Table of Contents

Single Particle Inclusive Spectra Resulting from the Collision of Relativistic Protons, Deuterons, Alpha Particles, and Carbon Ions with Nuclei

ABSTRACT

James C. Papp

We have measured the yields of positive and negative particles resulting from the collision of 1.05 GeV/nucleon and 2.1 GeV/nucleon protons, deuterons, alpha particles, and 1.05 GeV/nucleon carbon nuclei with various targets. Single particle inclusive cross sections for production of $\pi^{\pm}$, p, d, ^{3}H, ^{3}He, and ^{4}He at 2.5° (lab) were obtained. We discuss how the results bear on the concepts of limiting fragmentation and scaling, the structure of the alpha particle and deuteron, and the possibility of "coherent" production of pions by heavy ions.

I. Introduction

The availability of heavy ion beams having kinetic energies up to 2.5 GeV per nucleon at the Lawrence Berkeley Laboratory Bevatron has made possible the study of inclusive spectra from heavy ion-nucleus reactions. We hope that the experiment described in this thesis will shed light on a series of interesting questions:

1) Can heavy ions such as deuterons and alpha particles be considered in some sense "elementary" like protons and pions? In particular, can pions be produced in deuteron-nucleus and alpha-nucleus collisions with energies substantially greater than could be produced in proton-nucleus collisions at equal kinetic energy per nucleon? If so, can this production be understood in terms of the Fermi momentum of the constituents of the projectiles or is some other kind of collective effect necessary?

2) Are the ideas of limiting fragmentation[1] and scaling,[2] which are applicable to the "elementary" particle interactions at NAL and ISR energies, applicable to certain high energy heavy ion reactions? That is, is there a relation between the characteristic energies of a system, such as the spacing of energy levels, and the energy at which asymptotic considerations apply?

3) What can we learn about internal momentum distributions and correlations among nucleons in these projectiles? Can we think of a reaction such as d + Nucleus → p + anything in the region where the proton's velocity is about the same as the deuteron velocity as providing a sort of snap-shot of the deuteron structure at the time of the collision?

The results of this experiment certainly do not settle all of these questions though they do give some idea of what physics is involved in this type of reaction and point out the directions in which to seek more complete answers.

II. Theory and Phenomenology

A. Kinematics

Different sets of kinematic variables are useful for describing different physical phenomena. In this section we discuss those variables that have proved useful in the description of inclusive reactions.

The choice of variables is suggested by the experimental fact that transverse momenta in high energy multiparticle reactions are severely limited compared to longitudinal momenta. In high energy "elementary" particle reactions the average value of the transverse momentum, $p_\perp \simeq 0.3 - 0.4$ GeV/c, is approximately independent of the energy, type of particle produced, and multiplicity of the reaction. Since multiplicity

grows slowly, approximately like log E_{cm}, most of the energy available goes into longitudinal momentum. So if we consider a reaction of the form

$$a + b \to c + \text{anything} \tag{1}$$

we can write the Lorentz invariant cross section as

$$\frac{E^c d^3\sigma^c_{ab}}{d\vec{p}^3}\,(s,\ p^c_{\parallel},\ p^c_{\perp})$$

This cross section depends on the beam and target particles a and b; on the produced particle c; on the energy in the center of mass $\sqrt{s}$; and on the longitudinal and transverse momenta of particle c, $p^c_{\parallel}$ and $p^c_{\perp}$. Furthermore, in dealing with unpolarized beams and targets there is no azimuthal dependence.

A particularly elegant choice of longitudinal variable is the rapidity y. When presented in terms of y, the shape of the cross section is not dependent on the reference frame chosen. The rapidity is defined as

$$y = \frac{1}{2}\ln\left(\frac{E + p_{\parallel}}{E - p_{\parallel}}\right) = \sinh^{-1}\left(\frac{p_{\parallel}}{\mu}\right)$$

where $\mu = (m^2 + p_{\perp}^2)^{1/2}$ is called the longitudinal mass. From the definition it follows that, at fixed $p_{\perp}$, $dy = dp_{\parallel}/E$ so the cross section can be written as

$$\frac{E^c d^3\sigma^c_{ab}}{d\vec{p}^3}\,(s,\ p^c_{\parallel},\ p^c_{\perp}) = \frac{E^c d^3\sigma^c_{ab}}{dp^c_{\parallel} d^2\vec{p}^c_{\perp}}\,(s,\ p^c_{\parallel},\ p^c_{\perp})$$

$$= \frac{d^3\sigma^c_{ab}}{d^2\vec{p}^c_{\perp} dy}\,(s,\ p^c_{\perp},\ y)$$

we obtain

$$V(\vec{r}) \sim \gamma \int d^3r_2 \; \rho_1(\vec{r}_2 - \vec{r}) \; \rho_2(\vec{r}_2) \tag{4}$$

It can be shown that the appropriate constant in the limit of high energy nucleus-nucleus scattering is

$$\gamma = -\frac{2\pi\hbar^2}{M} f(0) \tag{5}$$

where M is the nucleon mass and f(0) is the complex forward nucleon-nucleon scattering amplitude evaluated at the incident lab energy per nucleon. This then yields our first and simplest approximation to the lowest order optical potential for ion-ion interactions

$$V_{opt}(\vec{r}) = -\frac{2\pi\hbar^2}{M} f(0) \int d^3r' \; \rho_1(\vec{r}' - \vec{r}) \; \rho_2(\vec{r}') \tag{6a}$$

It is already clear that this form of the model ignores the spin and isospin degrees of freedom of the nucleons though the above treatment is easily generalized to this level. Nowhere did the spin statistics enter so the Pauli principle has been ignored except to the extent it participates in the one body density distributions. Dispersive effects due to, among other things, the polarizability of the two distributions have not entered. Indeed, the analogy with Coulomb potentials clearly neglects <u>all</u> rearrangement processes. The internal Fermi motion of the constitutents and binding effects (off-shell effects) also remain to be included. Theoretical adjustments to f(0) that approximately correct for some of these inadequacies will be introduced and studied.

We explain in more detail below an extension to include finite

B. Energy Dependence of the Cross Sections

One aspect of this experiment was the determination of the energy dependence of certain heavy ion inclusive reactions. In particular we were interested in whether there is any similarity between the energy dependence of these cross sections in the 1-2 GeV/nucleon region and the energy dependence of elementary particle reactions at NAL and ISR energies.

Two ideas that have generally been confirmed[4] at NAL and the ISR are limiting fragmentation and scaling. The hypothesis of limiting fragmentation (HLF)[1] states

$$\frac{E^c d^3\sigma^c_{ab}}{d\vec{p}^3}\ (s,\ p^c_{\parallel},\ p^c_{\perp}) \underset{\substack{s\to\infty \\ p^c_{\parallel}\ \text{fixed}}}{\simeq} E^c\ \frac{d^3\sigma^c_{ab}}{d\vec{p}^3}\ (p^c_{a},\ p^c_{A})$$

That is, as the energy gets large, the cross section for producing slow particles in the lab (target fragments) becomes independent of the energy. Similarly, if one looks in the beam rest frame, the cross section for producing slow particles (beam fragments) becomes independent of the energy.

The energy at which limiting behavior starts depends on the reaction. For example, in the case of $p + p \to \pi^- + X$ limiting behavior has been seen at energies as low as 13 GeV.[5] One of the objectives of this experiment was to determine whether limiting behavior exists in reactions such as α + nucleus → p + anything at 1 - 2 GeV/nucleon.

The scaling hypothesis,[2] which is generally formulated in the center of mass frame, states

$$\frac{E^c d^3\sigma^c_{ab}}{dp^{\vec{}3}}(s, p_{\parallel}^{c*}, p_{\perp}^c) \overset{s}{\underset{s\to\infty}{\sim}} \frac{E^c d^3\sigma^c_{ab}}{dp^{\vec{}3}}(p_{\perp}^c, x).$$

That is, the cross section for large s does not depend separately on s and $p_{\parallel}^*$ but only on x, a combination of the two. In the beam and target fragmentation regions this statement is equivalent to HLF. However there is an additional prediction, based originally on the similarity of the reaction $p + p \to \pi + X$ to a bremstrahlung reaction, that in the region near $x = 0$ (the "wee x" region), which corresponds to neither beam nor target fragmentation,

$$\frac{E^c d^3\sigma^c_{ab}}{dp^{\vec{}3}}(p_{\perp}, x) \overset{x}{\underset{x\to 0}{\sim}} \frac{E^c d^3\sigma^c_{ab}}{dp^{\vec{}3}}(p_{\perp}).$$

That is, there is a central plateau in x. The origin of the equivalent central plateau in the rapidity variable is discussed in the next section.

C. Spectral Shapes at Fixed Energy

In this and the next section we discuss the shape of the spectra at fixed energy, that is, dependence on the rapidity y, and how these spectra approach their asymptotic values. We are particularly interested in seeing whether heavy ion reactions show behavior similar to that predicted for high energy elementary particle reactions and whether these inclusive reactions can help us learn about nuclear structure. Since a multitude of good review articles[6,7] discuss the various ideas and models regarding spectral shapes, we mention only two which are also

applicable to the question of approach to limiting behavior: (1) the short range correlation hypothesis, and (2) the Mueller Regge analysis.

If one considers the reaction (1) in terms of the rapidity y, then the correlation length hypothesis states that there is no correlation between two particles whose rapidities y_i and y_j are separated by an amount large compared to some correlation length L, that is if $|y_i - y_j| >> L$. Here L is not a length in the usual sense but rather a certain amount of rapidity. In particular, if y_a, y_b, and y_c are the beam, target, and produced particle rapidities, then there should be no correlation between the beam and produced particles as long as $|y_c - y_a| >> L$. Similarly there should be no correlation between the target and produced particles if $|y_b - y_c| >> L$. If the rapidity gap between beam and target is large enough, $|y_a - y_b| >> 2L$ then both $|y_b - y_c| >> L$ and $|y_a - y_c| >> L$ can be satisfied simultaneously. In this case there should be no correlation between the produced particle and either the beam or target. So we have a flat central plateau as shown in Fig. 1.

The correlation length idea gives no method for determining the magnitude of L and hence says nothing about how fast the asymptotic region is approached, which is one of the major concerns of this experiment. A different approach, due to Mueller overcomes this difficulty. The method hinges on a theorem that relates the cross section for the single particle inclusive

reaction (1) to the discontinuity of the forward amplitude for the elastic three-body reaction

$$a + b + \bar{c} \to a + b + \bar{c} \qquad (2)$$

If A(s, t, u,) is the proper absorptive part of the amplitude describing reaction (2) then the relationship is

$$E^c \frac{d^3\sigma_{ab}}{d\vec{p}^3} = \frac{1}{s} A(s, t, u)$$

where t and u are given by the usual relations

$$t = (p_b - p_c)^2$$
$$u = (p_a - p_c)^2$$

and p_a, p_b, and p_c are the 4-momenta of the indicated particles. A precise difinition of A(s, t, u) can be found in Ref. 3.

The utility of this approach comes from the possibility of applying Regge theory to learn about the asymptotic behavior of the amplitude A(s, t, u). Two kinematic regions of interest are the target fragmentation region, defined by the limit $s \to \infty$, $t \to -\infty$, u fixed, and the beam fragmentation region given by t fixed and u large. In each of these kinematic regions, assuming that Regge poles give the dominant contribution, a single Regge expansion is appropriate. The relevant Regge exchange diagrams are shown in Fig. 2a and 2b where the wavy lines indicate the Regge pole exchange and the loops indicate some more complicated process. Then for example in the target fragmentation region one has

$$E^c \frac{d^3\sigma^c_{ab}}{d\vec{p}^3}(s, p^c_{\parallel}, p^c_{\perp}) \simeq s^{\alpha_R(0)-1} f^c_{ab}(p^c_{\parallel}, p^c_{\perp})$$

If the leading Regge trajectory is the Pomeron, $\alpha_R(0) = \alpha_p(0) = 1$ we get

$$E^c \frac{d^3\sigma^c_{ab}}{d\vec{p}^3}(s,\ p^c_{\shortparallel},\ p^c_{\perp}) \simeq f^c_{ab}(p^c_{\shortparallel},\ p^c_{\perp}).$$

That is, the distribution is limiting (independent of s).

The central region is characterized by t and u large and comparable. The double Regge limit is appropriate here and the relevant diagram is shown in Fig. 2c. One finds the amplitude for this process is

$$A(s,\ t,\ u) = t^{\alpha_t(0)}\ u^{\alpha_u(0)}\ f^c_{ab}\ (p^c_{\perp})$$

which together with the result that $tu \simeq u^2 s$ gives for the invariant cross section

$$E^c \frac{d^3\sigma^c_{ab}}{d\vec{p}^3} = s^{\alpha(0)-1}\ \tilde{f}^c_{ab}\ (p^c_{\perp}).$$

If we have Pomeron dominance and $\alpha(0) = 1$, the single particle spectrum is independent of p^c as well as s. In other words, a central plateau in y develops. A more complete discussion of the application of Regge theory to inclusive processes can be found in Ref. 6.

D. Where is Asymptopia?

In this experiment an important question is at what energy asymptotic considerations become valid. Equivalently, in terms of the correlation length idea, what is a typical value of L? The Mueller method can provide an estimate.[8]

In the target fragmentation region, if a trajectory α_R in addition to the Pomeron is included in the analysis, the cross section becomes

$$\frac{E^c d^3\sigma^c_{ab}}{d\vec{p}^3}(s, p^c_{\parallel}, p^c_{\perp}) = f^c_{ab}(p^c_{\parallel}, p^c_{\perp}) + s^{\alpha_R(0)-1} g^c_{ab}(p^c_{\parallel}, p^c_{\perp}) \qquad (3)$$

If the vector meson trajectories contribute, $\alpha_R(0) \approx 1/2$ and the approach to limiting behavior is like $s^{-1/2}$. In the central plateau region, one can have a contribution from the Pomeron on one side of Fig. 2c, and a secondary trajectory on the other side. The result[8] is a slower approach to the limit, given by

$$s^{\frac{1}{2}(\alpha_p(0)+\alpha_R(0)-1)} \approx s^{-1/4}$$

It is necessary here to be careful regarding units. In the above equations, such as (3), one must really write $\left(\frac{s}{s_o}\right)$ for s. The constant s_o sets the energy scale and is usually chosen to be about 1 GeV^2 for elementary particle reactions. To express this approach to limiting behavior in terms of the correlation length L, we write the second term in eq. (3) as

$$\left(\frac{s}{s_o}\right)^{\alpha_R(0)-1} g^c_{ab}(p^c_{\parallel}, p^c_{\perp}) = \left(\frac{\mu^2 e^Y}{s_o}\right)^{\alpha_R(0)-1} g^c_{ab}(p^c_{\parallel}, p^c_{\perp})$$

$$= \left(\frac{s_o}{\mu^2}\right)^{1/2} e^{-Y/L} g^c_{ab}(p^c_{\parallel}, p^c_{\perp})$$

where $L = \frac{1}{1 - \alpha_R(0)} \approx 2$ is the correlation length and $Y = \ln\frac{s}{\mu^2}$ is the total length of the rapidity plot. So since $L \approx 2$, in order to see a limiting distribution one needs $Y \gtrsim 3 - 4$, or $E_{LAB} \approx 3.5$ GeV for a reaction like $p + p \to \pi + X$. A central plateau would not develop until $Y \gtrsim 6 - 8$ giving $E_{LAB} \approx 200$ GeV.

But now suppose we consider instead a heavy ion reaction such as

$$\alpha + A \rightarrow p + X. \qquad (4)$$

Here A is some nuclear target and the α particle is the projectile. What value do we choose for s_0 for such a reaction? It seems reasonable that if we are looking at the beam fragmentation region the characteristic energy of the process is of the order of a nuclear binding energy: a few MeV. If so, since the quantity (s_0/μ^2) will then be small, making the second term in eq. (3) small, we might expect limiting behavior at energies of only a few GeV for such heavy ion reactions.

Consider reaction (4) from a slightly different point of view. Suppose the beam kinetic energy is 1 - 2 GeV/nucleon and suppose the produced proton is in the beam fragmentation region. What we are describing is the familiar process of stripping. Physically we have a picture of an alpha particle moving toward a target nucleus which strips off one proton and two neutrons while the remaining proton proceeds ahead virtually undisturbed. So one might expect to find a peak in the spectrum of (4) when the proton rapidity equals the beam rapidity. The Fermi momentum in the alpha particle spreads out the peak somewhat, giving it a width typical of the momentum of the proton in the alpha. This is typically of the order of 100 MeV/c while the lab momentum of the proton is $\simeq$ 1.75 - 3 GeV/c depending on the incident beam

energy. So the width of the beam fragmentation region in rapidity $\Delta y \approx 0.175$ is very narrow in comparison to $Y = 2.3$, the total rapidity gap at 2 GeV/nucleon. If we say that for such a process the correlation length $L \approx \Delta y$, then we can satisfy the condition for the appearance of a central plateau region, namely $2L << Y$.

Measurements of appropriate single particle spectra from heavy ion induced reactions should determine the validity of this line of reasoning. If the ideas of scaling and limiting fragmentation and the predictions regarding the shapes of spectra at fixed energy are correct for these heavy ion reactions, we may have a new and rather powerful means for exploring high energy interaction mechanisms and also nuclear structure. Since the rapidity gap between beam and target is large, it is possible to identify beam and target fragments rather unambiguously, in contrast to nuclear reactions at lower energy.

E. Pion Production by Deuterons and Alpha Particles

A rather different aspect of this experiment was the search for some sort of "collective" effect in the production of pions by deuterons and alphas interacting with nuclei.

A variety of models exist to describe such reactions, ranging from macroscopic types[9,10,11] which try to describe heavy ion-nucleus reactions in terms of macroscopic parameters of the system such as impact parameters and temperatures, to

microscopic types which involve descriptions in terms of constituents, to Regge and particle type models.[12]

We are concerned primarily with microscopic models of pion production, and in particular deviations from such models. If it is not possible to construct a nucleon constituent model to describe deuteron and alpha production of pions then one can say some sort of collective effect is involved.

Where might such a collective effect show up? Perhaps in the production of fast pions: pions with energies beyond the kinematic limit for pions produced in nucleon-nucleus reactions. The kinematic limit for a reaction like $p + A \rightarrow \pi + X$, where A is some target nucleus, can be found by considering the mass of the system X:

$$m_X^2 = (p_p + p_A - p_\pi)^2$$

where the p's are the 4-momenta of the indicated particles. If the pion is observed at 0° to the incident beam, neglecting m_π compared to $|\vec{p}_\pi|$, and taking account of the inequality

$$m_X \geq m_p + m_A - m_\pi$$

we get that

$$p_\pi \leq T_p\left\{1 - \frac{E_p - p_p}{m_A}\right\}$$

where the second term is at most 3% and T_p is the proton kinetic energy. Thus protons cannot produce pions with momenta greater than the incident kinetic energy.

What about heavy ion projectiles? If they are treated in the same way as protons, and if the kinetic energy per nucleon is T, one expects $p_\pi \lesssim 2T$ for deuterons and $p_\pi \lesssim 4T$ for alphas. If instead we consider these projectiles to be assemblages of semi-free nucleons and that π production proceeds via the usual nucleon-nucleon interaction then one expects $p_\pi \lesssim T + T'$ where T' is some contribution due to the Fermi momentum in the projectile.

The question of whether pions produced with momenta $p_\pi > T$ in heavy ion collisions are due to collective effects or high internal momentum components in the projectile is not clear cut. For example, in the case of the deuteron, when the internal momentum is large, the nucleons tend to be close together and so correlated in space. The important question is whether there is any way to distinguish the effects of Fermi momentum from collective effects. The answer would seem to be yes. If we consider projectiles with A > 4 then to a fair approximation the internal momentum distributions are the same for all nuclei. So if we look at pion production spectra as a function of pion momentum in the beam fragmentation region, the spectral shapes should be very similar for all projectiles with a normalization depending on the A of the beam. If, however, collective effects are involved then it is possible that the spectra from the heavier projectiles would extend to significantly higher momenta than those for light projectiles.

With the help of a rather simple constituent type model we can calculate the spectral shape for π production by heavy ions assuming the mechanism is nucleon-nucleon collisions modified by Fermi momentum. Suppose $\vec{p}_o$ is the average incident momentum per nucleon and $\vec{p}$ is the momentum of the nucleon of interest inside the projectile. The momenta $\vec{p}$ and $\vec{p}_o$ differ of course because of the Fermi momentum. We are assuming here that we can neglect the projectile's binding energy and treat the incoming nucleons as free particles.

We want to calculate the cross section for producing a pion with momentum $\vec{k}$ by a heavy ion knowing the cross section for pion production by nucleons. The process can be visualized as in Fig. 3. If we let $W(\vec{p}_o,\vec{p})$ be the probability that if $\vec{p}_o$ is the beam momentum, then $\vec{p}$ is the momentum of the nucleon, we can write the cross section as

$$\sigma_H^-(\vec{p}_0, \vec{k}) = N_H\int\{Z\sigma_p^-(\vec{p}, \vec{k}) + (A - Z)\sigma_n^-(\vec{p}, \vec{k})\} \times W_H(\vec{p}_0, \vec{p})d^3\vec{p} \qquad (5)$$

where the superscript - means π^- production and the subscripts stand for the reactions

H: (d,α, or ^{12}C) + nucleus $\rightarrow \pi$ + X

p: proton + nucleus $\rightarrow \pi$ + X

n: neutron + nucleus $\rightarrow \pi$ + X

while σ stands for the invariant differential cross sections $\sigma = E\, d^3\sigma/d\vec{k}^3$. The factor N_H takes into account shielding effects

(N_H = 1 if there is no shielding). The quantities A and Z are the usual nucleon number and charge of the projectile in units of the proton charge. Furthermore, if the target is carbon, an isospin singlet in its ground state, charge symmetry allows us to replace

$$\sigma_n^-(\vec{p}, \vec{k}) = \sigma_p^+(\vec{p}, \vec{k})$$

a nice simplification since the reaction $p + A \rightarrow \pi^+ + X$ is easier to measure than $n + A \rightarrow \pi^- + X$.

If the beams are unpolarized, the cross section in eq. (5) depends on three quantities: $|\vec{p}|$, $|\vec{k}|$, and θ, the angle between $\vec{k}$ and $\vec{p}$. As a result, in order to explicitly carry out the integrations involved in eq. (5) it is necessary to measure the proton-induced pion production cross sections as functions of beam momentum, pion momentum, and production angle. In this experiment only $|\vec{p}|$ and $|\vec{k}|$ were variable; the production angle was fixed at 2.5° (lab). So in order to proceed some approximation to the transverse momentum dependence of the cross sections must be made.

We assume that we can write the cross sections in the following form[13]

$$\sigma^{\pm}_{p,n}(\vec{p}, \vec{k}) = f^{\pm}_{pn}(|\vec{p}|, |\vec{k}|) \cdot g^{\pm}_{p,n}(Q)$$

where $Q^2 = k^2 - \vec{k}\cdot\vec{p}/p^2$ is the magnitude of the component of $\vec{k}$ perpendicular to $\vec{p}$. We further assume that $g^{\pm}_{p,n}(Q) = e^{-cQ}$ where C is an adjustable constant. Higher energy data[14] suggest this is a reasonable parameterization with $C \approx 5(\text{GeV/c})^{-1}$. In other

words, we have assumed that the cross section σ can be written as a 0° cross section times some exponential function of transverse momentum.

The function $W(\vec{p}_0,\vec{p})$ can be obtained by using the momentum space wave functions $\phi(\vec{q})$ which describe the internal momentum of the nucleons in the projectiles. Here $\vec{q}$ is the momentum of the nucleon of interest in the rest frame of the projectile, i.e. the Fermi momentum. Then $W(\vec{q}) = |\phi(q)|^2$. Conservation of probability and Lorentz invariance require that $W(\vec{q})d^3\vec{q} = W(\vec{p},\vec{p}_0)d^3p$, or equivalently $E'W(\vec{q}) = EW(\vec{p},p_0)$ where E is the nucleon energy in the lab while E' is the energy in the rest frame of the projectile. So finally we can write

$$\sigma_H^-(\vec{p}_0,\vec{k}) = N_H\int\{f_p^-(|\vec{p}|,|\vec{k}|) + f_p^+(|\vec{p}|,|\vec{k}|)\} \times e^{-cQ}\frac{E'}{E}\, W\left(q_{\parallel}(\vec{p},\vec{p}_0),\, q_{\perp}(\vec{p},\vec{p}_0)\right) d^2p_{\perp}dp_{\parallel}.$$

The functions $f_p^{\pm}$ are obtained from our measured proton induced pion production cross sections. With suitable choices of W the integral can be performed numerically.

Since this is a rather general constituent type of model, it allows us to make a preliminary investigation of whether collective effects, that is deviations from this type of model, are important in pion production by heavy ions. In addition, the model may be applicable to baryon fragment production in reactions such as d + A → p + X, as discussed below in Section V-C

III. Experimental Method

The experiment essentially consisted of a single arm double focusing spectrometer which transported particles produced in our targets to our detection system and provided momentum analysis. The detection equipment identified the produced particles by momentum, time-of-flight, dE/dx, and Cerenkov information. The data was recorded in scalers and in a pulse height analyzer, the contents of which were subsequently read out on magnetic tape for later analysis.

A. Primary Beam

The experimental setup is shown in Fig. 4. The external beam of the Bevatron struck our targets at the third focus of what is called the septum channel--one of three main external beams from the accelerator. Typical fluxes on the targets were $1\text{-}3\times10^{11}$ protons, $10^{10}\text{-}10^{11}$ deuterons, $10^{9}\text{-}10^{10}$ alphas, and $1\text{-}3\times10^{6}$ carbon nuclei per pulse. There were approximately ten pulses per minute with a maximum spill length of about 1.2 seconds.

The primary beam intensity was monitored by a scintillation counter telescope consisting of three scintillators in coincidence. For most of the running the telescope was placed about 2 meters from the production targets at about 90° to the incident beam. Typically there were 200 counts in the monitor for 10^{10}

particles incident on the targets. Because the intensity of the carbon beam was so much lower than the intensity available with the other three types of beam particles, it was necessary to bring the monitor much closer to the target during this part of the experiment. As a result, the telescope was placed within six inches of the targets for the ^{12}C runs. This was the minimum distance allowed by the geometry of the target box.

The monitor of course only provided a relative normalization. In order to get an absolute normalization for our cross sections we needed to know precisely the incident flux. For this purpose we used an ion chamber and a secondary emission monitor placed in the primary beam upstream of our targets. The monitor was calibrated against the ion chamber and SEM according to the procedure described in section IV below.

The ion chamber itself was calibrated against a pair of scintillation counters placed directly in the beam in the following way. The charge created in the ion chamber by the beam was collected and measured by an electrometer. The full scale deflection of the meter which read out the electrometer charge could be adjusted from a maximum sensitivity of 3×10^7 up to 10×10^{10} incident charges per pulse. The charge produced in the ion chamber is proportional to Z^2 where Z is the charge of the beam particles. When a ^{12}C beam was used, the reading of the ion chamber was about 36 times the number of particles which actually passed through it.

So a beam rate of about 1×10^6 per pulse was within the range of both the ion chamber and scintillation counters. We used two scintillators 1/8 inch thick with RCA 8575 phototubes. The counters, one 4-inch square and one 3-inch disc, were placed in the beam one meter downstream of the ion chamber. The details of the calibration are discussed in section IV.

During most of the experiment, the primary beam was focused and steered onto the targets with the aid of a scintillation screen located in the target box which could be lowered into the beam about 6 inches behind the production targets. The scintillator was viewed by a TV camera providing an image in the main control room for the accelerator operating crew. The position of the beam was checked every time the targets were changed, approximately every 5 minutes. The low intensity of the carbon beam, however, made the use of a scintillation screen impossible. Instead a multiwire proportional system was used. For our particular application the MWPC system had the advantage that the profile of each beam pulse was displayed on a scope while data taking was going on. With the scintillator we could not take data and check the beam position at the same time because the scintillator itself was a significant source of secondary particles.

The targets were housed inside a box capable of holding up to four targets, two on each of two stands. The position of the targets was under the control of the operating crew of the

accelerator. Any of the 4 targets could be moved into the beam line, or it was possible to have no target in the beam line. About one minute was required to change targets. During running with the ^{12}C beam we used only two targets, C and Cu, each .32 cm thick, 3.2 cm high, 4.4 cm wide. During the remainder of the running we used 4 targets, each .64 cm thick except for a CH_2 target which was 1.32 cm thick. The targets were generally 1.9 cm high and 3.2 cm wide, while the beam spot was typically 1.3 cm high and 1.9 cm wide.

B. Secondary Beam Transport System

The secondary particles were momentum analyzed and transported to our detection apparatus by Beam 30 of the Bevatron, a double focusing spectrometer. The elements of the spectrometer are shown in Fig. 4. Particles produced at 2.5° enter the spectrometer and are steered by magnets M2/3 to the first focus. There a 61 cm long lead collimator was used to select the momentum acceptance, $\Delta p/p$, of the detected particles. Magnet M4 provided further momentum selection and brought the particles to the second focus where our detection apparatus was located. Typically we ran with a slit width of 5 cm for a $\Delta p/p$ of ± 1 1/2% when the spectrometer was set to transport negative particles. When the magnet polarities were reversed and positive particles were transmitted

we generally used a 1.25 cm wide slit for $\Delta p/p = \pm 3/8\%$. The measured intensity at the final focus as a function of slit width is shown in Fig. 5a. The linearity of the data points verifies the linear dependence of $\Delta p/p$ on the slit width. There was in addition an upstream collimator at the exit of magnet M1 which could be used to vary the angular acceptance of the channel. We usually ran with this collimator set at either 4 inches or 5 inches, so it would have no effect on the particles of interest.

We used a pre-existing beam which was designed so that there is virtually no access to the beam line between the production targets and the intermediate focus. Consequently it was impossible to directly measure the acceptance of the channel in momentum and solid angle. Instead it was necessary to measure the various magnetic elements and then to use the LBL computer program TRANSPORT to calculate the angular and momentum acceptances.

C. Detection System

When, for example, an alpha particle strikes a nucleus, pions, protons, deuterons, ^{3}He, ^{3}H, and alpha particles are all abundantly produced. If the beam is ^{12}C, an even wider variety of particles are produced. It was the function of the detection system to sort out and identify the particles reaching the final focus of our spectrometer. In order to do this, the detection system consisted essentially of five parts:

experiments. Let me finish my remarks by showing an example of how straightforward such an analysis might be. I choose the projectile fragmentation case and for simplicity attempt to naively estimate the inclusive cross section for

$$A+B \rightarrow (A-1)+X \tag{12}$$

where the A-1 system is detected intact. We shall assume that a surface nucleon has been removed suddenly leaving the (A-1) system, most of the time, in the ground state or some low lying excited state so that it does not subsequently break up. Actually, if we only desire the behavior of the inclusive cross section as a function of the target nucleus it is only necessary to assume that the population of the states of the (A-1) system is independent of the target. This seems reasonable. On the other hand, the more restrictive assumption permits the assignment of an absolute cross section to the theoretical results. A simple semi-microscopic analysis with the additional assumption that β, the previously mentioned ratio of real to imaginary nucleon-nucleon amplitude, is negligibly small proceeds as follows: we define a mean free path function, $\lambda(b,Z)$, for two interacting heavy ions in the impact parameter scheme by

$$1/\lambda(b,z) = \sigma T(b,z) \tag{13}$$

where $T(b,Z)$ is given by Eq. (10). Thus the total number of nucleon-nucleon collisions when two heavy ions collide at impact parameter b is $N(b)$ given by

The outputs from the Cerenkov's two photomultipliers were added together; then the triple coincidence S2•C•S3 was generated with the two scintillators immediately in front of and behind the Cerenkov. Fig. 7 shows a typical plot of S2•C•S3/10^3 MONITORS as a function of gas pressure, clearly showing contributions of e^-, μ^-, and π^-. Since the maximum pressure allowed in the counter was 330 PSI, the minimum momentum at which we could detect μ^- was 850 MeV/c, while electrons could easily be measured at all momenta studied in this experiment.

When the spectrometer was set to transport positively charged particles, complete identification of the various types of particles required measurements of both time-of-flight and energy loss (dE/dx). The system to do this is shown in Fig. 8. Basically time-of-flight was provided by counters S1 and S3, separated by about 50 Feet. The signal from S3 was used as a "start" pulse to a time-to-amplitude converter. S1, after a suitable delay, acted as the stop pulse for the TAC. The negative TAC output went to a 400 channel pulse height analyzer for storage. The TAC output was routed into either channels 0-200 or 200-400 according to whether or not the pulse height in counters S4 and S5 exceeded a certain level. This pulse height level was chosen at each momentum by setting the discriminator thresholds in such a way that particles with charge greater than or equal to 2 would be routed to the upper 200 channels while those with charge 1 would go to the lower 200 channels.

There were many variations on this system. Since it is very difficult to distinguish π^+ from protons above 1.75 GeV/c on the basis of time-of-flight alone, we occasionally used a routing signal based on the gas Cerenkov counter. With the counter set to fire on π^+ but not protons, a pulse from the Cerenkov would generate a high channel routing signal while its absence would generate a low channel routing.

Very often, especially when running with carbon and alpha beams, it was useful to take dE/dx spectra rather than TOF spectra. Basically we took a spectrum of pulse heights in counter S4, by running the signal from the phototube into the PHA after stretching it. This is shown in Fig. 9. The linear gate and stretcher allowed us to look at either all particles coming down the channel or to selectively gate through only such particles which satisfied a particular time-of-flight requirement. This is very useful in the identification of different particles having the same charge/mass ratio (e.g. deuterons and alphas), since such particles all have the same velocity at a particular momentum setting of the spectrometer, but have different pulse heights.

The remaining two elements in the system were a lucite total reflection Cerenkov counter sensitive to particles with $\beta \geq 0.9$, and the MWPC system. The Cerenkov counter was used in conjunction with the gas Cerenkov to distinguish protons from deuterons up to 3.5 GeV/c. We defined a deuteron by $[\overline{S2 \cdot C_{gas}} \cdot S3]$.

$[S1 \cdot S3] \cdot [\overline{C_{lucite}}]$, that is correct time-of-flight as determined by S1•S3, no pulse in the lucite counter, and no pulse in the gas counter, which fired only on pions. Then a proton was $[\overline{S2 \cdot C_{gas} \cdot S3}] \cdot [S1 \cdot S3] \cdot [C_{lucite}]$.

Finally, the MWPC system consisted of an X and Y plane located about one foot upstream of the final focus. The chamber generated an X-Y scatter plot on an oscilloscope display on a pulse by pulse basis. We used this to monitor the position and shape of the secondary beam at the final focus.

IV. Acquisition and Analysis of the Data

A. Data Acquisition

Our data taking was essentially done in three modes which we referred to as electronic runs, analyzer runs, and calibration runs. The data taken with the channel set for negative particles was all electronic. After setting the momentum of the channel, we cycled through the four targets recording the various scalers by hand for a fixed number of monitor counts. When we were looking at positive particles we set the relative timing of S1 and S3 to select the particular particle of interest and counted S1•S3 coincidences.

Most of our data on positive fragments came from analyzer runs. In this mode we took time-of-flight and/or dE/dx spectra in the pulse height analyzer for a particular number of monitor counts for each target and momentum. Each run was read out onto

magnetic tape for later computer analysis. In general, electronic and analyzer running went on simultaneously for the positive particles. Since we took the same data in several different ways, we have many cross checks.

Our last type of run was a calibration run. This consisted of calibrating the monitor telescope counts against the ion chamber readings for each target, beam particle, and beam energy. In addition, there was one run in which we calibrated the ion chamber against a pair of scintillation counters placed directly in the beam, and some runs to determine effects of target size and beam steering on our data.

B. Determination of the Cross Sections from Measured Quantities

The bulk of the data came in the form of time-of-flight and dE/dx spectra from the pulse height analyzer. Typical spectra are shown in Fig. 10. The particles were identified and counts in each peak were added manually and combined with electronic data taken at the same momentum and target to yield the total number of counts normalized to the monitor counts. Background subtraction was usually very easy due to the narrowness of the TOF peaks. For the scalar data, background subtraction was generally impossible so in cases where background was extensive we relied on the analyzer numbers for our final results.

The uncorrected single particle inclusive production cross section $d\sigma/d\Omega dk$ is given in terms of our counts/monitor by

$$\frac{d\sigma}{d\Omega dk} = \frac{\text{counts}}{\text{monitor}} \times F_1 \times F_2 \times \frac{A}{\rho N L} \times \frac{1}{d\Omega dk}$$

where the factors on the right hand side of the equation are defined as follows: the quantities $d\Omega$ and dk are the solid angle and momentum acceptance of the system; A, ρ, and L are respectively the atomic mass, density, and length of the target; N is Avogadro's number, 6.022×10^{23}; F_1 is the ratio (monitor counts)/(ion chamber reading) while F_2 is (ion chamber reading)/number of particles incident.

The quantities $d\Omega$ and dk were controlled by the collimators at the intermediate focus and at the exit of the first bending magnet. As mentioned above (sec. III-B) it was necessary to use computer calculations to determine values for $d\Omega$ and dk, though we were able to verify experimentally that the flux at our detectors varied linearly with the collimator slits (Figs. 5a and 5b). Uncertainty in the solid angle and momentum acceptance of the system constituted the major source of error in the absolute normalization of our data.

The factor F_1 was measured directly during our calibration runs described above (sec. IV-A). More difficult was the determination of F_2. The ion chamber had been calibrated to read out the number of singly-charged minimum-ionizing particles passing through, even though what it really measures is the charge produced in it. Since the charge produced depends on the type of beam particle and its energy, we had to recalibrate the ion chamber for each beam particle type and energy. In fact, the reading may be incorrect even for singly-charged minimum-ionizing particles, because of either a change in the chamber since the

time it was calibrated or an incorrect initial calibration. So we should write the factor $F_2 = z^2 F_2'(E)\, F_3$ where $F_2'(E)$ is the energy dependent factor which reduces to 1 at the "calibration" energy, and F_3 takes into account the error in the ion chamber reading at the "calibration" energy. $F_2'(E)$ can be calculated from standard energy loss tables; this is done in Appendix A. F_3 was measured by directly counting the beams with scintillation counters and comparing to the ion chamber.

C. Correction Factors

The important correction factors were rather different for the pion data and the baryon data. For pions, corrections for decay in flight and contamination by muons and electrons were most important.

To calculate the effect of pion decay, we let N_o be the number of pions produced in the target, N(x) be the number remaining a distance X from the target, τ be the pion proper lifetime, and p the momentum of the pion. Since the lifetime in the lab is $\gamma\tau$, the number remaining after a time t is

$$N(t) = N_o e^{-t/\gamma\tau}$$

Noting that $t = x/v = x/\beta c = Ex/pc = m\gamma c^2 x/pc$, we get

$$N(x) = N_0 e^{-\frac{x}{c\tau}\left(\frac{mc^2}{pc}\right)}$$

Numerically, if x is in meters and p in MeV/c

$$N(x) = N_0 e^{-17.89x/pc}$$

so $N_o = N(x)e^{17.89\ x/pc}$

In addition to the decay correction there is a correction due to lepton contamination. A muon which results from the decay of a pion after the Cerenkov counter will strike S5 and look exactly like a pion, so we ignore them. Consequently we can write for the number of pions created

$$N_\pi = (N_{total} - N_{lepton})e^{17.89\ x/pc}$$

where N_{total} is the total number of particles detected, while N_{lepton} is the number that were leptons. The appropriate value for x is the distance from the production target to the Cerenkov counter, 34.137 meters.

Our measured values for the lepton fraction are summarized in Table 1. The contamination is especially large for the case of electrons from Cu and Pb targets, as much as 1 % at 500 MeV/c, most likely because of conversion of γ's from π^0 decay. Unfortunately, the data being rather sketchy, it was necessary to make a model to calculate lepton contamination where there were no measurements. If we call L the lepton fraction and assume L depends on beam energy and target but is the same for *d* and α beams, we can try a parameterization of the form

$$L = A_e e^{-\alpha_e p} + A_\mu e^{-\alpha_\mu p}$$

for the electron and muon parts. Here p is the momentum. Fig. 11 shows a plot of lepton contamination as a function of momentum for 3.5 GeV protons on various targets. An exponential decrease with momentum seems to be reasonable.

Two additional corrections need to be mentioned: absorption and energy loss in the targets. For slow, heavy secondaries, energy loss is the major correction factor. For Be and C targets this effect is only about 7% in the worst case, but for Pb and Cu targets there is a 14% effect for 750 MeV/c ^{3}H and almost a 20% effect for ^{3}He at 1000 MeV/c.

In contrast, absorption is a much smaller effect. The fraction of particles that are absorbed is given approximately by $\rho NL/2A\ \sigma_{abs}$ where σ_{abs} is the absorption cross section. This is about 5% for pions in copper and about 1% in Be. For the case of baryons, absorption is at worst about 8% for α particles in Pb

D. Sources of Error

Probably as important as presenting final sets of data is knowing the likely sources of error. This knowledge allows one to estimate the accuracy of the data and to know how much faith to have in the results. In this experiment there were a variety of systematic errors which affect the final data in very different ways, ranging from an effect on the overall normalization of all data points to pulse-to-pulse variations affecting the data's self consistency.

The two major problems affecting the determination of the data's overall normalization were the inability to directly measure the system's solid angle and momentum acceptance, and the difficulty

in determining the incident flux. As mentioned above (sec. III-B), since there was essentially no access to the secondary beam line between the production targets and the intermediate focus, it was necessary to rely on a computer program to determine the acceptance of the channel. The accuracy of the LBL program TRANSPORT has been estimated by its authors at ±20% in determining acceptances.

Most experiments that utilize high intensity primary beams, that is intensities which make it impossible to count individual beam particles, suffer from errors in the range of 10%-20% associated with the necessary ion chambers or secondary emission monitors. For us this was not a great problem because we were able to calibrate our ion chamber against a pair of scintillators in the beam. By using a carbon beam with a charge of six proton charges, we found that the intensity ranges of the ion chamber and scintillators overlapped. In fact we found that the intensity as measured by the IC was about 13% less than that measured with the counters. So it is likely that the error involved in determining the incident flux is small compared to the error associated with the acceptance calculation.

These sorts of errors only affect the comparisons of this data with other experiments; they do not cause any internal variation in the data and so are perhaps less troublesome than the types that do. Among these more troublesome kinds are steering and focusing of the primary beam on the targets, inaccurate settings for the spectrometer magnets, dead time

effects in the control electronics, and problems associated with high rates in the detection system.

Steering and focusing of the primary beam affect the data in two possible ways. First it is possible that not all of the incident beam strikes the target, and second the production angle might be changed. We did several things to keep this problem to a minimum. During data taking we checked the beam condition before and after every target change, typically every 5-10 minutes. When the Bevatron seemed exceptionally unstable we recorded both monitor and ion chamber readings during running and checked each run for consistent monitor/IC ratios. Finally, in order to get some quantitative feeling for the problem, during one of the calibration runs we made some measurements of the effects of intentionally missteering the beam. We found that for the case of 500 MeV/c π^- produced by 2.66 GeV protons incident on Pb, displacing the primary beam by 1/4 inch from the center line produced a 10% change in our ratio π's/monitor. The effect was approximately linear up to displacements from the center line of ± 0.4 inch. So missteering problems could contribute errors in the 5-10% range for each data point.

Going from the primary beam to the secondary beam, the magnet setting error could at times be important. In certain cases the cross sections we measured were very momentum dependent; a momentum change of less than 10% could result in more than a

100% change in cross section. Therefore slight errors in our momentum determination could result in significant errors in the cross sections.

A source of error affecting both beam and fragment is multiple scattering. The effect is greatest for the case of slow heavy fragments. For deuterons and alpha fragments with p/z = 1 GeV/c the R.M.S. multiple scattering angle $(\bar{\theta}^2)^{1/2}$ varies from .25° for Be and C targets, up to 2.5° for a Pb target. The angle $(\bar{\theta}^2)^{1/2}$ decreases with momentum so that, when p/z = 2 GeV/c, $(\bar{\theta}^2)^{1/2}$ has decreased by a factor of 3. Multiple scattering is significant if $(\bar{\theta}^2)^{1/2}$ is comparable to some angle which characterizes the angular dependence of the cross section. Since our data was taken at only one angle, we must assume some angular dependence to estimate the significance of multiple scattering. Heckman, et al.[21] have found that in the rest frame of the beam, fragmentation of heavy projectiles, such as ^{16}O into various nuclear fragments is given approximately by the form $e^{-p^2/2m_\pi^2}$. If we assume a similar form for the cross section away from the fragmentation peaks, then for our case the angular dependence is essentially $e^{-25p^2\theta^2}$. If p = 1 GeV/c the distribution is $e^{-\theta^2/\theta_0^2}$ with $\theta_0^2 = 1/25$ or $\theta_0 = 1/5 = 11.4°$. This is larger than the worst case multiple scattering angle (Pb target) by a factor of 4, suggesting that for the experiment, especially for data with Be, C, and even Cu targets, multiple scattering is rather unimportant.

Finally we mention errors due to high rates and background subtractions. The main consequence of high rates in the spectrometer

was the introduction of background into the TOF spectra. Since momentum selection by magnet M4 occurred after counter S1, the rate in S1 was significantly larger than in S3, especially in regions where the cross sections were very momentum-dependent; that is, near the fragmentation peaks which were the regions of high rates. Since S3 provided the start pulse to our time-to-amplitude converter and S1 provided the stop pulse, with high rates there was a chance that the stop pulse was generated by a different particle from the start pulse, thus producing background. Generally our TOF spectra were very clean, as Fig. 10 shows. However, in certain instances this background was very significant. For example, the proton production cross section by 1.05 GeV/nucleon alpha particles is very large at a momentum of 1.75 GeV/c, more than 1500 times the size of the ^{3}H production cross section. As a result, the signal-to-noise ratio for ^{3}H could be as bad as 1:1. This effect differs from those mentioned above in that the presence of background is obvious while, for example, missteering the beam is not. So, in the cases where background was severe, the errors on those points were increased.

V. Results

A. General

The range of parameters involved in the experiment is shown in Fig. 12. Not all possible combinations of parameters were measured; for example, for 2.66, 3.5, and 4.8 GeV proton beams, only negative produced particles were measured. Also, $e^{\pm}$ and $\mu^{\pm}$ were measured only to the extent necessary to determine the contamination of the pion data. We first discuss the pion production results, then move on to the data on the heavier fragments.

B. Pion Production

The measured cross sections for $\pi^{\pm}$ production by protons are summarized in Tables 2-8. Tables 9 and 10 give the results for deuteron beams, Tables 11 and 12 for alpha beams, and Table 13 for a ^{12}C beam. All the corrections discussed in Section IV above, lepton contamination, decay in flight, and absorption in the target have been applied to the data.

Plotted in Fig. 13 and Fig. 14 are the data on π^- and π^+ production by protons on carbon. The 1.05 GeV/nucleon deuteron and alpha results are plotted in Fig. 15, along with the 1.05 GeV proton data for comparison. Fig. 16 shows similar data at 2.1 GeV/nucleon. The effects of the kinematic limit discussed in Section II-A are evident in these three figures: the 1.05 GeV proton data cuts off at about 1 GeV, while the spectra from 1.05 GeV/nucleon deuterons and alphas extend far beyond 1 GeV/c. The 2.1 GeV/nucleon results show similar features.

The Lorentz invariant cross sections $E/k^2\ d^2\sigma/d\Omega dk$ for these processes are plotted against the scaling variable x' in Figs. 17, 18, and 19. Here x' is the usual $x' = k_{\pi}^*/(k_{\pi}^*)_{max}$, where the asterisk denotes center-of-mass. The quantity $(k_{\pi}^*)_{max}$ is found by calculating the missing mass for the reaction beam + target $\rightarrow \pi$ + MM and then finding the pion momentum which corresponds to minimum missing mass consistent with baryon conservation. One finds the rather remarkable result that all the π^- spectra tend to fall

on top of each other. Scaling is familiar from higher energies, though here the cross sections show approximate scaling all the way down to 1 GeV. If one plots the data taken with a Be target and compares them with results of other experiments[15,16,17] at higher energies (12, 19, 24 GeV) the agreement is quite good.

One must remember in looking at these data that the measurements were made at fixed angle in the lab, 2.5°, rather than fixed transverse momentum. Consequently $k_\perp$ varies from 22 MeV/c at k_π = 500 MeV/c to $k_\perp$ = 210 MeV/c when k_π = 4.8 GeV/c. If we assume a transverse momentum dependence[14] of $e^{-5\ k_\perp}$ we would expect an effect of the order of a factor of 2 when comparing data from two energies at fixed x' near x' = 1. For fixed x', the larger the beam energy the larger is $k_\perp$. As a result one would expect that the cross section for pion production at fixed x' by higher energy beams would be less than the cross section for pions produced by lower energy beams. The deuteron and alpha induced spectra in Figs. 18 and 19 show this is the case.

While the π^- data in Fig. 17 show approximate scaling, the π^+ data does not. This might be expected since at higher energies the reaction $p + p \to \pi^- + X$ scales much earlier than $p + p \to \pi^+ + X$. This agrees with the general observation that reactions requiring "exotic" exchanges in the t-channel scale before those which require non-exotic exchanges.

Comparing the proton data in Fig. 17 with the deuteron and alpha data in Figs. 18 and 19, it is evident that the distributions fall much more steeply with x' as the mass of the projectile

increases. This indicates that a loosely bound object like a deuteron tends not to transfer a large fraction of its kinetic energy to an individual pion. If one wanted to regard a nucleus as elementary in the sense of a proton, then one might expect protons and light nuclei to behave similarly at equal <u>total</u> kinetic energy. We show in Table 14 the results for the ratio

$$R_{d,\alpha}(X') = \frac{\frac{d^2\sigma}{d\Omega dk}(d,\alpha + C \to \pi^- + X)}{\frac{d^2\sigma}{d\Omega dk}(p + C \to \pi^- + X)}$$

at equal total kinetic energies. We see in fact that R(x') decreases rapidly over the range $.25 \leq x' \leq .7$. This disagrees with the results of a recent Russian experiment in which Baldin et al.[18] report R(x') is a constant over the range $0.7 \leq x' \leq 1.0$ and that this result cannot be explained in terms of the Fermi motion of the projectile. It must be remembered that their experiment was performed at 0° and at an energy of 4 GeV/nucleon, though it is unlikely that these differences alone could account for the disagreement.

To understand the effects of Fermi momentum we compare the data of this experiment with the results of a calculation based on the model discussed in Section II-E. Using eq. (6) we have inserted in the right hand side our measured proton induced pion production cross sections. The function $W_d(\vec{p},\vec{p}_o)$ was derived from a standard Hulthen wave function $\phi(\vec{q}) = C_1\left[1/(q^2+\alpha^2) - 1/(q^2+\beta^2)\right]$ with $\alpha = 45.7$ MeV, $\beta = 5.2\alpha$. C_1 is chosen to give the right normalization.

Wave functions for alpha particles are much harder to come by. The usual measured quantity is the form factor for electron scattering off He. This is in turn related to the charge distribution of the alpha particle by way of a Fourier transform. In order to find a function $W_\alpha(\vec{p},\vec{p}_o)$ we made the following assumptions: that the configuration space alpha particle wave function is real, and that the charge density distribution describes the matter density distribution for both protons and neutrons in the alpha. We then took the measured form factors[19] and numerically performed the necessary Fourier transforms to calculate $\phi(\vec{q})$.

The data for the reaction $d + C \rightarrow \pi^- + X$ at 1.05 and 2.1 GeV/nucleon are shown in Fig. 20, along with the results of the model calculation (solid curve). Similarly Fig. 21 shows the results for an alpha particle beam. The shielding factor was set equal to one, leaving no adjustable parameters in the calculation. The agreement in the case of the deuterons is striking. For the alphas the agreement is good at the lower momentum, but there is only qualitative agreement at the higher momenta. When interpreting these results it must be kept in mind that the predictions of the model for high momentum pions are very dependent on the high Fermi momentum components in the function W which are not very well known. Considering strong assumptions involved in the above method for determining W_α, it would be surprising if the model and the data were in very good agreement.

The very good agreement between the model and the data in the case of deuterons where the wave function is well-known suggests that at least in this case a constituent type model can explain the main features of pion production without invoking a description in terms of collective effects. For alphas, given the accuracy of the function W, one can say that the data is consistent with there being no large collective effects involved.

These conclusions also disagree with some recent results from Dubna,[20] where Baldin, et al. measured pion production at 180° using 8.4 GeV/c deuterons incident on various targets. They claim to see much more pion production than could be explained by Fermi momentum alone. Their results are, of course, in a very different kinematic region, though it would be quite strange to have large collective effects show up in one region and not the other. It would be very useful to have additional independent data to check the results from these two experiments.

Another thing that would be very useful would be extensive data on pion production by ^{12}C and heavier beams. Our data, shown in Table 13, does not extend to high enough momenta to search for collective effects. One might expect such effects to be larger for heavier beams while Fermi momenta would be relatively unchanged. This would check the Dubna experiment[20] where, by looking at backward pions, they have essentially reversed the roles of beam and target.

We next examine the target dependence of these reactions. Fig. 22 shows the cross section for π^- production by 2.1 GeV/nucleon

alphas on four targets: Be, C, Cu, and Pb. The shapes of the cross sections as a function of momentum is essentially independent of the target at momenta $\geq$ 1 GeV/c, suggesting that the particles are "beam fragments."

The magnitude of the cross sections depends, of course, on the atomic mass A of the target. Fig. 23 shows the cross section for producing negative pions of a particular momentum as a function of A of the target. For momenta $\geq$ 1 GeV/c the data has an $A^{1/3}$ dependence, suggesting a sort of peripheral production mechanism. At lower momenta the A dependence increases, implying that slower pions are produced in more central collisions.

Another interesting question bearing on the pion spectra is that of charge symmetry. Since deuterons, alphas, and ^{12}C are all isospin 0 nuclei, in collisions of deuteron and alpha beams with carbon, equal numbers of π^+ and π^- would be produced if charge independence is valid. Table 15 lists the results of the ratio of π^+/π^- production for 2.1 GeV/nucleon beams. There is no evidence of violation of charge independence to the level of precision of the data, ±10%.

One final remark should be made on the subject of pions. When heavy ion beams first became available at the Bevatron, it was hoped that it would be possible to produce beams of very energetic pions; after all, the kinetic energy of ^{12}C at 2 GeV/nucleon is 24 GeV. If there are no collective effects, only the Fermi momentum is available for making super-energetic pions, and that alone is not enough. Even if there are significant collective

effects with heavier beams, something for which we see no evidence using deuterons and alphas, the available flux is so low that the prospect of getting usable beams by such a means seems very remote.

C. Baryonic Fragment Production

The heavy fragment production cross sections are summarized in Tables 16-47. Unmeasured cross sections are listed as zero in the tables. The momentum listed in these tables is the momentum setting of the spectrometer and does not include energy loss in the target. Table 48 shows the correspondence between the momentum setting of the channel and the momentum with which the particle is produced. The difference is rather small and the format of the data tables would make it very cumbersome to include the effect there.

The Lorentz invariant cross section for 1.05 GeV/nucleon alphas fragmenting into p, d, ^{3}He, ^{3}H, and ^{4}He is plotted in Fig. 24 as a function of lab momentum for a carbon target. The structure of the alpha particle is clearly indicated. Not only does the alpha fragment into protons, but there is significant production of deuterons, tritons, and ^{3}He. Since the data were taken at fixed angle in the lab (2.5°), care must be taken when interpreting the height of the peaks, where the transverse momentum is about 75 MeV/c per nucleon, comparable to the Fermi momentum of the nucleons in the alpha. Also the factor E/k^2 lowers the deuteron peak by a factor of 2 relative to the proton

peak, while the ^{3}He and ^{3}H peaks are down by a factor of 3. Nevertheless, the invariant cross sections for fragmentation into ^{3}He, deuterons, and protons are within about an order of magnitude of each other. They are approximately in the ratio 1:3.5:11.4.

If instead of plotting the data as a function of laboratory momentum one plots it as a function of rapidity y, Fig. 25 results. Several features stand out:

1) The peaks of the distributions all occur at the same rapidity--the rapidity of the beam particle.
2) The widths of the distributions decrease as the mass of the fragment increases. One expects this since in Fig. 24 all the distributions have comparable widths in momentum. Since increasing mass means decreasing y for fixed momentum, the distributions for heavier fragments should be narrower in y.
3) The diffractive fragmentation peak is well separated from the target fragmentation region and stands out clearly from the central region.

Similar features are evident in the fragmentation of deuterons. Fig. 26 shows the Lorentz invariant cross section for the fragmentation of 1.05 GeV/nucleon deuterons on carbon. Here the production of ^{3}H and ^{3}He decreases rapidly with momentum, as one would expect if these particles were being punched out of the target. Pick-up processes are infrequent since in order for them to occur the momentum of the nucleon in the target

"picked up" would have to be comparable to the momentum per nucleon of the beam particle, in this case about 1.75 GeV/c. The probability for such a large Fermi momentum is very low. In the figure the proton peak is evident and is narrower than in the case of an alpha beam, due to the fact that a deuteron is more loosely bound than an alpha. The deuteron distribution is similar to spectra from other inelastic scattering processes. There is a sharp elastic peak, a quasi-elastic shoulder, and a "deep inelastic" region.

It is interesting to try to apply the model we used for pion production to the proton production spectra. In terms of the diagram shown in Fig. 3, this means substituting a proton for the outgoing pion. In this case equation 5 becomes, neglecting the possibility of charge exchange,

$$\sigma_H^p(\vec{p}_0, \vec{k}) = Z\int \sigma_p^p(\vec{p}, \vec{k})\, W(\vec{p}_0, \vec{p})\, d^3\vec{p} \qquad (7)$$

In order to calculate the entire spectrum we would need to use the cross section for the process of p + C → p + anything. Instead we try only to calculate the cross section in the neighborhood of the proton peaks and use the elastic scattering cross section for σ_{pC}^p. In other words, we visualize the peaks to be the result of elastic scattering, smeared out by Fermi momentum. We use the same functions for W as in the pion case. The elastic p + C scattering

cross section is $d\sigma/dt \approx 7.5e^{65t}$(barns/(GeV/c)^2). Since this cross section falls very rapidly with momentum transfer, we can make the approximation that $k_{\parallel} = p_{\parallel}$ and that the energy of the incoming and outgoing protons are the same. Then t reduces to $t = -(\vec{p}_{\perp} - \vec{k}_{\perp})^2$. Then after inserting a δ-function in $(p_{\parallel} - k_{\parallel})$ under the integral in eq. 7 it reduces to

$$\sigma = Z \int p_{\perp} d^2\vec{p}_{\perp} W(k, p_{\perp}, p_0)\ 7.5e^{-(p_{\perp}-k_{\perp})^2 65}$$

$$= Z \int p_{\perp} dp_{\perp} W(k, p_{\perp}, p_0)\ e^{-65(p_{\perp}^2+k_{\perp}^2)} \int_0^{2\pi} d\phi e^{-130 p_{\perp} k_{\perp} \cos\phi}$$

The integral over ϕ is the modified Bessel function $\frac{1}{\pi} I_0(130 p_{\perp} k_{\perp})$. The remaining integral over p must be done numerically. The results of the calculation for deuteron and alpha beams are shown in Figs. 27 and 28. As in the case of pion production, the agreement between the calculation and the data is much better for the deuterons than the alphas, suggesting that our choice of alpha particle wave function is not very good. The model of course may be wrong, but its success in dealing with deuterons implies that it should be applicable to heavier projectiles. If a function W could be found which correctly predicted both the proton distribution and the pion production spectra, it would be a strong candidate for the correct internal momentum distribution of the alpha. If carried out in a systematic way with measurements not limited to lab angles of 2.5°, experiments of this type could prove to be very useful for determining wave functions of many nuclei.

We next turn to the energy dependence of these spectra and questions of limiting fragmentation and scaling. Since in this experiment we look at particles in the lab with momenta $\gtrsim$.75 GeV/c, the applicable statement of limiting fragmentation is that the cross section for production of slow particles in the rest frame of the beam is independent of the energy. Therefore we need to compare the cross sections for processes such as d + A → p + x where A is some nucleus in the region of the peaks of the proton distributions at 1.05 and 2.1 GeV/nucleon. Unfortunately, since the lab angle is fixed at 2.5°, the transverse momenta at the peaks are different for the two energies, making a direct comparison of the invariant cross sections impossible. However, if we adopt the viewpoint of the model discussed above that in the regions of the peaks we are seeing basically elastic scattering smeared by Fermi momentum, then we can correct for the $k_\perp$ variation. We assume again that for protons elastically scattering off carbon that $d\sigma/dt = 7.5e^{65t}$. The proton peaks occur at 1.75 GeV/c and 2.875 GeV/c for 1.05 and 2.1 GeV/nucleon deuterons or alphas incident. Then $t = -2k^2(1-\cos\theta)$ where k is the proton momentum and $\theta = 2.5°$ (43.6 milliradians). Since θ is small, $t \simeq -k^2\theta^2$, and we get that at k = 1.75 GeV/c, $t_1 = -62.0 \times 10^{-4}$ and at k = 2.875, $t_2 = -167 \times 10^{-4}$. Therefore the ratio of the invariant cross sections $\sigma_{1.05\ \text{GeV/nucleon}}/\sigma_{2.1\ \text{GeV/nucleon}} = e^{65(t_1-t_2)} \simeq 2.0$

We can compare two reactions: $d + C \rightarrow p + X$ and $\alpha + C \rightarrow p + X$. Table 49 shows this comparison for various targets at $y = y_{beam}$. The average for all targets is 2.67 ± 0.48. The result is hardly undeniable proof of the validity of limiting fragmentation but it is certainly consistent with the idea, considering the size of the error.

In the regions of the rapidity plots away from the peaks, the fragmentation cross sections are much flatter but still decrease as k (and hence $k_\perp$) increases until they approach the region of the peaks. We could again try to apply our model using the inclusive cross sections for $p + C \rightarrow p + X$, but this calculation is prohibitively difficult because of the unknown angle dependence and our limited data on energy dependence of these cross sections. One would expect these regions to be flat, based on the models discussed in section II. The experimental results are consistent with this, though the inability to separate out the $k_\perp$ dependence makes any strong statement impossible. Performing the experiment at a range of angles would be very illuminating here.

As for the energy dependence of these plateau regions, it is not clear that one should expect them to be energy independent on the basis of scaling. In the high energy "elementary particle" domain where one looks at reactions like $p + p \rightarrow \pi + X$ scaling predicts energy independence in the central region. Once the beam and target fragmentations reach limiting behavior, going

to higher energies necessarily adds pions to the central region. Since the multiplicity seems to grow logarithmically with the energy, and the length of the rapidity plot also grows logarithmically, the number of pions per unit rapidity remains constant as the energy goes up. In these heavy ion reactions, on the other hand, as the energy increases the rapidity gap between beam and target fragmentation regions grows, but one cannot create more nucleons in the same way one creates pions at the ISR. So with a constant number of nucleons to fill an ever-widening rapidity gap, one might expect the cross sections in the central plateau region to decrease with energy, and the effect should be greater for reactions like $\alpha + C \rightarrow {}^{3}He + X$ than for $\alpha + C \rightarrow p + X$. Figs. 28 and 29 bear out this expectation. We are again faced with non-constant $k_{\perp}$ which produces the same effects, so no certain conclusions can be drawn about scaling.

We turn next to the question of target dependence. For Be, C, and CH_2 targets the shapes of the spectra are virtually identical, as would be expected since these targets are very similar. The only very different target we can compare to is Pb.

In the regions near the peaks, the spectra have the same shape for all targets. If one assumes a power law behavior where the cross section is proportional to A^N where A is the atomic mass of the target and N is some power, then near the peaks, $N \approx 1/3$ for all fragments as for the case of pion production. This differs from the results of Heckman et al.[21] who found

that with heavier beams, such as ^{16}O that the target dependence was approximately $A^{0.26}$.

At lower momenta the power N increases, especially for the heavier fragments. We have plotted in Fig. 30 the power N as a function of momentum for the three reactions α + Nucleus → {p, d, ^3He} + anything. One can see that in the case of ^3H production, the power N is about 2 at 750 MeV/c, greater than the geometric $A^{2/3}$.

Finally, we examine the results on fragmentation of 1.05 GeV/nucleon ^{12}C on carbon and copper targets. Tables 50 and 51 list the cross sections for production of p, d, ^3H, ^3He, and ^4He while Tables 52 and 53 give the results for Li, Be, B, and C fragments.

Fig. 31 shows a plot of the invariant cross sections for carbon on carbon vs. laboratory momentum. It is very reminiscent of the results on fragmentation of alphas. In the peak region the proton spectra from α and ^{12}C beams are essentially identical, as are the deuteron spectra, implying that the momentum distributions of nucleons are very similar in the two types of beam particles. On the other hand, the ^3H-^3He peak is significantly wider in the case of a ^{12}C beam than in the case of an alpha beam. This is reasonable since in an alpha particle a triton or ^3He can only recoil against a nucleon, limiting its momentum. Inside a ^{12}C nucleus, a tri-nucleon can recoil against 9 nucleons allowing a wider spread while still conserving momentum. Also, in the case of

^{12}C there is much more ^{3}H and ^{3}He production in the central region compared to the peak than in the case of alphas, a feature that would be interesting to study as a function of energy and angle.

The production of the heavier fragments is shown in Fig. 32, where again the invariant cross section is plotted against the lab momentum. Here the 2.5° production angle is very significant. In the area of the ^{6}Li peak, near 10 GeV/c the transverse momentum is about 440 MeV/c while for ^{7}Be and ^{10}B it is about 525 MeV/c and 760 MeV/c. So to produce these fragments at 2.5° requires either very large Fermi momentum or large momentum transfer; the first is very unlikely while the second would tend to break up such fragile nuclei. It would be interesting to study these fragments as a function of energy and angle and thereby to directly measure transverse momentum effects.

VI. Summary and Conclusions

A vast amount of data was collected during this experiment. In this section we try to briefly summarize the results and their implications.

First, in pion production by deuterons and alphas, we find that effects due to "collective" behavior of the projectile nucleons are very small--beyond the level of precision of this experiment. Pion production by deuterons can be well understood in terms of an independent particle model with Fermi momentum. In the case of an alpha particle beam, the lack of a good wave

function for the alpha makes it impossible to rule out collective effects, but if they are involved, they are too small for this experiment to detect.

We have also found that for π^- production by protons, deuterons, or alphas, scaling is approximately valid down to energies of 1 GeV/nucleon--not the case for π^+ production by protons. Charge symmetry has been verified: the ratio of production cross sections of π^+ and π^- is 1 for deuteron and alpha beams on a carbon target. The target dependence for fast pion production is approximately $A^{1/3}$, increasing toward $A^{2/3}$ for pion momenta near 500 MeV/c.

As for production of particles with baryon number ≥ 1, the data is consistent with limiting fragmentation of the projectile. This conclusion, along with all others here, is model dependent because the experiment was performed at fixed lab angle rather than fixed transverse momentum.

Regarding the spectral shapes of reactions such as α + target $\rightarrow$ d + X, we find in addition to a diffractive fragmentation peak a central, rather flat region. The data is consistent with the prediction of a flat region at fixed $k_\perp$, though our inability to separate out the $k_\perp$ dependence makes a stronger conclusion impossible.

The independent particle model used to discuss pion production does a fair job of describing the fragmentation of deuterons into protons, though it does badly in describing alphas fragmenting into protons. This may again be due to a poor choice of the

alpha wave function. It seems that this model, together with comprehensive measurements of both pion production and beam fragmentation cross sections could result in a powerful new technique for determining nuclear wave functions. Measurements of fragmentation of light nuclear projectiles into deuterons, tritons, etc. should lead to new information about correlations inside nuclei.

Certainly the questions raised in the introduction to this thesis have not been completely answered. Nevertheless, we hope that it has been a useful introductory survey of this kind of physics which has a great potential in helping us understand particles and nuclei.

Acknowledgements

No experiment of this sort, much less an entire graduate career, is the work of one person. A few lines of acknowledgements can hardly do justice to the many whose efforts contributed to this experiment and who made my stay at Berkeley both fun and exciting.

Thanks go to my graduate advisor, Professor Gilbert Shapiro and to our research Group Leader, Professor Owen Chamberlain, against whose lunchtime expertise with pen and napkin no problem dared to remain unsolved.

Special thanks have to go to Professor Herbert Steiner who dragged me kicking and screaming through this experiment. He gave limitlessly of his time, energy, and enthusiasm to both the experiment and this thesis. His whole-hearted effort in everything he does is an inspiration--I'll never know how he does it all.

Much of the credit for the design of the experiment and for getting it moving goes to Dr. Lee Schroeder who shouldered a large amount of the responsibility and the work. Without his help, that of Dr. Albrecht Wagner, and that of Dr. John Staples, our beam expert, who for some unknown reason actually preferred 4 AM to noon shifts, the experiment would have been almost impossible.

My fellow graduate students deserve a chapter to themselves; unfortunately a paragraph will have to suffice. First on the list has to be James Wiss without whose efforts the model calculations would have never been satisfactorily done. I appreciate it, Jim! Next comes John Jaros whom I must thank both for taking lots of miserable shifts and for the discussions, during which we convinced each other that what we were doing was of some value after all. In addition, Leonard Anderson and Geoffrey O'Keefe both helped overcome our continual short-handedness when it came to data taking. Finally, there is Gary Godfrey. What can you say about Gary? He has yet to make me understand why the universe is a quantum singlet. Though if anyone ever will, Gary will someday understand it all and explain it to the rest of us--again.

I also want to express my appreciation to our able secretary, Jeanne Miller, and to our superb mechanical technician, Ray Fuzesy. If it weren't for Ray, I would have never got its cylinder head back into my Mustang nor learned many of the intricacies of machines. He is an artist at his craft as well as a gypsy and a connoisseur of living. Jeanne Miller typed these endless pages and made sure my drawings turned into figures when I of necessity had to be elsewhere.

The Bevatron crew did their usual superb job of running the accelerator. Needless to say, no beams means no experiment.

My sincere thanks to you all.

In a class by herself stands my wife, Ellice, who contributed endless love and encouragement. In exchange she had to put up with a sometimes cantankerous character. She shared in all the tough times. She must share in the credit for the finished product; it's half yours, Cutie!

References

1. J. Benecke, T. Chou, C. Yang, E. Yen, Phys. Rev. 188, 2159 (1969).
2. R. P. Feynman, Phys. Rev. Lett. 23, 1415 (1969).
3. A. H. Mueller, Phys. Rev. D2, 2963 (1970).
4. G. Belletini, P. L. Braccini, C. Bradaschia, R. Castaldi, T. Del Prete, L. Foa, P. Firomini, P. Laurelli, A. Menzione, M. Valdata, G. Finocchiara, P. Grannis, D. Green, R. Mustard, R. Thun, Phys. Lett. 45B, 69 (1973).
5. D. Smith, UCRL-20632, Berkeley (1971), Ph.D. Thesis (unpublished).
6. W. Frazer, L. Ingber, C. H. Mehta, C. H. Poon, D. Silverman, K. Stowe, P. D. Ping, and H. J. Yesian, Rev. Mod. Phys. 44, 284 (1972).
7. H. Boggild and T. Ferbel, Ann. Rev. Nucl. Sci., to be published (preprint COO-3065-76).
8. H. D. Abarbanel, Phys. Rev. D3, 2227 (1971).
9. J. D. Bowman, W. J. Swiatecki, and C. F. Tsang, "Abrasion and Ablation of Heavy Ions," LBL Internal Report, July 1973 (unpublished).
10. A. Mullensiefen, Nucl. Phys. B28, 368 (1971).
11. W. Czyz and L. C. Maximon, Phys. Lett. 27B, 354 (1968), 52, 59 (1969).
12. G. F. Chew, "Large and Small Baryon Numbers in High Energy Collision Theory," LBL Internal Report, May 1973 (unpublished).
13. D. C. Carey, J. R. Johnson, R. Kammerud, M. Peters, D. J. Ritche, A. Roberts, J. R. Sauer, R. Shafer, O. Therist, J. K. Walker, and F. E. Taylor, Phys. Rev. Lett. 33, 330 (1974).
14. H. Steiner, J. Jaros, private communication.

15. D. Dekkers, J. A. Gierb, R. Mermod, G. Weber, T. R. Willits, K. Winter, B. Jordan, M. Vivorgent, N. M. King, E. J. N. Wilson, Phys. Rev. 137, 4B, B962 (1965).

16. G. J. Marmer, D. Lundquist, Phys. Rev. D3, 1089 (1971).

17. G. J. Marmer, K. Reibel, D. M. Schwartz, A. Stevens, R. Winston, D. Wolfe, P. R. Phillips, E. C. Swallow, and T. Ramanowski, Phys. Rev. 179, 1294 (1969).

18. A. M. Baldin, S. B. Gerasimov, H. Guiordenescu, V. N. Zubarev, L. K. Ivanova, A. D. Kirillov, V. A. Kuznetsov, N. S. Moroz, V. B. Radomanov, V. N. Ramzhin, V. S. Stavinsky, M. I. Yatsuta, Yad. Fis. 18, 79 (1973).

19. R. F. Frosch, J. S. McCarthy, R. E. Rand, and M. R. Yearian, Phys. Rev. 160, 874 (1967).

20. A. M. Baldin, N. Ghiordanescu, L. K. Ivanova, N. S. Moroz, A. A. Povtorejko, V. B. Radomanov, V. S. Stavinsky, V. N. Zubarev, Preprint Joint Institute for Nuclear Research E1-8054, "An Experimental Investigation of Cumulative Meson Production," Dubna, 1974.

21. H. H. Heckman, D. E. Greiner, P. J. Lindstrom, and F. S. Bieser, Phys. Rev. Lett. 28, 926 (1972).

22. E. Segrè, ed., Experimental Nuclear Physics (John Willy and Sons, Inc., New York, 1953), Vol. 1, p. 233.

23. W. P. Trower, "High Energy Particle Data," Vol. II, UCRL-2426, 1966.

Appendix

Ion Chamber Calibration

In order to determine the flux through the ion chamber and thereby the flux on the target, it is necessary to relate the flux of particles to the charge collected by the ion chamber. The characteristics of the chamber are as follows. The gas in the chamber was argon, atomic weight A = 40. The gas pressure was 800 mm Hg at a temperature of 22°C, giving density $\rho = 1.737 \times 10^{-3} g/cm^3$. The distance x traversed by a particle passing through the chamber was 3.175 cm.

If we define $\xi = \rho x$, then $\xi = 5.515 \times 10^{-3} g/cm^2$. Furthermore, if $dE/d\xi$ is the rate of energy loss of the incident particle, then the total energy loss per particle is $\Delta E = dE/d\xi \cdot \xi$. So the number of ion pairs produced in the argon by each beam particle is $N_I = \Delta E/\epsilon = dE/d\xi \cdot \xi \cdot 1/\epsilon$ where ϵ is the energy required to produce an ion pair.

The electrometer is calibrated to read 10^8 particles when the charge collected is 6.3×10^{-9} coulombs. So if one beam particle traverses the chamber and creates a charge Q, the electrometer will read

$$\frac{10^8}{6.3 \times 10^{-9}} \times Q = 2.54 \times 10^{-3} \frac{dE}{d\xi} \xi \frac{1}{\epsilon}$$

Using $\epsilon = 26.4$ eV[22] as the energy to produce an ion pair in Argon, we find if one particle passes through the ion chamber the electrometer

will read .531 $dE/d\xi$ where $dE/d\xi$ is in units of MeV-cm^2/g.

In the text we defined the function $z^2F_2'(E)$ = (ion chamber reading)/(number of particles traversing ion chamber), which is the same function as that calculated above, $Z^2F_2'(E) = .531\ dE/d\xi$. This function is tabulated in Table A-1 for various beam particles and energies using standard values for $dE/d\xi$.[23]

$Z^2F_2'(E)$ for

Kinetic Energy per Nucleon / Beam Particle	p	d	α	^{12}C
1.05	.876	.828	3.37	30.3
1.73	.823			
2.1	.818	.791	3.21	
2.66	.818			
3.5	.823			
4.2	.834			
4.8	.839			

The factor F3 defined in section V-B was determined by placing two thin (1/8") scintillation counters in the beam downstream of the ion chamber. The scintillators, equipped with RCA8575 photomultiplier tubes, showed no pulse sagging even at rates of 1.7×10^6/second. Using a 1.05 GeV/nucleon ^{12}C beam we counted scintillation counter coincidences and compared them with the ion chamber reading. From Table A1 one expects a ratio R = ion chamber/scintillator coincidences = 30.3, independent of intensity. There was however a slight intensity dependence as well as a small effect depending on which electrometer scale was used. A change in intensity by a factor of 10 caused a 6% change in R while the scale effect was about 2%. A straight line least-squares fit was made to the intensity dependent data and extrapolated to zero intensity resulting in a ratio $R = 26.4 \pm 0.5$; so $F3 = 26.4/30.3 = 0.87$.

MOMENTUM (GeV/c)	LEPTON	TARGETS			
		Be 1/4"	C 1/4"	Cu 1/4"	Pb 1/4"
		1.73 GeV Proton Beam			
0.5	e^-	5.16±0.23	5.73±0.23	24.7±0.5	29.9±0.6
0.9	e^-	2.64±0.16	2.97±0.17	5.44±0.23	6.90±0.26
1.0	e^-	1.49±0.12	1.60±0.13	3.90±0.20	4.16±0.20
1.25	e^-	0.69±0.08	0.68±0.08	1.21±0.11	1.44±0.12
0.9	μ^-	5.33±0.32	4.91±0.33	5.56±0.40	4.39±0.43
1.0	μ^-	5.24±0.27	5.36±0.29	4.66±0.31	4.85±0.36
1.25	μ^-	4.71±0.24	4.99±0.44	4.85±0.27	4.50±0.26
		3.5 GeV Proton Beam			
0.5	e^-	10.8±0.3	12.0±0.4	44.2±0.7	54.1±0.7
0.75	e^-	5.39±0.23	6.27±0.25	24.7±0.5	31.4±0.6
0.9	e^-	4.43±0.21	5.15±0.23	18.6±0.4	23.3±0.5
1.0	e^-	3.39±0.18	3.80±0.19	14.0±0.4	19 6±0.4
1.25	e^-	1.50±0.12	1.94±0.14	7.31±0.27	9.50±0.31
0.9	μ^-	8.70±0.42	8.60±0.43	6.65±0.66	7.07±0.73
1.0	μ^-	8.55±0.38	8.25±0.39	7.08±0.59	5.23±0.66
1.25	μ^-	7.00±0.31	7.41±0.33	7.21±0.47	7.44±0.51

Table 1. Percent Lepton Contamination in π^- Signal

MOMENTUM (GeV/c)	LEPTON	TARGETS			
		Be 1/4"	C 1/4"	Cu 1/4"	Pb 1/4"
		4.2 GeV Proton Beam			
0.5	e^-	11.3±0.3	12.8±0.4	41.5±0.6	50.7±0.7
0.75	e^-	6.81±0.26	7.60±0.27	27.2±0.5	35.0±0.6
0.9	e^-	5.23±0.23	5.89±0.24	21.4±0.5	28.5±0.5
1.0	e^-	3.73±0.19	4.80±0.22	17.5±0.4	22.8±0.5
1.25	e^-	2.09±0.14	2.09±0.14	10.3±0.3	13.9±0.4
0.9	μ^-	8.83±0.43	8.67±0.45	6.24±0.70	--
1.0	μ^-	8.14±0.39	6.45±0.40	6.82±0.60	5.91±0.72
1.25	μ^-	6.48±0.32	6.54±0.32	5.39±0.51	5.83±0.57

MOMENTUM (GeV/c)	LEPTON	TARGETS			
		Be 1/4"	C 1/4"	CH_2(0.52")	Pb 1/4"
		2.1 GeV/nucleon Alpha Beam			
0.75	e^-	1.67±0.13	2.12±0.14	2.03±0.14	10.3±0.32
1.0	e^-	1.49±0.12	1.71±0.13	1.82±0.13	4.43±0.21
1.25	e^-	0.62±0.08	0.71±0.08	0.53±0.07	2.02±0.14
1.5	e^-	0.60±0.35	0.90±0.15	0.60±0.35	1.60±0.29
1.75	e^-	0.42±0.10	0.60±0.35	0.60±0.35	1.05±0.20
1.0	μ^-	6.37±0.30	6.67±0.32	6.48±0.32	5.73±0.38
1.25	μ^-	5.52±0.26	5.48±0.26	5.61±0.26	5.58±0.31
1.5	μ^-	3.50±0.57	3.40±0.35	4.30±0.60	4.20±0.61
1.75	μ^-	3.63±0.33	4.35±0.60	4.15±0.60	4.05±0.54

Table 1. Continued.

MOMENTUM (GeV/c)	LEPTON	TARGETS			
		Be 2"	C 1"	Cu 3/8"	Pb 1/4"
		1.05 GeV/Nucleon Deuteron Beam			
1.0	$e^- + \mu^-$	--	5.58±0.23	--	--
1.25	$e^- + \mu^-$	4.13±0.56	3.67±0.42	3.94±0.82	5.95±1.24
		2.1 GeV/Nucleon Deuteron Beam			
1.0	$e^- + \mu^-$	8.14±0.06	8.03±0.06	9.14±0.07	9.35±0.07
1.5	$e^- + \mu^-$	4.55±0.15	4.41±0.15	5.14±0.16	5.23±0.16
2.0	$e^- + \mu^-$	3.52±0.13	3.49±0.13	3.62±0.19	3.39±0.18
2.5	$e^- + \mu^-$	1.76±0.09	--	--	--
		2.1 GeV/Nucleon Alpha Beam			
1.0	$e^- + \mu^-$	8.48±0.29	8.16±0.28	10.2±0.32	11.3±0.34
1.5	$e^- + \mu^-$	5.13±0.23	5.17±0.23	5.35±0.23	5.21±0.23
2.0	$e^- + \mu^-$	3.79±0.19	3.95±0.20	4.08±0.20	4.74±0.22

Table 1. Continued.

Pion Momentum (GeV/c)	Target	π^- Production $\frac{d\sigma}{d\Omega dk}$(mb/sr/GeV/c)	π^+ Production $\frac{d\sigma}{d\Omega dk}$(mb/sr/GeV/c)
0.5	Be	10.7 ± 0.2	50.4 ± 0.9
0.5	C	11.1 ± 0.5	63.3 ± 1.2
0.5	Cu	24.0 ± 0.6	110. ± 2.
0.5	Pb	45.2 ± 1.2	140. ± 2.
0.6	Be	8.34 ± 0.15	--
0.6	C	8.06 ± 0.17	--
0.6	Cu	16.3 ± 0.4	--
0.6	Pb	30.4 ± 0.8	--
0.65	Be	--	40.2 ± 1.5
0.65	C	--	51.4 ± 1.1
0.65	Cu	--	82.3 ± 1.8
0.65	Pb	--	102. ± 3.
0.7	Be	4.18 ± 0.19	--
0.7	C	4.10 ± 0.24	--
0.7	Cu	7.36 ± 0.24	--
0.7	Pb	14.0 ± 0.4	--
0.75	Be	2.53 ± 0.12	14.9 ± 0.3
0.75	C	2.07 ± 0.12	18.7 ± 0.4
0.75	Cu	4.66 ± 0.24	30.6 ± 1.0
0.75	Pb	6.98 ± 0.42	41.2 ± 1.2
0.9	Be	$(2.92 \pm 0.31)\times10^{-1}$	1.69 ± 0.04
0.9	C	$(3.06 \pm 0.39)\times10^{-1}$	2.04 ± 0.06
0.9	Cu	$(6.40 \pm 0.27)\times10^{-1}$	3.52 ± 0.13
0.9	Pb	$(8.80 \pm 0.45)\times10^{-1}$	4.03 ± 0.19

Table 2. Pion Production cross-sections
Beam = 1.05 GeV Protons

Errors quoted are statistical only.

Pion Momentum (GeV/c)	Target	π^- Production $\frac{d\sigma}{d\Omega dk}$(mb/sr/GeV/c)	π^+ Production $\frac{d\sigma}{d\Omega dk}$(mb/sr/GeV/c)
.95	Be	$(2.88 \pm 0.50)\times10^{-2}$	--
.95	C	$(2.81 \pm 0.61)\times10^{-2}$	--
.95	Cu	$(5.42 \pm 1.06)\times10^{-2}$	--
.95	Pb	$(8.34 \pm 1.86)\times10^{-2}$	--
1.0	Be	$(4.84 \pm 1.96)\times10^{-3}$	$(1.29 \pm 0.64)\times10^{-1}$
1.0	C	$(3.70 \pm 2.13)\times10^{-3}$	$(0.987 \pm 0.700)\times10^{-1}$
1.0	Cu	$(7.71 \pm 3.14)\times10^{-3}$	$(2.93 \pm 0.67)\times10^{-1}$
1.0	Pb	$(19.3 \pm 8.6)\times10^{-3}$	$(3.70 \pm 1.07)\times10^{-1}$

Table 2. Continued.

Pion Momentum (GeV/c)	Target	π^- Production $\frac{d\sigma}{d\Omega dk}$(mb/sr/GeV/c)	π^+ Production $\frac{d\sigma}{d\Omega dk}$(mb/sr/GeV/c)
0.5	Be	21.1 ± 0.3	44.3 ± 0.8
0.5	C	24.9 ± 0.4	57.1 ± 1.1
0.5	Cu	60.4 ± 1.0	112. ± 2.
0.5	Pb	112. ± 2.	161. ± 4.
0.75	Be	17.0 ± 0.2	66.3 ± 0.9
0.75	C	18.6 ± 0.3	85.6 ± 0.8
0.75	Cu	39.1 ± 0.6	149. ± 2.
0.75	Pb	69.8 ± 1.2	209. ± 4.
1.0	Be	8.02 ± 0.12	39.7 ± 0.5
1.0	C	8.60 ± 0.14	51.7 ± 0.4
1.0	Cu	17.1 ± 0.4	81.9 ± 1.0
1.0	Pb	29.9 ± 0.6	112. ± 2.
1.25	Be	3.23 ± 0.05	9.97 ± 0.18
1.25	C	2.96 ± 0.06	11.9 ± 0.2
1.25	Cu	6.48 ± 0.15	19.5 ± 0.4
1.25	Pb	11.9 ± 0.3	28.1 ± 0.9
1.5	Be	$(4.59 \pm 0.15)\times10^{-1}$	1.48 ± 0.05
1.5	C	$(4.19 \pm 0.17)\times10^{-1}$	1.78 ± 0.07
1.5	Cu	$(10.1 \pm 0.4)\times10^{-1}$	2.99 ± 0.17
1.5	Pb	$(18.1 \pm 0.7)\times10^{-1}$	4.16 ± 0.30
1.625	Be	$(4.46 \pm 0.30)\times10^{-2}$	--
1.625	C	$(5.02 \pm 0.25)\times10^{-2}$	--
1.625	Cu	$(7.88 \pm 0.41)\times10^{-2}$	--
1.625	Pb	$(17.7 \pm 1.7)\times10^{-2}$	--

Table 3. Pion Production Cross-Sections
Beam = 1.73 GeV Protons

Errors quoted are statistical only.

Pion Momentum (GeV/c)	Target	π^- Production $\frac{d\sigma}{d\Omega dk}$(mb/sr/GeV/c)	π^+ Production $\frac{d\sigma}{d\Omega dk}$(mb/sr/GeV/c)
1.75	Be	$(4.05 \pm 1.20)\times10^{-3}$	--
1.75	C	$(6.84 \pm 1.97)\times10^{-3}$	--
1.75	Cu	$(21.2 \pm 4.5)\times10^{-3}$	--
1.75	Pb	$(20.2 \pm 6.7)\times10^{-3}$	--

Table 3. Continued.

Pion Momentum (GeV/c)	Target	π^- Production $\frac{d\sigma}{d\Omega dk}$(mb/sr/GeV/c)	π^+ Production $\frac{d\sigma}{d\Omega dk}$(mb/sr/GeV/c)
.5	Be	24.5 ± 0.2	37.7 ± 0.7
.5	C	28.9 ± 0.2	47.8 ± 1.0
.5	Cu	68.2 ± 0.6	78.6 ± 2.0
.5	Pb	122. ± 1.	118. ± 4.
.65	Be	22.9 ± 0.1	--
.65	C	27.0 ± 0.2	--
.65	Cu	58.4 ± 0.5	--
.65	Pb	108. ± 1.	--
.75	Be	22.7 ± 0.1	60.1 ± 0.8
.75	C	26.9 ± 0.2	97.4 ± 1.1
.75	Cu	57.4 ± 0.4	131. ± 2.
.75	Pb	100. ± 1.	194. ± 4.
.9	Be	19.7 ± 0.1	--
.9	C	22.3 ± 0.1	--
.9	Cu	44.6 ± 0.3	--
.9	Pb	77.6 ± 0.6	--
1.0	Be	--	76.9 ± 0.7
1.0	C	--	97.4 ± 0.9
1.0	Cu	--	157. ± 2.
1.0	Pb	--	227. ± 3.
1.25	Be	7.69 ± 0.05	28.7 ± 0.3
1.25	C	8.32 ± 0.06	36.0 ± 0.4
1.25	Cu	15.9 ± 0.2	59.8 ± 0.8
1.25	Pb	27.7 ± 0.3	86.2 ± 1.3

Table 4. Pion Production Cross-Sections
Beam = 2.1 GeV Protons

Errors quoted are statistical only.

Pion Momentum (GeV/c)	Target	π^- Production $\frac{d\sigma}{d\Omega dk}$(mb/sr/GeV/c)	π^+ Production $\frac{d\sigma}{d\Omega dk}$(mb/sr/GeV/c)
1.5	Be	4.08 ± 0.03	11.3 ± 0.1
1.5	C	4.25 ± 0.04	13.4 ± 0.2
1.5	Cu	8.08 ± 0.09	21.4 ± 0.4
1.5	Pb	15.2 ± 0.20	30.2 ± 0.7
1.75	Be	2.08 ± 0.02	4.59 ± 0.10
1.75	C	1.91 ± 0.02	5.31 ± 0.12
1.75	Cu	3.48 ± 0.06	8.28 ± 0.28
1.75	Pb	6.53 ± 0.12	12.6 ± 0.5
1.875	Be	$(4.75 \pm 0.08)\times10^{-1}$	--
1.875	C	$(4.63 \pm 0.10)\times10^{-1}$	--
1.875	Cu	$(7.48 \pm 0.24)\times10^{-1}$	--
1.875	Pb	$(13.1 \pm 0.5)\times10^{-1}$	--
2.0	Be	$(1.09 \pm 0.12)\times10^{-2}$	--
2.0	C	$(1.10 \pm 0.15)\times10^{-2}$	--
2.0	Cu	$(2.90 \pm 0.45)\times10^{-2}$	--
2.0	Pb	$(3.32 \pm 0.76)\times10^{-2}$	--

Table 4. Continued.

Pion Momentum (GeV/c)	Target	π^- Production $\frac{d\sigma}{d\Omega dk}$(mb/sr/GeV/c)
.5	Be	25.9 ± 0.1
.5	C	31.7 ± 0.2
.5	Cu	73.8 ± 0.4
.5	Pb	134. ± 1.
.75	Be	25.1 ± 0.1
.75	C	30.9 ± 0.1
.75	Cu	67.1 ± 0.3
.75	Pb	125. ± 1.
.9	Be	24.0 ± 0.1
.9	C	29.0 ± 0.2
.9	Cu	60.3 ± 0.3
.9	Pb	111. ± 1.
1.0	Be	22.8 ± 0.1
1.0	C	27.2 ± 0.1
1.0	Cu	55.6 ± 0.2
1.0	Pb	99.4 ± 0.5
1.25	Be	15.6 ± 0.1
1.25	C	17.8 ± 0.1
1.25	Cu	33.9 ± 0.2
1.25	Pb	60.4 ± 0.3
1.5	Be	9.11 ± 0.04
1.5	C	10.31 ± 0.04
1.5	Cu	19.5 ± 0.1
1.5	Pb	33.9 ± 0.1

Table 5. Pion Production Cross-sections
Beams = 2.66 GeV Protons

Errors quoted are statistical only.

Pion Momentum (GeV/c)	Target	π^- Production $\frac{d\sigma}{d\Omega dk}$(mb/sr/GeV/c)
1.75	Be	5.98 ± 0.02
1.75	C	6.55 ± 0.03
1.75	Cu	12.2 ± 0.1
1.75	Pb	22.0 ± 0.1
2.0	Be	3.86 ± 0.02
2.0	C	4.01 ± 0.02
2.0	Cu	7.46 ± 0.04
2.0	Pb	14.2 ± 0.1
2.125	Be	2.33 ± 0.01
2.125	C	2.32 ± 0.01
2.125	Cu	4.36 ± 0.03
2.125	Pb	8.72 ± 0.07
2.25	Be	1.23 ± 0.01
2.25	C	1.11 ± 0.01
2.25	Cu	1.96 ± 0.02
2.25	Pb	3.83 ± 0.04
2.375	Be	$(3.02 \pm 0.03)\times10^{-1}$
2.375	C	$(2.93 \pm 0.04)\times10^{-1}$
2.375	Cu	$(4.88 \pm 0.09)\times10^{-1}$
2.375	Pb	$(9.82 \pm 0.20)\times10^{-1}$
2.5	Be	$(1.33 \pm 0.06)\times10^{-2}$
2.5	C	$(1.62 \pm 0.08)\times10^{-2}$
2.5	Cu	$(2.71 \pm 0.20)\times10^{-2}$
2.5	Pb	$(6.03 \pm 0.48)\times10^{-2}$

Table 5. Continued.

Pion Momentum (GeV/c)	Target	π^- Production $\frac{d\sigma}{d\Omega dk}$(mb/sr/GeV/c)
2.625	Cu	$(1.39 \pm 0.98)\times10^{-5}$
2.625	Pb	$(2.45 \pm 1.73)\times10^{-5}$

Table 5. Continued.

Pion Momentum (GeV/c)	Target	π^- Production $\frac{d\sigma}{d\Omega dk}$(mb/sr/GeV/c)
.5	Be	39.0 ± 0.3
.5	C	50.5 ± 0.4
.5	Cu	126. ± 1.
.5	Pb	216. ± 2.
.75	Be	39.7 ± 0.2
.75	C	50.2 ± 0.2
.75	Cu	116. ± 1.
.75	Pb	218. ± 1.
1.0	Be	37.7 ± 0.2
1.0	C	47.7 ± 0.2
1.0	Cu	102. ± 1.
1.0	Pb	186. ± 1.
1.25	Be	31.8 ± 0.1
1.25	C	39.8 ± 0.2
1.25	Cu	81.2 ± 0.4
1.25	Pb	141. ± 1.
1.5	Be	27.2 ± 0.1
1.5	C	32.4 ± 0.1
1.5	Cu	63.4 ± 0.3
1.5	Pb	108. ± 1.
2.0	Be	13.7 ± 0.1
2.0	C	15.9 ± 0.1
2.0	Cu	29.5 ± 0.2
2.0	Pb	50.5 ± 0.4

Table 6. Pion Production Cross-sections
Beam = 3.5 GeV Protons

Errors quoted are statistical only.

Pion Momentum (GeV/c)	Target	π^- Production $\frac{d\sigma}{d\Omega dk}$(mb/sr/GeV/c)
2.5	Be	6.05 ± 0.03
2.5	C	6.48 ± 0.04
2.5	Cu	12.0 ± 0.1
2.5	Pb	21.8 ± 0.2
3.0	Be	1.00 ± 0.01
3.0	C	.986 ± 0.012
3.0	Cu	1.75 ± 0.03
3.0	Pb	3.48 ± 0.07
3.25	Be	$(5.74 \pm 0.22)\times10^{-2}$
3.25	C	$(5.86 \pm 0.28)\times10^{-2}$
3.25	Cu	$(11.8 \pm 0.8)\times10^{-2}$
3.25	Pb	$(21.4 \pm 1.7)\times10^{-2}$

Table 6. Continued.

Pion Momentum (GeV/c)	Target	π^- Production $\frac{d\sigma}{d\Omega dk}$(mb/sr/GeV/c)	π^+ Production $\frac{d\sigma}{d\Omega dk}$(mb/sr/GeV/c)
.5	Be	50.4 ± 0.3	53.3 ± 0.7
.5	C	65.7 ± 0.4	78.6 ± 1.0
.5	Cu	166. ± 1.	164. ± 2.
.5	Pb	314. ± 2.	278. ± 4.
.75	Be	53.0 ± 0.3	78.8 ± 0.8
.75	C	68.3 ± 0.3	105. ± 1.
.75	Cu	158. ± 1.	211. ± 2.
.75	Pb	308. ± 2.	389. ± 5.
1.0	Be	54.2 ± 0.2	99.1 ± 0.8
1.0	C	68.8 ± 0.3	128. ± 1.
1.0	Cu	146. ± 1.	241. ± 2.
1.0	Pb	253. ± 1.	411. ± 5.
1.25	Be	--	117. ± 1.
1.25	C	--	146. ± 1.
1.25	Cu	--	266. ± 2.
1.25	Pb	--	445. ± 5.
1.5	Be	42.1 ± 0.2	146. ± 1.
1.5	C	52.2 ± 0.2	183. ± 1.
1.5	Cu	99.4 ± 0.5	305. ± 3.
1.5	Pb	181. ± 1.	522. ± 5.
1.75	Be	--	150. ± 1.
1.75	C	--	182. ± 1.
1.75	Cu	--	315. ± 3.
1.75	Pb	--	493. ± 5.

Table 7. Pion Production Cross-sections
Beam = 4.2 GeV Protons

Errors quoted are statistical only.

Pion Momentum (GeV/c)	Target	π^- Production $\frac{d\sigma}{d\Omega dk}$(mb/sr/GeV/c)	π^+ Production $\frac{d\sigma}{d\Omega dk}$(mb/sr/GeV/c)
2.0	Be	29.0 ± 0.1	95.6 ± 0.7
2.0	C	34.7 ± 0.1	118. ± 1.
2.0	Cu	60.7 ± 0.3	197. ± 2.
2.0	Pb	110. ± 1.	326. ± 3.
2.5	Be	15.3 ± 0.1	39.8 ± 0.5
2.5	C	17.6 ± 0.1	49.1 ± 0.6
2.5	Cu	29.7 ± 0.2	84.9 ± 1.2
2.5	Pb	53.1 ± 0.4	129. ± 2.
3.0	Be	7.90 ± 0.04	19.9 ± 0.4
3.0	C	8.90 ± 0.05	25.1 ± 1.0
3.0	Cu	15.5 ± 0.1	40.8 ± 2.1
3.0	Pb	26.3 ± 0.2	62.3 ± 2.8
3.5	Be	1.85 ± 0.01	9.79 ± 0.30
3.5	C	1.87 ± 0.02	13.0 ± 0.3
3.5	Cu	3.33 ± 0.04	24.0 ± 0.8
3.5	Pb	6.20 ± 0.10	35.6 ± 1.5
3.75	Be	$(2.13 \pm 0.04)\times10^{-2}$	--
3.75	C	$(1.92 \pm 0.05)\times10^{-2}$	--
3.75	Cu	$(3.98 \pm 0.14)\times10^{-2}$	--
3.75	Pb	$(7.45 \pm 0.33)\times10^{-2}$	--
4.0	Be	$(1.42 \pm 0.33)\times10^{-3}$	--
4.0	C	$(1.30 \pm 0.28)\times10^{-3}$	--
4.0	Cu	$(4.89 \pm 1.07)\times10^{-3}$	--
4.0	Pb	$(10.3 \pm 2.7)\times10^{-3}$	--

Table 7. Continued.

Pion Momentum (GeV/c)	Target	π^- Production $\frac{d\sigma}{d\Omega dk}$(mb/sr/GeV/c)
.5	Be	69.8 ± 2.9
.5	C	89.0 ± 4.0
.5	Cu	244. ± 11.
.5	Pb	415. ± 21.
1.0	Be	71.9 ± 0.8
1.0	C	93.5 ± 1.1
1.0	Cu	237. ± 3.
1.0	Pb	389. ± 5.
1.5	Be	63.0 ± 0.6
1.5	C	79.5 ± 0.9
1.5	Cu	170. ± 2.
1.5	Pb	274. ± 3.
2.0	Be	52.0 ± 0.5
2.0	C	61.9 ± 0.7
2.0	Cu	140. ± 2.
2.0	Pb	188. ± 3.
2.5	Be	27.7 ± 0.3
2.5	C	33.9 ± 0.4
2.5	Cu	66.8 ± 0.8
2.5	Pb	102. ± 2.
3.0	Be	17.5 ± 0.2
3.0	C	21.9 ± 0.2
3.0	Cu	44.0 ± 0.6
3.0	Pb	61.7 ± 1.0

Table 8. Pion Production Cross-sections
Beam = 4.8 GeV Protons

Errors quoted are statistical only.

Pion Momentum (GeV/c)	Target	π^- Production $\frac{d\sigma}{d\Omega dk}$(mb/sr/GeV/c)
3.5	Be	9.45 ± 0.11
3.5	C	10.7 ± 0.1
3.5	Cu	22.1 ± 0.3
3.5	Pb	36.2 ± 0.7
4.0	Be	1.89 ± 0.03
4.0	C	1.83 ± 0.03
4.0	Cu	3.45 ± 0.10
4.0	Pb	6.23 ± 0.23
4.5	Be	$(3.13 \pm 0.19)\times10^{-2}$
4.5	C	$(4.12 \pm 0.19)\times10^{-2}$
4.5	Cu	$(10.8 \pm 0.5)\times10^{-2}$
4.5	Pb	$(15.8 \pm 1.1)\times10^{-2}$
4.75	Cu	$(8.43 \pm 4.22)\times10^{-4}$
4.75	Pb	$(6.62 \pm 6.62)\times10^{-4}$

Table 8. Continued.

Pion Momentum (GeV/c)	Target	π^- Production $\frac{d\sigma}{d\Omega dk}$(mb/sr/GeV/c)	π^+ Production $\frac{d\sigma}{d\Omega dk}$(mb/sr/GeV/c)
.5	Be	45.6 ± 0.7	--
.5	C	47.1 ± 0.8	--
.5	Cu	83.8 ± 1.8	--
.5	Pb	143. ± 3.	--
.6	Be	38.5 ± 0.5	--
.6	C	37.2 ± 0.6	--
.6	Cu	68.2 ± 1.4	--
.6	Pb	112. ± 3.	--
.75	Be	15.5 ± 0.3	12.6 ± 0.2
.75	C	15.8 ± 0.3	18.8 ± 0.3
.75	Cu	26.1 ± 0.7	32.5 ± 0.4*
.75	Pb	42.9 ± 1.3	35.5 ± 0.9
1.0	Be	1.09 ± 0.04	.887 ± 0.040
1.0	C	1.06 ± 0.05	1.35 ± 0.07
1.0	Cu	1.85 ± 0.13	1.97 ± 0.12*
1.0	Pb	2.95 ± 0.25	2.32 ± 0.21
1.25	Be	$(1.11 \pm 0.11)\times10^{-1}$	$(1.11 \pm 0.17)\times10^{-1}$
1.25	C	$(1.31 \pm 0.16)\times10^{-1}$	$(1.23 \pm 0.24)\times10^{-1}$
1.25	Cu	$(2.36 \pm 0.40)\times10^{-1}$	$(2.50 \pm 0.37)\times10^{-1}$*
1.25	Pb	$(3.13 \pm 0.70)\times10^{-1}$	$(1.99 \pm 0.75)\times10^{-1}$
1.5	Be	$(7.98 \pm 1.54)\times10^{-3}$	--
1.5	C	$(11.6 \pm 2.1)\times10^{-3}$	--
1.5	Cu	$(17.3 \pm 3.0)\times10^{-3}$	--
1.5	Pb	$(27.9 \pm 5.8)\times10^{-3}$	--

*Target = CH_2

Table 9. Pion Production Cross-sections
Beam = 1.05 GeV/Nucleon Deuterons

Errors quoted are statistical only.

Pion Momentum (GeV/c)	Target	π^- Production $\frac{d\sigma}{d\Omega dk}$(mb/sr/GeV/c)	π^+ Production $\frac{d\sigma}{d\Omega dk}$(mb/sr/GeV/c)
1.75	Be	$(1.44 \pm 1.02)\times10^{-4}$	--
1.75	Pb	$(13.2 \pm 6.6)\times10^{-4}$	--

Table 9. Continued.

Pion Momentum (GeV/c)	Target	π^- Production $\frac{d\sigma}{d\Omega dk}$(mb/sr/GeV/c)	π^+ Production $\frac{d\sigma}{d\Omega dk}$(mb/sr/GeV/c)
0.5	Be	104.2 ± 0.4	76.8 ± 1.5
0.5	C	110.0 ± 0.4	84.8 ± 1.9
0.5	Cu	250. ± 1.	121. ± 2.*
0.5	Pb	544. ± 2.	276. ± 8.
0.75	Be	101.9 ± 0.2	107. ± 2.
0.75	C	117.9 ± 0.4	114. ± 2.
0.75	Cu	482. ± 2.	135. ± 2.*
0.75	Pb	616. ± 2.	289. ± 7.
1.0	Be	92.8 ± 1.0	104. ± 1.
1.0	C	109. ± 1.	112. ± 2.
1.0	Cu	213. ± 3.	173. ± 2.*
1.0	Pb	336. ± 5.	277. ± 6.
1.25	Be	45.6 ± 0.5	48.0 ± 0.7
1.25	C	50.6 ± 0.6	51.8 ± 0.8
1.25	Cu	97.0 ± 1.4	78.8 ± 1.1*
1.25	Pb	157. ± 2.8	119. ± 3.
1.5	Be	17.2 ± 0.2	18.5 ± 0.3
1.5	C	19.4 ± 0.3	18.9 ± 0.4
1.5	Cu	33.1 ± 0.2	28.6 ± 0.5*
1.5	Pb	54.0 ± 0.4	44.9 ± 1.6
1.75	Be	8.0[illegible] ± 0.11	8.17 ± 0.28
1.75	C	8.29 ± 0.13	8.64 ± 0.22
1.75	Cu	19.4 ± 0.4	12.9 ± 0.3*
1.75	Pb	29.3 ± 0.6	18.9 ± 0.9

*Target = CH_2

Table 10. Pion Production Cross-sections
Beam = 2.1 GeV/Nucleon Deuterons

Errors quoted are statistical only.

Pion Momentum (GeV/c)	Target	π^- Production $\frac{d\sigma}{d\Omega dk}$(mb/sr/GeV/c)	π^+ Production $\frac{d\sigma}{d\Omega dk}$(mb/sr/GeV/c)
2.0	Be	2.25 ± 0.05	2.95 ± 0.14
2.0	C	2.59 ± 0.07	2.76 ± 0.11
2.0	Cu	4.56 ± 0.06	4.74 ± 0.16*
2.0	Pb	7.84 ± 0.12	6.83 ± 0.10
2.5	Be	$(2.37 \pm 0.13)\times10^{-1}$	--
2.5	C	$(2.55 \pm 0.18)\times10^{-1}$	--
2.5	Cu	$(4.61 \pm 0.15)\times10^{-1}$	--
2.5	Pb	$(7.98 \pm 0.34)\times10^{-1}$	--
3.0	Be	$(1.40 \pm 0.09)\times10^{-2}$	--
3.0	C	$(1.77 \pm 0.13)\times10^{-2}$	--
3.0	Cu	$(2.56 \pm 0.32)\times10^{-2}$	--
3.0	Pb	$(4.87 \pm 0.74)\times10^{-2}$	--
3.5	Cu	$(19.7 \pm 8.1)\times10^{-5}$	--
3.5	Pb	$(9.48 \pm 9.48)\times10^{-5}$	--

*Target = CH_2

Table 10. Continued.

Pion Momentum (GeV/c)	Target	π^- Production $\frac{d\sigma}{d\Omega dk}$(mb/sr/GeV/c)	π^+ Production $\frac{d\sigma}{d\Omega dk}$(mb/sr/GeV/c)
.5	Be	99.7 ± 4.0	78.4 ± 5.1
.5	C	112. ± 5.	105. ± 7
.5	CH_2	110. ± 5.	--
.5	Pb	340. ± 19.	--
.65	Be	61.0 ± 2.4	--
.65	C	63.2 ± 2.8	--
.65	CH_2	62.6 ± 2.8	--
.65	Pb	201. ± 12.	--
.75	Be	45.0 ± 1.8	--
.75	C	47.4 ± 2.1	53.6 ± 3.6
.75	CH_2	46.8 ± 2.1	77.1 ± 3.9
.75	Pb	137. ± 8.	99.6 ± 4.6
.9	Be	13.4 ± 0.7	--
.9	C	13.9 ± 0.8	--
.9	CH_2	13.9 ± 0.8	--
.9	Pb	34.8 ± 3.2	--
1.0	Be	7.21 ± 0.42	6.15 ± 0.35
1.0	C	6.27 ± 0.47	8.59 ± 0.53
1.0	CH_2	7.60 ± 0.53	12.8 ± 0.7
1.0	Pb	20.7 ± 2.2	18.3 ± 0.8
1.1	Be	3.52 ± 0.18	--
1.1	C	3.13 ± 0.21	--
1.1	CH_2	3.22 ± 0.21	--
1.1	Pb	8.99 ± 0.95	--

Table 11. Pion Production Cross-sections
Beam = 1.05 GeV/nucleon alphas

Errors quoted are statistical only.

Pion Momentum (GeV/c)	Target	π^- Production $\frac{d\sigma}{d\Omega dk}$(mb/sr/GeV/c)	π^+ Production $\frac{d\sigma}{d\Omega dk}$(mb/sr/GeV/c)
1.25	Be	1.12 ± 0.07	$(9.18 \pm 0.11)\times10^{-1}$
1.25	C	1.13 ± 0.09	$(13.9 \pm 0.2)\times10^{-1}$
1.25	CH_2	1.16 ± 0.09	$(17.4 \pm 0.2)\times10^{-1}$
1.25	Pb	3.00 ± 0.40	$(26.8 \pm 0.7)\times10^{-1}$
1.5	Be	$(2.26 \pm 0.21)\times10^{-1}$	--
1.5	C	$(2.11 \pm 0.26)\times10^{-1}$	--
1.5	CH_2	$(2.06 \pm 0.26)\times10^{-1}$	--
1.5	PB	$(6.55 \pm 1.26)\times10^{-1}$	--
1.75	Be	$(4.49 \pm 1.67)\times10^{-2}$	--
1.75	CH_2	$(3.39 \pm 0.94)\times10^{-2}$	--
1.75	Pb	$(5.89 \pm 3.40)\times10^{-2}$	--

Table 11. Continued.

Pion Momentum (GeV/c)	Target	π^- Production $\frac{d\sigma}{d\Omega dk}$(mb/sr/GeV/c)	π^+ Production $\frac{d\sigma}{d\Omega dk}$(mb/sr/GeV/c)
.5	Be	168. ± 2.	--
.5	C	237. ± 3.	--
.5	Cu	439. ± 6.	--
.5	Pb	703. ± 11.	--
.75	Be	205. ± 2.	192. ± 9.
.75	C	276. ± 3.	274. ± 14.
.75	Cu	486. ± 6.	493. ± 29.
.75	Pb	746. ± 7.	652. ± 87.
.9	Be	211. ± 2.	--
.9	C	282. ± 3.	--
.9	Cu	454. ± 6.	--
.9	Pb	714. ± 7.	--
1.0	Be	196. ± 2.	168. ± 8.
1.0	C	256. ± 2.	268. ± 12.
1.0	Cu	455. ± 5.	380. ± 27.
1.0	Pb	644. ± 6.	582. ± 41.
1.25	Be	109. ± 1.	95.7 ± 5.2
1.25	C	142. ± 1.	135. ± 7.
1.25	Cu	234. ± 3.	191. ± 14.
1.25	Pb	347. ± 5.	40[illegible]. ± 30.
1.5	Be	51.0 ± 0.6	47.8 ± 3.3
1.5	C	64.6 ± 0.8	65.2 ± 4.7
1.5	Cu	101. ± 2.	93.6 ± 8.9
1.5	Pb	164. ± 3.	157. ± 16.

Table 12. Pion Production Cross-sections
Beam = 2.1 GeV/nucleon alphas

Errors quoted are statistical only.

Pion Momentum (GeV/c)	Target	π^- Production $\frac{d\sigma}{d\Omega dk}$(mb/sr/GeV/c)	π^+ Production $\frac{d\sigma}{d\Omega dk}$(mb/sr/GeV/c)
1.75	Be	26.5 ± 0.2	25.2 ± 1.6
1.75	C	33.0 ± 0.3	35.8 ± 2.4
1.75	Cu	52.1 ± 0.6	53.4 ± 5.4
1.75	Pb	82.8 ± 1.2	80.7 ± 10.0
2.0	Be	11.1 ± 0.1	11.3 ± 1.0
2.0	C	14.8 ± 0.2	15.3 ± 1.2
2.0	Cu	24.5 ± 0.4	26.4 ± 3.5
2.0	Pb	35.6 ± 0.5	28.7 ± 5.4
2.5	Be	2.22 ± 0.04	--
2.5	C	2.94 ± 0.06	--
2.5	Cu	4.55 ± 0.12	--
2.5	Pb	6.56 ± 0.24	--
3.0	Be	$(3.77 \pm 0.12)\times10^{-1}$	--
3.0	C	$(5.09 \pm 0.19)\times10^{-1}$	--
3.0	Cu	$(7.69 \pm 0.37)\times10^{-1}$	--
3.0	Pb	$(11.9 \pm 0.72)\times10^{-1}$	--
3.5	Be	$(2.26 \pm 0.27)\times10^{-2}$	--
3.5	C	$(2.67 \pm 0.31)\times10^{-2}$	--
3.5	Cu	$(4.47 \pm 0.57)\times10^{-2}$	--
3.5	Pb	$(8.58 \pm 1.25)\times10^{-2}$	--
4.0	Be	$(8.99 \pm 4.02)\times10^{-4}$	--
4.0	C	$(23.9 \pm 10.7)\times10^{-4}$	--
4.0	Cu	$(7.43 \pm 5.25)\times10^{-4}$	--
4.0	Pb	$(18.8 \pm 13.3)\times10^{-4}$	--

Table 12. Continued.

Pion Momentum (GeV/c)	Target	π^- Production $\frac{d\sigma}{d\Omega dk}$ (mb/sr/GeV/c)
0.75	Be	115 ± 7
0.75	C	147 ± 10
0.75	Cu	390 ± 31
0.75	Pb	394 ± 37
1.0	C	26.8 ± 3.1
1.0	Cu	100 ± 12

Table 13. Pion production cross sections

Beam = 1.05 GeV/nucleon ^{12}C

Errors quoted are statistical only

Momentum GeV/c / R	.5	.75	1.0	1.5	2.0	2.5	3.0
$\frac{\text{2.1 deuterons}}{\text{4.2 protons}}$	1.67	1.73	1.58	0.37	7.46×10^{-2}	1.67×10^{-2}	1.99×10^{-3}
$\frac{\text{1.05 alphas}}{\text{4.2 protons}}$	1.70	0.694	9.11×10^{-2}	4.04×10^{-3}	---	---	---

Table 14. Ratios of the cross sections for π^- production by protons, deuterons, and alphas of equal total kinetic energy

Momentum GeV/c R	.75	1.0	1.25	1.5	1.75	2.0	Avg
$d + C \rightarrow \pi^{\pm}$	.966	1.03	1.02	.974	1.04	1.07	1.02 ± .03
$\alpha + C \rightarrow \pi^{\pm}$	.993	1.05	---	1.01	1.08	1.03	1.02 ± .04

Table 15. Ratio R for π^+/π^- production by 2.1 GeV/nucleon beams

1.85 GEV PROTONS
TARGET = BE

	PLAB/Z	PROTONS	DEUTERONS	H-3	HE-3	HE-4
CROSS SECTION	.500	5.162E+01	0.	0.	0.	0.
CROSS SECTION ERROR		4.748E-01	0.	0.	0.	0.
CROSS SECTION	.750	1.187E+02	3.425E+00	5.143E-02	1.575E-01	0.
CROSS SECTION ERROR		2.184E+00	1.579E-01	1.820E-02	2.264E-02	0.
CROSS SECTION	.900	1.679E+02	6.580E+00	1.187E-01	1.484E-01	0.
CROSS SECTION ERROR		3.376E+00	2.533E-01	2.977E-02	2.364E-02	0.
CROSS SECTION	1.000	2.071E+02	1.031E+01	0.	9.824E-02	0.
CROSS SECTION ERROR		7.419E+00	5.988E-01	0.	3.292E-02	0.
CROSS SECTION	1.250	2.731E+02	1.412E+01	2.568E-01	0.	0.
CROSS SECTION ERROR		8.043E+00	9.789E-01	5.634E-02	0.	0.
CROSS SECTION	1.500	3.816E+02	1.603E+01	2.889E-01	0.	0.
CROSS SECTION ERROR		8.194E+00	9.672E-01	5.887E-02	0.	0.
CROSS SECTION	1.563	2.187E+02	0.	0.	0.	0.
CROSS SECTION ERROR		6.844E+00	0.	0.	0.	0.
CROSS SECTION	1.625	1.858E+02	0.	0.	0.	0.
CROSS SECTION ERROR		6.852E+00	0.	0.	0.	0.
CROSS SECTION	1.750	7.86?E+02	1.163E+01	0.	0.	0.
CROSS SECTION ERROR		4.550E+01	1.826E+00	0.	0.	0.
CROSS SECTION	1.790	9.453E+05	0.	0.	0.	0.
CROSS SECTION ERROR		1.891E+05	0.	0.	0.	0.
CROSS SECTION	2.000	1.019E+02	2.979E+01	1.269E-01	0.	0.
CROSS SECTION ERROR		4.178E-03	3.487E-01	1.125E-02	0.	0.

Table 16.

1.85 GEV PROTONS
TARGET = BE

	PLAB/Z	PROTONS	DEUTERONS	H-3	HE-3	HE-4
CROSS SECTION	2.250	3.510E-03	1.765E-03	1.110E-02	0.	0.
CROSS SECTION ERROR		1.241E-03	0.827E-04	2.221E-03	0.	0.

Table 16 (continued).

1.85 GEV PROTONS
TARGET = C

	PLAB/Z	PROTONS	DEUTERONS	H-3	HE-3	HE-4
CROSS SECTION	.500	7.420E+01	0.	0.	0.	0.
CROSS SECTION ERROR		9.846E-01	0.	0.	0.	0.
CROSS SECTION	.750	1.554E+02	5.374E+00	7.478E-02	2.721E-01	0.
CROSS SECTION ERROR		2.894E+00	2.550E-01	2.826E-02	3.838E-02	0.
CROSS SECTION	.900	2.191E+02	9.338E+00	1.994E-01	2.706E-01	0.
CROSS SECTION ERROR		3.503E+00	2.923E-01	3.788E-02	3.131E-02	0.
CROSS SECTION	1.000	2.632E+02	1.429E+01	1.638E-01	1.638E-01	0.
CROSS SECTION ERROR		9.363E+00	8.356E-01	7.347E-02	5.210E-02	0.
CROSS SECTION	1.250	3.751E+02	1.926E+01	4.627E-01	0.	0.
CROSS SECTION ERROR		7.536E+00	5.552E-01	6.428E-02	0.	0.
CROSS SECTION	1.500	3.695E+02	1.754E+01	3.396E-01	0.	0.
CROSS SECTION ERROR		8.202E+00	5.205E-01	5.286E-02	0.	0.
CROSS SECTION	1.563	2.740E+02	0.	0.	0.	0.
CROSS SECTION ERROR		8.946E+00	0.	0.	0.	0.
CROSS SECTION	1.625	2.567E+02	0.	0.	0.	0.
CROSS SECTION ERROR		8.388E+00	0.	0.	0.	0.
CROSS SECTION	1.750	1.171E+03	1.70AE+01	0.	0.	0.
CROSS SECTION ERROR		6.583E+01	1.332E+00	0.	0.	0.
CROSS SECTION	1.790	7.758E+04	0.	0.	0.	0.
CROSS SECTION ERROR		8.959E+03	0.	0.	0.	0.
CROSS SECTION	2.000	3.659E-02	3.469E-01	1.739E-01	0.	0.
CROSS SECTION ERROR		7.328E-03	4.191E-01	1.618E-02	0.	0.

Table 17.

1.85 GEV PROTONS
TARGET = CU

	PLAB/Z	PROTONS	DEUTERONS	H-3	HE-3	HE-4
CROSS SECTION	.500	2.677E+02	0.	0.	0.	0.
CROSS SECTION ERROR		2.432E+00	0.	0.	0.	0.
CROSS SECTION	.750	4.214E+02	2.487E+01	3.898E-01	6.863E-01	0.
CROSS SECTION ERROR		6.558E+00	8.075E-01	9.449E-02	8.370E-02	0.
CROSS SECTION	.900	5.009E+02	3.425E+01	9.323E-01	3.716E-01	0.
CROSS SECTION ERROR		6.127E+00	7.561E-01	1.089E-01	4.856E-02	0.
CROSS SECTION	1.000	5.357E+02	3.692E+01	1.399E+00	1.632E-01	0.
CROSS SECTION ERROR		7.839E+00	9.252E-01	1.538E-01	3.913E-02	0.
CROSS SECTION	1.250	6.974E+02	4.231E+01	1.354E+00	0.	0.
CROSS SECTION ERROR		1.798E+01	1.703E+00	2.455E-01	0.	0.
CROSS SECTION	1.500	7.868E+02	3.687E+01	1.035E+00	0.	0.
CROSS SECTION ERROR		1.632E+01	1.338E+00	1.790E-01	0.	0.
CROSS SECTION	1.563	6.809E+02	0.	0.	0.	0.
CROSS SECTION ERROR		2.240E+01	0.	0.	0.	0.
CROSS SECTION	1.625	5.772E+02	0.	0.	0.	0.
CROSS SECTION ERROR		1.908E+01	0.	0.	0.	0.
CROSS SECTION	1.750	6.866E+03	3.518E+01	0.	0.	0.
CROSS SECTION ERROR		3.906E+02	3.185E+00	0.	0.	0.
CROSS SECTION	1.798	1.112E+06	0.	0.	0.	0.
CROSS SECTION ERROR		1.527E+05	0.	0.	0.	0.
CROSS SECTION	2.000	3.858E-01	4.707E+01	3.582E-01	0.	0.
CROSS SECTION ERROR		3.749E-02	6.716E-01	4.887E-02	0.	0.

Table 18.

1.05 GEV PROTONS
TARGET = CU

	PLAB/Z	PROTONS	DEUTERONS	H-3	HE-3	HE-4
CROSS SECTION	2.250	0.	1.265E-02	4.427E-02	0.	0.
CROSS SECTION ERROR		0.	4.217E-03	7.955E-03	0.	0.

Table 18 (continued).

1.85 GEV PROTONS
TARGET = PB

	PLAB/Z	PROTONS	DEUTERONS	H-3	HE-3	HE-4
CROSS SECTION	.500	5.146E+02	0.	0.	0.	0.
CROSS SECTION ERROR		5.194E+00	0.	0.	0.	0.
CROSS SECTION	.750	6.964E+02	5.141E+01	1.345E+00	8.269E-01	0.
CROSS SECTION ERROR		8.615E+00	1.312E+00	1.947E-01	1.688E-01	0.
CROSS SECTION	.900	7.721E+02	1.307E+02	3.488E+00	2.832E-01	0.
CROSS SECTION ERROR		9.364E+00	2.256E+00	2.888E-01	9.879E-02	0.
CROSS SECTION	1.000	8.087E+02	6.438E+01	3.825E+00	2.378E-01	0.
CROSS SECTION ERROR		9.265E+00	1.305E+00	2.782E-01	4.868E-02	0.
CROSS SECTION	1.250	1.053E+03	6.382E+01	2.782E+00	0.	0.
CROSS SECTION ERROR		2.265E+01	2.331E+00	4.865E-01	0.	0.
CROSS SECTION	1.500	1.190E+03	5.448E+01	1.776E+00	0.	0.
CROSS SECTION ERROR		2.654E+01	2.877E+00	3.163E-01	0.	0.
CROSS SECTION	1.563	9.850E+02	0.	0.	0.	0.
CROSS SECTION ERROR		3.290E+01	0.	0.	0.	0.
CROSS SECTION	1.625	9.643E+02	0.	0.	0.	0.
CROSS SECTION ERROR		2.276E+01	0.	0.	0.	0.
CROSS SECTION	1.750	1.600E+04	5.299E+01	0.	0.	0.
CROSS SECTION ERROR		8.959E+02	5.886E+00	0.	0.	0.
CROSS SECTION	1.790	2.721E+06	0.	0.	0.	0.
CROSS SECTION ERROR		3.773E+05	0.	0.	0.	0.
CROSS SECTION	2.000	3.193E+00	5.842E+01	8.873E-01	0.	0.
CROSS SECTION ERROR		1.747E-01	9.500E-01	9.245E-02	0.	0.

Table 19.

1.73 GEV PROTONS
TARGET = BE

	PLAB/Z	PROTONS	DEUTERONS	H-3	HE-3	HE-4
CROSS SECTION	.500	4.272E+01	0.	0.	0.	0.
CROSS SECTION ERROR		5.874E-01	0.	0.	0.	0.
CROSS SECTION	.750	7.153E+01	2.674E+00	0.	1.155E-01	0.
CROSS SECTION ERROR		8.325E-01	8.681E-02	0.	1.223E-02	0.
CROSS SECTION	1.000	1.034E+02	3.519E+00	1.636E-01	9.527E-02	0.
CROSS SECTION ERROR		1.126E+00	8.928E-02	1.782E-02	9.622E-03	0.
CROSS SECTION	1.250	1.577E+02	4.839E+00	1.355E-01	4.696E-02	0.
CROSS SECTION ERROR		1.651E+00	9.873E-02	1.451E-02	6.831E-03	0.
CROSS SECTION	1.500	2.197E+02	6.308E+00	1.193E-01	6.416E-03	0.
CROSS SECTION ERROR		2.259E+00	1.896E-01	1.243E-02	2.030E-03	0.
CROSS SECTION	1.750	2.681E+02	7.882E+00	1.056E-01	0.	0.
CROSS SECTION ERROR		2.735E+00	1.218E-01	1.083E-02	0.	0.
CROSS SECTION	2.000	3.761E+02	8.412E+00	0.	0.	0.
CROSS SECTION ERROR		5.978E+00	1.938E-01	0.	0.	0.
CROSS SECTION	2.250	5.038E+02	9.692E+00	0.	0.	0.
CROSS SECTION ERROR		5.072E+00	1.328E-01	0.	0.	0.
CROSS SECTION	2.375	2.093E+02	6.144E+00	0.	0.	0.
CROSS SECTION ERROR		4.569E+00	2.801E-01	0.	0.	0.
CROSS SECTION	2.435	3.689E+02	0.	0.	0.	0.
CROSS SECTION ERROR		3.648E+00	0.	0.	0.	0.
CROSS SECTION	2.625	6.739E-01	6.064E+00	0.	0.	0.
CROSS SECTION ERROR		2.319E-02	8.939E-02	0.	0.	0.

Table 20.

1.73 GEV PROTONS
TARGET = BE

	PLAB/Z	PROTONS	DEUTERONS	H-3	HE-3	HE-4
CROSS SECTION	2.750	1.038E-01	3.528E+00	0.	0.	0.
CROSS SECTION ERROR		8.534E-03	6.082E-02	0.	0.	0.
CROSS SECTION	2.825	7.945E-02	1.896E+00	0.	0.	0.
CROSS SECTION ERROR		7.357E-03	4.055E-02	0.	0.	0.

Table 20 (continued).

1.73 GEV PROTONS
TARGET = C

	PLAB/Z	PROTONS	DEUTERONS	H-3	HE-3	HE-4
CROSS SECTION	.500	6.229E+01	0.	0.	0.	0.
CROSS SECTION ERROR		6.155E-01	0.	0.	0.	0.
CROSS SECTION	.750	1.095E+02	4.978E+00	0.	2.890E-01	0.
CROSS SECTION ERROR		1.278E+00	1.495E-01	0.	2.368E-02	0.
CROSS SECTION	1.000	1.360E+02	5.696E+00	2.582E-01	1.522E-01	0.
CROSS SECTION ERROR		1.501E+00	1.423E-01	2.758E-02	1.522E-02	0.
CROSS SECTION	1.250	1.926E+02	6.963E+00	2.653E-01	6.873E-02	0.
CROSS SECTION ERROR		2.042E+00	1.467E-01	2.543E-02	9.130E-03	0.
CROSS SECTION	1.500	2.763E+02	8.539E+00	2.412E-01	1.407E-02	0.
CROSS SECTION ERROR		2.860E+00	1.567E-01	2.215E-02	3.762E-03	0.
CROSS SECTION	1.750	3.242E+02	9.850E+00	2.205E-01	0.	0.
CROSS SECTION ERROR		3.320E+00	1.630E-01	1.961E-02	0.	0.
CROSS SECTION	2.000	4.683E+02	1.015E+01	0.	0.	0.
CROSS SECTION ERROR		6.136E+00	2.060E-01	0.	0.	0.
CROSS SECTION	2.250	6.867E+02	1.091E+01	0.	0.	0.
CROSS SECTION ERROR		6.133E+00	1.626E-01	0.	0.	0.
CROSS SECTION	2.435	5.667E+02	0.	0.	0.	0.
CROSS SECTION ERROR		5.726E+00	0.	0.	0.	0.
CROSS SECTION	2.625	1.899E+00	6.878E+00	0.	0.	0.
CROSS SECTION ERROR		5.808E-02	1.121E-01	0.	0.	0.
CROSS SECTION	2.750	1.694E-01	4.322E+00	0.	0.	0.
CROSS SECTION ERROR		1.363E-02	8.108E-02	0.	0.	0.

Table 21.

1.73 GEV PROTONS
TARGET = C

	PLAB/Z	PROTONS	DEUTERONS	H-3	HE-3	HE-4
CROSS SECTION	2.825	1.809E-01	2.586E+00	0.	0.	0.
CROSS SECTION ERROR		1.834E-02	5.839E-02	0.	0.	0.

Table 21 (continued).

1.73 GEv PROTONS
TARGET = CU

	PLAB/Z	PROTONS	DEUTERONS	H-3	HE-3	HE-4
CROSS SECTION	.500	2.319E+02	0.	0.	0.	0.
CROSS SECTION ERROR		2.238E+00	0.	0.	0.	0.
CROSS SECTION	.750	3.204E+02	2.512E+01	0.	1.882E+00	0.
CROSS SECTION ERROR		3.886E+00	6.326E-01	0.	0.326E-02	0.
CROSS SECTION	1.000	3.467E+02	2.696E+01	2.348E+00	3.086E-01	0.
CROSS SECTION ERROR		3.929E+00	5.852E-01	1.530E-01	4.475E-02	0.
CROSS SECTION	1.250	4.229E+02	2.476E+01	2.135E+00	1.106E-01	0.
CROSS SECTION ERROR		4.607E+00	5.105E-01	1.339E-01	2.206E-02	0.
CROSS SECTION	1.500	5.287E+02	2.289E+01	1.282E+00	1.704E-02	0.
CROSS SECTION ERROR		5.606E+00	4.439E-01	9.435E-02	7.624E-03	0.
CROSS SECTION	1.750	5.487E+02	1.943E+01	8.649E-01	8.766E-03	0.
CROSS SECTION ERROR		5.762E+00	3.866E-01	7.162E-02	5.062E-03	0.
CROSS SECTION	2.000	8.327E+02	1.778E+01	4.580E-01	0.	0.
CROSS SECTION ERROR		8.579E+00	3.488E-01	4.810E-02	0.	0.
CROSS SECTION	2.250	1.118E+03	2.468E+01	0.	0.	0.
CROSS SECTION ERROR		1.140E+01	4.130E-01	0.	0.	0.
CROSS SECTION	2.375	5.292E+02	9.478E+00	0.	0.	0.
CROSS SECTION ERROR		9.866E+00	3.988E-01	0.	0.	0.
CROSS SECTION	2.435	1.874E+03	0.	0.	0.	0.
CROSS SECTION ERROR		1.894E+01	0.	0.	0.	0.
CROSS SECTION	2.625	4.134E+00	9.854E+00	0.	0.	0.
CROSS SECTION ERROR		1.313E-01	2.179E-01	0.	0.	0.

Table 22.

1.73 GEV PROTONS
TARGET = CU

	PLAB/Z	PROTONS	DEUTERONS	H-3	HE-3	HE-4
CROSS SECTION	2.750	4.953E-01	6.661E+00	0.	0.	0.
CROSS SECTION ERROR		4.25[illegible]E-02	1.665E-01	0.	0.	0.
CROSS SECTION	2.825	[illegible].	2.829E+00	0.	0.	0.
CROSS SECTION ERROR		0.	1.643E-01	0.	0.	0.

Table 22 (continued).

1.73 GEV PROTONS
TARGET = PB

	PLAB/Z	PROTONS	DEUTERONS	H-3	HE-3	HE-4
CROSS SECTION	.500	5.674E+02	0.	0.	0.	0.
CROSS SECTION ERROR		7.674E+00	0.	0.	0.	0.
CROSS SECTION	.750	6.473E+02	8.584E+01	0.	2.999E+00	0.
CROSS SECTION ERROR		7.887E+00	1.865E+00	0.	2.225E-01	0.
CROSS SECTION	1.000	5.925E+02	5.976E+01	6.598E+00	6.930E-01	0.
CROSS SECTION ERROR		7.003E+00	1.337E+00	4.057E-01	9.205E-02	0.
CROSS SECTION	1.250	7.060E+02	5.837E+01	6.811E+00	1.167E-01	0.
CROSS SECTION ERROR		7.945E+00	1.112E+00	3.472E-01	3.371E-02	0.
CROSS SECTION	1.500	8.053E+02	3.601E+01	2.464E+00	2.432E-02	0.
CROSS SECTION ERROR		8.802E+00	8.334E-01	2.014E-01	1.404E-02	0.
CROSS SECTION	1.750	9.943E+02	3.531E+01	1.445E+00	0.	0.
CROSS SECTION ERROR		1.059E+01	7.79.E-01	1.424E-01	0.	0.
CROSS SECTION	2.000	1.270E+03	2.875E+01	0.	0.	0.
CROSS SECTION ERROR		1.328E+01	6.535E-01	0.	0.	0.
CROSS SECTION	2.259	1.777E+03	3.406E+01	0.	0.	0.
CROSS SECTION ERROR		1.828E+01	6.919E-01	0.	0.	0.
CROSS SECTION	2.375	1.893E+03	1.556E+01	0.	0.	0.
CROSS SECTION ERROR		1.938E+01	7.134E-01	0.	0.	0.
CROSS SECTION	2.435	2.270E+03	0.	0.	0.	0.
CROSS SECTION ERROR		2.316E+01	0.	0.	0.	0.
CROSS SECTION	2.625	8.681E+00	1.560E+01	0.	0.	0.
CROSS SECTION ERROR		2.906E-01	4.083E-01	0.	0.	0.

Table 23.

1.73 GEV PROTONS
TARGET = PB

	PLAB/Z	PROTONS	DEUTERONS	H-3	HE-3	HE-4
CROSS SECTION	2.750	1.411E+00	9.858E+00	0.	0.	0.
CROSS SECTION ERROR		1.100E-01	2.951E-01	0.	0.	0.
CROSS SECTION	2.825	0.	4.960E+00	0.	0.	0.
CROSS SECTION ERROR		0.	2.110E-01	0.	0.	0.

Table 23 (continued).

2.1 GEV PROTONS
TARGET = BE

	PLAB/Z	PROTONS	DEUTERONS	H-3	HE-3	HE-4
CROSS SECTION	.500	3.983E+01	3.843E-01	0.	1.409E-02	0.
CROSS SECTION ERROR		5.632E-01	3.941E-02	0.	5.329E-03	0.
CROSS SECTION	.750	6.172E+01	2.276E+00	0.	0.	0.
CROSS SECTION ERROR		7.381E-01	8.120E-02	0.	0.	0.
CROSS SECTION	1.000	8.883E+01	3.575E+00	1.731E-01	8.959E-02	0.
CROSS SECTION ERROR		9.828E-01	9.183E-02	1.875E-02	9.539E-03	0.
CROSS SECTION	1.250	1.288E+02	4.870E+00	1.538E-01	5.879E-02	0.
CROSS SECTION ERROR		1.365E+00	9.841E-02	1.577E-02	6.906E-03	0.
CROSS SECTION	1.500	2.038E+02	4.733E+00	1.302E-01	1.476E-02	0.
CROSS SECTION ERROR		1.488E+00	6.514E-02	9.393E-03	2.228E-03	0.
CROSS SECTION	1.750	2.814E+02	5.926E+00	1.208E-01	3.451E-03	0.
CROSS SECTION ERROR		2.870E+00	1.014E-01	1.185E-02	1.409E-03	0.
CROSS SECTION	2.000	3.168E+02	6.327E+00	1.037E-01	0.	0.
CROSS SECTION ERROR		3.216E+00	1.017E-01	1.027E-02	0.	0.
CROSS SECTION	2.250	4.289E+02	6.579E+00	0.	0.	0.
CROSS SECTION ERROR		4.333E+00	1.089E-01	0.	0.	0.
CROSS SECTION	2.500	6.136E+02	5.644E+00	0.	0.	0.
CROSS SECTION ERROR		1.953E+01	2.776E-01	0.	0.	0.
CROSS SECTION	2.750	2.496E+02	3.785E+00	0.	0.	0.
CROSS SECTION ERROR		8.687E+00	2.017E-01	0.	0.	0.
CROSS SECTION	3.000	1.715E+00	3.639E+00	0.	0.	0.
CROSS SECTION ERROR		3.784E-02	6.126E-02	0.	0.	0.

Table 24.

2.1 GEV PROTONS
TARGET = BE

	PLAB/Z	PROTONS	DEUTERONS	H-3	HE-3	HE-4
CROSS SECTION	3.125	1.630E-01	2.775E+00	0.	0.	0.
CROSS SECTION ERROR		1.032E-02	5.047E-02	0.	0.	0.
CROSS SECTION	2.125	4.020E+02				
CROSS SECTION ERROR		1.206E+01				
CROSS SECTION	2.375	6.231E+02				
CROSS SECTION ERROR		1.869E+01				
CROSS SECTION	2.625	8.242E+02				
CROSS SECTION ERROR		2.472E+01				
CROSS SECTION	2.6875	8.040E+02				
CROSS SECTION ERROR		2.412E+01				
CROSS SECTION	2.8125	4.530E+02				
CROSS SECTION ERROR		1.360E+01				
CROSS SECTION	2.875	3.234E+03				
CROSS SECTION ERROR		9.702E+01				

Table 24 (continued).

2.1 GEV PROTONS
TARGET = C

	PLAB/Z	PROTONS	DEUTERONS	H-3	HE-3	HE-4
CROSS SECTION	.500	6.241E+01	7.112E-01	0.	4.119E-02	0.
CROSS SECTION ERROR		8.825E-01	6.726E-02	0.	1.143E-02	0.
CROSS SECTION	.750	8.891E+01	3.495E+00	0.	0.	0.
CROSS SECTION ERROR		1.077E+00	1.260E-01	0.	0.	0.
CROSS SECTION	1.000	1.241E+02	5.945E+00	3.644E-01	1.426E-01	0.
CROSS SECTION ERROR		1.388E+00	1.491E-01	3.417E-02	1.519E-02	0.
CROSS SECTION	1.250	1.699E+02	6.498E+00	3.092E-01	6.971E-02	0.
CROSS SECTION ERROR		1.819E+00	1.435E-01	2.817E-02	9.425E-03	0.
CROSS SECTION	1.500	2.532E+02	6.582E+00	1.646E-01	1.795E-02	0.
CROSS SECTION ERROR		2.534E+00	1.360E-01	1.873E-02	4.358E-03	0.
CROSS SECTION	1.750	3.417E+02	7.900E+00	2.354E-01	3.621E-03	0.
CROSS SECTION ERROR		3.505E+00	1.430E-01	2.478E-02	1.811E-03	0.
CROSS SECTION	2.000	3.797E+02	8.187E+00	1.616E-01	0.	0.
CROSS SECTION ERROR		3.874E+00	1.399E-01	1.608E-02	0.	0.
CROSS SECTION	2.250	5.130E+02	8.813E+00	0.	0.	0.
CROSS SECTION ERROR		5.198E+00	1.329E-01	0.	0.	0.
CROSS SECTION	2.500	7.162E+02	6.275E+00	0.	0.	0.
CROSS SECTION ERROR		1.615E+01	2.433E-01	0.	0.	0.
CROSS SECTION	2.750	3.686E+02	4.966E+00	0.	0.	0.
CROSS SECTION ERROR		1.184E+01	2.855E-01	0.	0.	0.
CROSS SECTION	3.000	2.989E+00	3.853E+00	0.	0.	0.
CROSS SECTION ERROR		6.326E-02	7.434E-02	0.	0.	0.

Table 25.

2.1 GEV PROTONS
TARGET = C

	PLAB/Z	PROTONS	DEUTERONS	H-3	HE-3	HE-4
CROSS SECTION	3.125	2.326E-01	2.868E+00	0.	0.	0.
CROSS SECTION ERROR		1.541E-02	6.861E-02	0.	0.	0.
CROSS SECTION	2.125	3.620E+02				
CROSS SECTION ERROR		6.516E+00				
CROSS SECTION	2.375	5.330E+02				
CROSS SECTION ERROR		9.594E+00				
CROSS SECTION	2.625	7.930E+02				
CROSS SECTION ERROR		1.427E+01				
CROSS SECTION	2.6875	9.398E+02				
CROSS SECTION ERROR		2.819E+01				
CROSS SECTION	2.8125	4.591E+02				
CROSS SECTION ERROR		1.377E+01				
CROSS SECTION	2.875	3.484E+03				
CROSS SECTION ERROR		3.832E+01				

Table 25(continued).

2.1 GEV PROTONS
TARGET = CU

	PLAB/Z	PROTONS	DEUTERONS	H-3	HE-3	HE-4
CROSS SECTION	.500	2.471E+02	3.517E+00	0.	1.887E-01	0.
CROSS SECTION ERROR		3.376E+00	2.794E-01	0.	4.588E-02	0.
CROSS SECTION	.750	2.795E+02	2.839E+01	0.	0.	0.
CROSS SECTION ERROR		3.436E+00	5.818E-01	0.	0.	0.
CROSS SECTION	1.000	3.180E+02	2.935E+01	3.141E+00	4.773E-01	0.
CROSS SECTION ERROR		3.676E+00	6.378E-01	1.893E-01	5.169E-02	0.
CROSS SECTION	1.250	3.856E+02	2.526E+01	2.619E+00	1.643E-01	0.
CROSS SECTION ERROR		4.263E+00	5.463E-01	1.547E-01	2.706E-02	0.
CROSS SECTION	1.500	5.127E+02	2.027E+01	1.369E+00	5.920E-02	0.
CROSS SECTION ERROR		5.473E+00	4.344E-01	1.016E-01	1.481E-02	0.
CROSS SECTION	1.750	6.230E+02	1.873E+01	8.943E-01	0.	0.
CROSS SECTION ERROR		6.528E+00	3.898E-01	7.584E-02	0.	0.
CROSS SECTION	2.000	6.596E+02	1.623E+01	6.326E-01	0.	0.
CROSS SECTION ERROR		6.858E+00	3.391E-01	5.959E-02	0.	0.
CROSS SECTION	2.250	8.850E+02	1.411E+01	0.	0.	0.
CROSS SECTION ERROR		9.085E+00	2.973E-01	0.	0.	0.
CROSS SECTION	2.500	1.220E+03	1.871E+01	0.	0.	0.
CROSS SECTION ERROR		1.242E+01	2.414E-01	0.	0.	0.
CROSS SECTION	2.750	7.241E+02	7.110E+00	0.	0.	0.
CROSS SECTION ERROR		2.351E+01	5.770E-01	0.	0.	0.
CROSS SECTION	3.000	3.287E+00	2.491E+00	0.	0.	0.
CROSS SECTION ERROR		1.132E-01	9.843E-02	0.	0.	0.

Table 26.

2.1 GEV PROTONS
TARGET = CU

	PLAB/Z	PROTONS	DEUTERONS	H-3	HE-3	HE-4
CROSS SECTION	3.125	9.113E-01	4.247E+00	0.	0.	0.
CROSS SECTION ERROR		5.661E-02	1.290E-01	0.	0.	0.
CROSS SECTION	2.125	8.107E+02				
CROSS SECTION ERROR		1.215E+01				
CROSS SECTION	2.375	1.138E+03				
CROSS SECTION ERROR		1.698E+01				
CROSS SECTION	2.625	1.555E+03				
CROSS SECTION ERROR		1.710E+01				
CROSS SECTION	2.6875	1.346E+03				
CROSS SECTION ERROR		5.384E+01				
CROSS SECTION	2.8125	1.195E+03				
CROSS SECTION ERROR		3.585E+01				
CROSS SECTION	2.875	2.062E+04				
CROSS SECTION ERROR		2.269E+02				

Table 26(continued).

2.1 GEV PROTONS
TARGET = PB

	PLAB/Z	PROTONS	DEUTERONS	H-3	HE-3	HE-4
CROSS SECTION	.500	6.398E+02	1.464E+01	0.	6.784E-01	0.
CROSS SECTION ERROR		8.681E+00	9.093E-01	0.	1.370E-01	0.
CROSS SECTION	.750	5.837E+02	7.818E+01	0.	0.	0.
CROSS SECTION ERROR		7.423E+00	1.751E+00	0.	0.	0.
CROSS SECTION	1.000	5.898E+02	8.416E+01	1.240E+01	7.961E-01	0.
CROSS SECTION ERROR		7.122E+00	1.739E+00	6.015E-01	1.857E-01	0.
CROSS SECTION	1.250	6.616E+02	5.736E+01	7.508E+00	4.134E-01	0.
CROSS SECTION ERROR		7.620E+00	1.262E+00	4.164E-01	6.809E-02	0.
CROSS SECTION	1.500	8.525E+02	3.991E+01	3.910E+00	1.862E-02	0.
CROSS SECTION ERROR		9.382E+00	9.441E-01	2.727E-01	1.317E-02	0.
CROSS SECTION	1.750	1.014E+03	3.204E+01	2.011E+00	0.	0.
CROSS SECTION ERROR		1.089E+01	7.787E-01	1.803E-01	0.	0.
CROSS SECTION	2.000	1.133E+03	2.768E+01	1.173E+00	0.	0.
CROSS SECTION ERROR		1.199E+01	6.763E-01	1.205E-01	0.	0.
CROSS SECTION	2.250	1.409E+03	2.142E+01	0.	0.	0.
CROSS SECTION ERROR		1.468E+01	5.549E-01	0.	0.	0.
CROSS SECTION	2.500	1.924E+03	1.595E+01	0.	0.	0.
CROSS SECTION ERROR		6.251E+01	1.413E+00	0.	0.	0.
CROSS SECTION	2.750	1.208E+03	1.051E+01	0.	0.	0.
CROSS SECTION ERROR		3.973E+01	1.078E+00	0.	0.	0.
CROSS SECTION	3.000	1.394E+01	8.676E+00	0.	0.	0.
CROSS SECTION ERROR		3.807E-01	2.951E-01	0.	0.	0.

Table 27.

2.1 GEV PROTONS
TARGET = PB

	PLAB/Z	PROTONS	DEUTERONS	H-3	HE-3	HE-4
CROSS SECTION	3.125	2.265E+00	6.542E+00	0.	0.	0.
CROSS SECTION ERROR		1.418E-01	2.487E-01	0.	0.	0.
CROSS SECTION	2.125	1.335E+03				
CROSS SECTION ERROR		1.468E+01				
CROSS SECTION	2.375	1.939E+03				
CROSS SECTION ERROR		2.132E+01				
CROSS SECTION	2.625	2.496E+03				
CROSS SECTION ERROR		2.746E+01				
CROSS SECTION	2.6875	2.151E+03				
CROSS SECTION ERROR		6.363E+01				
CROSS SECTION	2.8125	2.296E+03				
CROSS SECTION ERROR		4.174E+01				
CROSS SECTION	2.875	2.413E+04				
CROSS SECTION ERROR		1.340E+03				

Table 27 (continued).

4.2 GEV PROTONS
TARGET = BE

	PLAB/Z	PROTONS	DEUTERONS	H-3	HE-3	HE-4
CROSS SECTION	.500	3.477E+01	3.290E-01	0.	2.106E-02	0.
CROSS SECTION ERROR		5.494E-01	4.168E-02	0.	7.458E-03	0.
CROSS SECTION	.750	5.542E+01	1.756E+00	0.	2.106E-02	0.
CROSS SECTION ERROR		7.067E-01	8.822E-02	0.	6.884E-03	0.
CROSS SECTION	1.000	7.887E+01	2.379E+00	1.105E-01	4.871E-02	0.
CROSS SECTION ERROR		8.286E-01	8.243E-02	1.778E-02	8.023E-03	0.
CROSS SECTION	1.250	7.976E+01	2.115E+00	9.908E-02	4.845E-02	0.
CROSS SECTION ERROR		8.957E-01	6.983E-02	1.448E-02	7.168E-03	0.
CROSS SECTION	1.500	1.002E+02	2.164E+00	6.846E-02	2.721E-02	0.
CROSS SECTION ERROR		1.005E+00	6.515E-02	1.098E-02	4.894E-03	0.
CROSS SECTION	1.750	1.277E+02	2.363E+00	4.514E-02	1.730E-02	0.
CROSS SECTION ERROR		1.349E+00	6.338E-02	8.253E-03	3.212E-03	0.
CROSS SECTION	2.000	1.452E+02	2.289E+00	4.213E-02	1.514E-02	0.
CROSS SECTION ERROR		1.515E+00	5.913E-02	7.459E-03	3.161E-03	0.
CROSS SECTION	3.000	3.053E+02	2.688E+00	0.	0.	0.
CROSS SECTION ERROR		1.232E+01	1.716E-01	0.	0.	0.
CROSS SECTION	3.500	4.556E+02	0.	0.	0.	0.
CROSS SECTION ERROR		1.027E+01	0.	0.	0.	0.
CROSS SECTION	4.000	5.794E+02	0.	0.	0.	0.
CROSS SECTION ERROR		5.826E+00	0.	0.	0.	0.
CROSS SECTION	4.500	7.348E+02	0.	0.	0.	0.
CROSS SECTION ERROR		7.377E+00	0.	0.	0.	0.

Table 28.

4.2 GEV PROTONS
TARGET = BE

	PLAB/Z	PROTONS	DEUTERONS	H-3	HE-3	HE-4
CROSS SECTION	4.625	6.946E+02	0.	0.	0.	0.
CROSS SECTION ERROR		6.974E+00	0.	0.	0.	0.
CROSS SECTION	4.758	5.538E+02	0.	0.	0.	0.
CROSS SECTION ERROR		5.556E+00	0.	0.	0.	0.
CROSS SECTION	4.875	8.546E+02	0.	0.	0.	0.
CROSS SECTION ERROR		8.573E+00	0.	0.	0.	0.
CROSS SECTION	5.000	4.390E+03	0.	0.	0.	0.
CROSS SECTION ERROR		4.392E+01	0.	0.	0.	0.

Table 28 (continued).

4.2 GEV PROTONS
TARGET = C

	PLAB/Z	PROTONS	DEUTERONS	H-3	HE-3	HE-4
CROSS SECTION	.500	5.057E+01	5.719E-01	0.	1.270E-02	0.
CROSS SECTION ERROR		9.117E-01	6.950E-02	0.	7.334E-03	0.
CROSS SECTION	.750	8.966E+01	7.847E+00	0.	0.	0.
CROSS SECTION ERROR		1.141E+00	2.109E-01	0.	0.	0.
CROSS SECTION	1.000	1.055E+02	4.663E+00	2.710E-01	1.000E-01	0.
CROSS SECTION ERROR		1.246E+00	1.476E-01	3.398E-02	1.516E-02	0.
CROSS SECTION	1.250	1.141E+02	3.966E+00	2.866E-01	5.750E-02	0.
CROSS SECTION ERROR		1.297E+00	1.221E-01	2.653E-02	9.891E-03	0.
CROSS SECTION	1.500	1.397E+02	3.824E+00	1.665E-01	4.516E-02	0.
CROSS SECTION ERROR		1.530E+00	1.104E-01	2.174E-02	7.996E-03	0.
CROSS SECTION	1.750	1.681E+02	3.760E+00	1.452E-01	2.540E-02	0.
CROSS SECTION ERROR		1.796E+00	1.025E-01	1.880E-02	5.549E-03	0.
CROSS SECTION	2.000	1.958E+02	3.438E+00	1.418E-01	2.329E-02	0.
CROSS SECTION ERROR		2.052E+00	9.170E-02	1.739E-02	4.970E-03	0.
CROSS SECTION	3.000	5.227E+02	3.967E+00	0.	0.	0.
CROSS SECTION ERROR		1.675E+01	2.671E-01	0.	0.	0.
CROSS SECTION	3.500	5.308E+02	0.	0.	0.	0.
CROSS SECTION ERROR		9.798E+00	0.	0.	0.	0.
CROSS SECTION	4.000	7.787E+02	0.	0.	0.	0.
CROSS SECTION ERROR		7.839E+00	0.	0.	0.	0.
CROSS SECTION	4.500	8.821E+02	0.	0.	0.	0.
CROSS SECTION ERROR		8.867E+00	0.	0.	0.	0.

Table 29.

4.2 GEV PROTONS
TARGET = C

	PLAB/Z	PROTONS	DEUTERONS	H-3	HE-3	HE-4
CROSS SECTION	4.625	7.943E+02	0.	0.	0.	0.
CROSS SECTION ERROR		7.988E+00	0.	0.	0.	0.
CROSS SECTION	4.750	6.881E+02	0.	0.	0.	0.
CROSS SECTION ERROR		6.925E+00	0.	0.	0.	0.
CROSS SECTION	4.875	1.336E+03	0.	0.	0.	0.
CROSS SECTION ERROR		1.340E+01	0.	0.	0.	0.
CROSS SECTION	5.000	4.708E+03	0.	0.	0.	0.
CROSS SECTION ERROR		4.712E+01	0.	0.	0.	0.

Table 29 (continued).

4.2 GEV PROTONS
TARGET = CU

	PLAB/Z	PROTONS	DEUTERONS	H-3	HE-3	HE-4
CROSS SECTION	.500	2.650E+02	3.359E+00	0.	2.677E-01	0.
CROSS SECTION ERROR		3.946E+00	3.343E-01	0.	6.698E-02	0.
CROSS SECTION	.750	3.411E+02	2.635E+01	0.	0.	0.
CROSS SECTION ERROR		4.356E+00	8.849E-01	0.	0.	0.
CROSS SECTION	1.000	3.369E+02	3.297E+01	3.263E+00	5.522E-01	0.
CROSS SECTION ERROR		4.098E+00	8.872E-01	2.359E-01	6.819E-02	0.
CROSS SECTION	1.250	3.112E+02	2.469E+01	2.637E+00	2.744E-01	0.
CROSS SECTION ERROR		3.701E+00	6.214E-01	1.897E-01	4.294E-02	0.
CROSS SECTION	1.500	3.286E+02	1.655E+01	1.629E+00	8.366E-02	0.
CROSS SECTION ERROR		3.786E+00	4.879E-01	1.448E-01	2.162E-02	0.
CROSS SECTION	1.750	3.945E+02	1.691E+01	1.253E+00	7.171E-02	0.
CROSS SECTION ERROR		4.382E+00	4.332E-01	1.101E-01	1.853E-02	0.
CROSS SECTION	2.000	3.976E+02	1.211E+01	1.004E+00	4.601E-02	0.
CROSS SECTION ERROR		4.361E+00	3.382E-01	9.219E-02	1.388E-02	0.
CROSS SECTION	3.000	7.718E+02	7.026E+00	0.	0.	0.
CROSS SECTION ERROR		2.524E+01	6.596E-01	0.	0.	0.
CROSS SECTION	3.500	9.858E+02	0.	0.	0.	0.
CROSS SECTION ERROR		1.841E+01	0.	0.	0.	0.
CROSS SECTION	4.000	1.219E+03	0.	0.	0.	0.
CROSS SECTION ERROR		1.239E+01	0.	0.	0.	0.
CROSS SECTION	4.500	1.424E+03	0.	0.	0.	0.
CROSS SECTION ERROR		1.442E+01	0.	0.	0.	0.

Table 30.

4.2 GEV PROTONS
TARGET = CU

	PLAB/Z	PROTONS	DEUTERONS	H-	HE-3	HE-4
CROSS SECTION	4.625	1.344E+03	0.	0.	0.	0.
CROSS SECTION ERROR		1.361E+01	0.	0.	0.	0.
CROSS SECTION	4.750	1.184E+03	0.	0.	0.	0.
CROSS SECTION ERROR		1.201E+01	0.	0.	0.	0.
CROSS SECTION	4.875	3.232E+03	0.	0.	0.	0.
CROSS SECTION ERROR		3.240E+01	0.	0.	0.	0.
CROSS SECTION	5.000	1.316E+04	0.	0.	0.	0.
CROSS SECTION ERROR		1.017E+02	0.	0.	0.	0.

Table 30 (continued).

4.2 GEV PROTONS
TARGET = PB

	PLAB/Z	PROTONS	DEUTERONS	H-3	HE-3	HE-4
CROSS SECTION	.500	8.805E+02	1.448E+01	0.	1.813E+00	0.
CROSS SECTION ERROR		1.274E+01	1.207E+00	0.	3.026E-01	0.
CROSS SECTION	.750	9.823E+02	1.321E+02	0.	3.827E+00	0.
CROSS SECTION ERROR		1.266E+01	3.238E+00	0.	3.604E-01	0.
CROSS SECTION	1.000	8.049E+02	1.248E+02	2.118E+01	1.485E+00	0.
CROSS SECTION ERROR		1.019E+01	2.772E+00	1.852E+00	1.939E-01	0.
CROSS SECTION	1.250	6.962E+02	8.304E+01	1.611E+01	8.862E-01	0.
CROSS SECTION ERROR		8.694E+00	1.996E+00	8.216E-01	1.339E-01	0.
CROSS SECTION	1.500	6.749E+02	5.317E+01	8.862E+00	3.357E-01	0.
CROSS SECTION ERROR		8.213E+00	1.428E+00	5.526E-01	7.513E-02	0.
CROSS SECTION	1.750	6.814E+02	3.931E+01	4.719E+00	0.	0.
CROSS SECTION ERROR		8.087E+00	1.126E+00	3.715E-01	0.	0.
CROSS SECTION	2.000	7.363E+02	2.653E+01	2.518E+00	8.811E-02	0.
CROSS SECTION ERROR		8.494E+00	8.534E-01	2.530E-01	3.332E-02	0.
CROSS SECTION	3.000	1.535E+03	1.273E+01	0.	0.	0.
CROSS SECTION ERROR		3.610E+01	1.065E+00	0.	0.	0.
CROSS SECTION	3.500	1.718E+03	0.	0.	0.	0.
CROSS SECTION ERROR		3.261E+01	0.	0.	0.	0.
CROSS SECTION	4.000	2.065E+03	0.	0.	0.	0.
CROSS SECTION ERROR		2.125E+01	0.	0.	0.	0.
CROSS SECTION	4.500	2.395E+03	0.	0.	0.	0.
CROSS SECTION ERROR		2.448E+01	0.	0.	0.	0.

Table 31.

4.2 GEV PROTONS
TARGET = PB

	PLAB/Z	PROTONS	DEUTERONS	H-3	HE-3	HE-4
CROSS SECTION	4.625	2.380E+03	0.	0.	0.	0.
CROSS SECTION ERROR		2.432E+01	0.	0.	0.	0.
CROSS SECTION	4.750	2.045E+03	0.	0.	0.	0.
CROSS SECTION ERROR		2.096E+01	0.	0.	0.	0.
CROSS SECTION	4.875	5.354E+03	0.	0.	0.	0.
CROSS SECTION ERROR		5.494E+01	0.	0.	0.	0.
CROSS SECTION	5.000	4.160E+04	0.	0.	0.	0.
CROSS SECTION ERROR		4.165E+02	0.	0.	0.	0.

Table 31 (continued).

1.85 GEV/NUCLEON DEUTERONS
TARGET = BE

	PLAB/Z	PROTONS	DEUTERONS	H-3	HE-3	HE-4
CROSS SECTION	.750	1.487E+02	6.598E+00	9.693E-02	2.867E-01	0.
CROSS SECTION ERROR		1.534E+00	1.484E-01	1.618E-02	1.986E-02	0.
CROSS SECTION	.750	1.416E+02	6.657E+00	9.693E-02	2.867E-01	0.
CROSS SECTION ERROR		1.544E+00	1.492E-01	1.618E-02	1.986E-02	0.
CROSS SECTION	.750	1.392E+02	6.523E+00	9.693E-02	2.867E-01	0.
CROSS SECTION ERROR		1.519E+00	1.474E-01	1.618E-02	1.986E-02	0.
CROSS SECTION	1.000	2.434E+02	1.504E+01	6.785E-01	5.937E-01	0.
CROSS SECTION ERROR		2.532E+00	2.298E-01	3.763E-02	2.519E-02	0.
CROSS SECTION	1.000	2.347E+02	1.392E+01	4.443E-01	2.948E-01	0.
CROSS SECTION ERROR		2.445E+00	2.175E-01	3.028E-02	1.750E-02	0.
CROSS SECTION	1.250	4.671E+02	2.133E+01	5.889E-01	2.552E-01	0.
CROSS SECTION ERROR		4.750E+00	2.824E-01	2.912E-02	1.458E-02	0.
CROSS SECTION	1.500	1.854E+03	2.313E+01	5.304E-01	2.639E-01	0.
CROSS SECTION ERROR		2.646E+01	4.109E-01	3.853E-02	1.921E-02	0.
CROSS SECTION	1.750	1.138E+04	2.714E+01	4.039E-01	1.442E-01	0.
CROSS SECTION ERROR		3.599E+02	1.024E+00	6.945E-02	2.921E-02	0.
CROSS SECTION	1.875	4.109E+03	4.283E+01	0.	0.	0.
CROSS SECTION ERROR		1.301E+02	1.514E+00	0.	0.	0.
CROSS SECTION	2.000	1.174E+03	2.658E+01	5.149E-01	9.887E-02	0.
CROSS SECTION ERROR		3.727E+01	9.865E-01	7.392E-02	2.161E-02	0.
CROSS SECTION	2.125	1.887E+02	1.621E+01	0.	0.	0.
CROSS SECTION ERROR		5.862E+00	6.449E-01	0.	0.	0.

Table 32.

1.05 GEV/NUCLEON DEUTERONS
TARGET = BE

	PLAB/Z	PROTONS	DEUTERONS	H-3	HE-3	HE-4
CROSS SECTION	2.250	6.221E+01	1.250E+01	2.962E-01	0.	0.
CROSS SECTION ERROR		2.103E+00	5.175E-01	5.240E-02	0.	0.
CROSS SECTION	2.375	3.781E+01	1.276E+01	0.	0.	0.
CROSS SECTION ERROR		1.322E+00	5.204E-01	0.	0.	0.
CROSS SECTION	2.500	2.099E+01	2.139E+01	1.696E-01	0.	0.
CROSS SECTION ERROR		7.797E-01	7.933E-01	3.748E-02	0.	0.
CROSS SECTION	2.750	6.967E-01	6.092E+01	3.157E-01	0.	0.
CROSS SECTION ERROR		7.444E-02	2.035E+00	4.918E-02	0.	0.
CROSS SECTION	3.000	0.	1.592E+02	3.366E-01	0.	0.
CROSS SECTION ERROR		0.	5.107E+00	4.677E-02	0.	0.
CROSS SECTION	3.125	0.	2.771E+02	0.	0.	0.
CROSS SECTION ERROR		0.	8.664E+00	0.	0.	0.
CROSS SECTION	3.250	0.	3.137E+02	3.355E-01	0.	0.
CROSS SECTION ERROR		0.	1.002E+01	4.687E-02	0.	0.
CROSS SECTION	3.250	0.	3.117E+02	3.542E-01	0.	0.
CROSS SECTION ERROR		0.	9.953E+00	4.823E-02	0.	0.
CROSS SECTION	3.313	0.	2.333E+02	0.	0.	0.
CROSS SECTION ERROR		0.	7.474E+00	0.	0.	0.
CROSS SECTION	3.375	0.	4.050E+02	0.	0.	0.
CROSS SECTION ERROR		0.	1.298E+01	0.	0.	0.
CROSS SECTION	3.438	0.	3.154E+03	0.	0.	0.
CROSS SECTION ERROR		0.	9.962E+01	0.	0.	0.

Table 32 (continued).

1.05 GEV/NUCLEON DEUTERONS
TARGET = BE

	PLAB/Z	PROTONS	DEUTERONS	H-3	HE-3	HE-4
CROSS SECTION	3.469	0.	9.756E+03	0.	0.	0.
CROSS SECTION ERROR		0.	1.821E+02	0.	0.	0.
CROSS SECTION	3.588	0.	4.531E+04	0.	0.	0.
CROSS SECTION ERROR		0.	1.433E+03	0.	0.	0.
CROSS SECTION	3.531	0.	4.311E+02	0.	0.	0.
CROSS SECTION ERROR		0.	1.372E+01	0.	0.	0.

Table 32 (continued).

1.88 GEV/NUCLEON DEUTERONS
TARGET = C

	PLAB/Z	PROTONS	DEUTERONS	H-3	HE-3	HE-4
CROSS SECTION	.750	2.193E+02	1.385E+01	3.389E-01	5.177E-01	0.
CROSS SECTION ERROR		2.442E+00	2.936E-01	4.216E-02	3.753E-02	0.
CROSS SECTION	.750	2.218E+02	1.340E+01	3.389E-01	5.177E-01	0.
CROSS SECTION ERROR		2.467E+00	2.993E-01	4.216E-02	3.753E-02	0.
CROSS SECTION	.750	2.164E+02	1.385E+01	3.389E-01	5.177E-01	0.
CROSS SECTION ERROR		2.413E+00	3.043E-01	4.216E-02	3.753E-02	0.
CROSS SECTION	1.000	3.466E+02	2.329E+01	1.125E+00	4.704E-01	0.
CROSS SECTION ERROR		3.650E+00	3.033E-01	6.494E-02	3.131E-02	0.
CROSS SECTION	1.000	3.399E+02	2.389E+01	1.141E+00	5.264E-01	0.
CROSS SECTION ERROR		3.598E+00	3.089E-01	6.654E-02	3.288E-02	0.
CROSS SECTION	1.250	6.368E+02	3.272E+01	1.249E+00	3.827E-01	0.
CROSS SECTION ERROR		6.523E+00	4.599E-01	6.446E-02	2.585E-02	0.
CROSS SECTION	1.500	2.339E+03	3.179E+01	9.785E-01	2.891E-01	0.
CROSS SECTION ERROR		4.294E+01	7.860E-01	9.499E-02	3.625E-02	0.
CROSS SECTION	1.750	1.594E+04	3.558E+01	9.836E-01	1.944E-01	0.
CROSS SECTION ERROR		5.044E+02	1.448E+00	1.532E-01	4.756E-02	0.
CROSS SECTION	1.875	5.488E+03	5.831E+01	0.	0.	0.
CROSS SECTION ERROR		1.711E+02	2.153E+00	0.	0.	0.
CROSS SECTION	2.000	1.580E+03	3.560E+01	0.687E-01	1.981E-01	0.
CROSS SECTION ERROR		4.881E+01	1.488E+00	1.340E-01	4.483E-02	0.
CROSS SECTION	2.125	2.414E+02	2.088E+01	0.	0.	0.
CROSS SECTION ERROR		7.923E+00	8.799E-01	0.	0.	0.

Table 33.

1.05 GEV/NUCLEON DEUTERONS
TARGET = C

	PLAB/Z	PROTONS	DEUTERONS	H-3	HE-3	HE-4
CROSS SECTION	2.250	9.078E+01	1.013E+01	4.278E-01	0.	0.
CROSS SECTION ERROR		3.136E+00	8.856E-01	8.828E-02	0.	0.
CROSS SECTION	2.250	8.484E+01	1.578E+01	2.847E-01	0.	0.
CROSS SECTION ERROR		2.947E+00	7.265E-01	7.173E-02	0.	0.
CROSS SECTION	2.375	4.849E+01	1.815E+01	0.	0.	0.
CROSS SECTION ERROR		1.776E+00	7.957E-01	0.	0.	0.
CROSS SECTION	2.500	3.383E+01	3.131E+01	4.644E-01	0.	0.
CROSS SECTION ERROR		1.295E+00	1.216E+00	8.747E-02	0.	0.
CROSS SECTION	2.750	1.175E+00	8.198E+01	4.876E-01	0.	0.
CROSS SECTION ERROR		1.358E-01	2.812E+00	7.818E-02	0.	0.
CROSS SECTION	3.125	0.	3.433E+02	0.	0.	0.
CROSS SECTION ERROR		0.	1.185E+01	0.	0.	0.
CROSS SECTION	3.250	0.	3.957E+02	3.879E-01	0.	0.
CROSS SECTION ERROR		0.	1.271E+01	6.235E-02	0.	0.
CROSS SECTION	3.250	0.	4.203E+02	5.858E-01	0.	0.
CROSS SECTION ERROR		0.	1.348E+01	8.847E-02	0.	0.
CROSS SECTION	3.313	0.	3.397E+02	0.	0.	0.
CROSS SECTION ERROR		0.	1.393E+01	0.	0.	0.
CROSS SECTION	3.375	0.	6.095E+02	0.	0.	0.
CROSS SECTION ERROR		0.	1.376E+01	0.	0.	0.
CROSS SECTION	3.438	0.	4.916E+03	0.	0.	0.
CROSS SECTION ERROR		0.	1.556E+02	0.	0.	0.

Table 33 (continued).

1.05 GEV/NUCLEON DEUTERONS
TARGET = C

	PLAB/Z	PROTONS	DEUTERONS	H-3	HE-3	HE-4
CROSS SECTION	3.469	0.	7.673E+03	0.	0.	0.
CROSS SECTION ERROR		0.	2.428E+02	0.	0.	0.
CROSS SECTION	3.500	0.	4.350E+04	0.	0.	0.
CROSS SECTION ERROR		0.	1.376E+03	0.	0.	0.
CROSS SECTION	3.531	0.	9.486E+02	0.	0.	0.
CROSS SECTION ERROR		0.	2.992E+01	0.	0.	0.

Table 33 (continued).

1.85 GEV/NUCLEON DEUTERONS
TARGET = PB

	PLAB/Z	PROTONS	DEUTERONS	H-3	HE-3	HE-4
CROSS SECTION	.750	8.604E+02	1.106E+02	3.418E+00	2.587E+00	0.
CROSS SECTION ERROR		1.001E+01	2.153E+00	3.292E-01	2.031E-01	0.
CROSS SECTION	.750	8.661E+02	1.126E+02	3.630E+00	2.462E+00	0.
CROSS SECTION ERROR		1.006E+01	2.170E+00	3.397E-01	1.900E-01	0.
CROSS SECTION	.750	8.716E+02	1.138E+02	0.	0.	0.
CROSS SECTION ERROR		1.012E+01	2.193E+00	0.	0.	0.
CROSS SECTION	1.000	1.013E+03	1.192E+02	1.463E+01	1.094E+00	0.
CROSS SECTION ERROR		1.121E+01	2.046E+00	6.046E-01	1.139E-01	0.
CROSS SECTION	1.000	9.836E+02	1.164E+02	1.388E+01	1.329E+00	0.
CROSS SECTION ERROR		1.091E+01	2.012E+00	5.879E-01	1.257E-01	0.
CROSS SECTION	1.250	1.675E+03	1.844E+02	9.582E+00	6.821E-01	0.
CROSS SECTION ERROR		1.764E+01	1.739E+00	4.334E-01	7.550E-02	0.
CROSS SECTION	1.500	5.944E+03	8.356E+01	4.845E+00	4.312E-01	0.
CROSS SECTION ERROR		6.819E+01	1.418E+00	2.551E-01	5.830E-02	0.
CROSS SECTION	1.750	1.856E+05	8.671E+01	3.360E+00	2.680E-01	0.
CROSS SECTION ERROR		3.349E+03	4.359E+00	6.003E-01	1.347E-01	0.
CROSS SECTION	1.875	1.844E+04	1.643E+02	0.	0.	0.
CROSS SECTION ERROR		5.851E+02	6.878E+00	0.	0.	0.
CROSS SECTION	2.000	4.103E+03	7.773E+01	2.940E+00	1.176E-01	0.
CROSS SECTION ERROR		1.315E+02	3.879E+00	5.953E-01	8.324E-02	0.
CROSS SECTION	2.125	5.867E+02	4.623E+01	0.	0.	0.
CROSS SECTION ERROR		2.818E+01	2.679E+00	0.	0.	0.

Table 34.

1.05 GEV/NUCLEON DEUTERONS
TARGET = PB

	PLAB/Z	PROTONS	DEUTERONS	H-3	HE-3	HE-4
CROSS SECTION	2.250	1.954E+02	3.861E+01	1.673E+00	0.	0.
CROSS SECTION ERROR		7.613E+00	2.338E+00	4.215E-01	0.	0.
CROSS SECTION	2.375	4.876E+02	1.146E+02	0.	0.	0.
CROSS SECTION ERROR		1.432E+01	4.931E+00	0.	0.	0.
CROSS SECTION	2.500	5.996E+01	6.305E+01	1.317E+00	0.	0.
CROSS SECTION ERROR		3.009E+00	3.161E+00	3.545E-01	0.	0.
CROSS SECTION	2.750	1.654E+00	1.759E+02	1.197E+00	0.	0.
CROSS SECTION ERROR		3.736E-01	6.765E+00	3.222E-01	0.	0.
CROSS SECTION	3.000	0.	4.336E+02	1.098E+00	0.	0.
CROSS SECTION ERROR		0.	1.486E+01	2.954E-01	0.	0.
CROSS SECTION	3.125	0.	7.357E+02	0.	0.	0.
CROSS SECTION ERROR		0.	2.441E+01	0.	0.	0.
CROSS SECTION	3.250	0.	9.139E+02	5.798E-01	0.	0.
CROSS SECTION ERROR		0.	3.089E+01	2.055E-01	0.	0.
CROSS SECTION	3.313	0.	8.942E+02	0.	0.	0.
CROSS SECTION ERROR		0.	2.936E+01	0.	0.	0.
CROSS SECTION	3.375	0.	1.787E+03	0.	0.	0.
CROSS SECTION ERROR		0.	3.893E+01	0.	0.	0.
CROSS SECTION	3.438	0.	1.281E+04	0.	0.	0.
CROSS SECTION ERROR		0.	4.868E+02	0.	0.	0.
CROSS SECTION	3.469	0.	2.523E+04	0.	0.	0.
CROSS SECTION ERROR		0.	7.998E+02	0.	0.	0.

Table 34 (continued).

1.05 GEV/NUCLEON DEUTERONS
TARGET = PB

	PLAB/Z	PROTONS	DEUTERONS	H-3	HE-3	HE-4
CROSS SECTION	3.500	0.	1.084E+05	0.	0.	0.
CROSS SECTION ERROR		0.	5.950E+03	0.	0.	0.
CROSS SECTION	3.531	0.	1.663E+03	0.	0.	0.
CROSS SECTION ERROR		0.	9.362E+01	0.	0.	0.

Table 34 (continued).

1.89 GEV/NUCLEON DEUTERONS
TARGET = CH2

	PLAB/Z	PROTONS	DEUTERONS	H-3	HE-3	HE-4
CROSS SECTION	.750	2.679E+02	1.296E+01	2.346E-01	5.131E-01	0.
CROSS SECTION ERROR		2.953E+00	3.037E-01	3.716E-02	3.912E-02	0.
CROSS SECTION	.750	2.697E+02	1.338E+01	2.346E-01	5.131E-01	0.
CROSS SECTION ERROR		2.972E+00	3.054E-01	3.716E-02	3.912E-02	0.
CROSS SECTION	.750	2.757E+02	1.337E+01	2.346E-01	5.131E-01	0.
CROSS SECTION ERROR		3.032E+00	3.894E-01	3.716E-02	3.912E-02	0.
CROSS SECTION	1.000	4.383E+02	2.350E+01	1.138E+00	5.000E-01	0.
CROSS SECTION ERROR		4.595E+00	3.974E-01	7.140E-02	3.300E-02	0.
CROSS SECTION	1.250	8.254E+02	3.775E+01	1.004E+00	4.107E-01	0.
CROSS SECTION ERROR		8.425E+00	5.230E-01	6.269E-02	2.746E-02	0.
CROSS SECTION	1.500	2.905E+03	3.931E+01	3.460E-01	4.984E-01	0.
CROSS SECTION ERROR		4.129E+01	7.335E-01	4.531E-02	3.807E-02	0.
CROSS SECTION	1.750	2.158E+04	4.999E+01	3.770E-01	4.900E-01	0.
CROSS SECTION ERROR		6.829E+02	1.936E+00	9.006E-02	7.999E-02	0.
CROSS SECTION	1.875	7.745E+03	9.109E+01	0.	0.	0.
CROSS SECTION ERROR		2.453E+02	3.228E+00	0.	0.	0.
CROSS SECTION	2.000	2.138E+03	4.892E+01	0.356E-01	4.895E-02	0.
CROSS SECTION ERROR		6.796E+01	1.861E+00	1.381E-01	3.313E-02	0.
CROSS SECTION	2.125	3.165E+02	2.695E+01	0.	0.	0.
CROSS SECTION ERROR		1.032E+01	1.131E+00	0.	0.	0.
CROSS SECTION	2.250	1.278E+02	2.102E+01	4.185E-01	0.	0.
CROSS SECTION ERROR		4.309E+00	9.221E-01	9.051E-02	0.	0.

Table 35.

1.05 GEV/NUCLEON DEUTERONS
TARGET = CH2

	PLAB/Z	PROTONS	DEUTERONS	H-3	HE-3	HE-4
CROSS SECTION	2.375	2.005E+01	8.074E+00	0.	0.	0.
CROSS SECTION ERROR		0.762E-01	4.623E-01	0.	0.	0.
CROSS SECTION	2.500	5.615E+01	3.987E+01	4.398E-01	0.	0.
CROSS SECTION ERROR		2.031E+00	1.496E+00	0.905E-02	0.	0.
CROSS SECTION	2.750	1.086E+00	1.157E+02	3.198E-01	0.	0.
CROSS SECTION ERROR		1.352E-01	3.903E+00	7.223E-02	0.	0.
CROSS SECTION	3.000	0.	3.080E+02	4.691E-01	0.	0.
CROSS SECTION ERROR		0.	9.967E+00	0.424E-02	0.	0.
CROSS SECTION	3.125	0.	4.832E+02	0.	0.	0.
CROSS SECTION ERROR		0.	1.550E+01	0.	0.	0.
CROSS SECTION	3.250	0.	6.819E+02	5.887E-01	0.	0.
CROSS SECTION ERROR		0.	2.177E+01	0.382E-02	0.	0.
CROSS SECTION	3.313	0.	4.391E+02	0.	0.	0.
CROSS SECTION ERROR		0.	1.439E+01	0.	0.	0.
CROSS SECTION	3.375	0.	6.531E+02	0.	0.	0.
CROSS SECTION ERROR		0.	1.475E+01	0.	0.	0.
CROSS SECTION	3.438	0.	5.960E+03	0.	0.	0.
CROSS SECTION ERROR		0.	1.887E+02	0.	0.	0.
CROSS SECTION	3.469	0.	1.295E+04	0.	0.	0.
CROSS SECTION ERROR		0.	4.097E+02	0.	0.	0.
CROSS SECTION	3.500	0.	7.495E+04	0.	0.	0.
CROSS SECTION ERROR		0.	2.370E+03	0.	0.	0.

Table 35 (continued).

1.85 GEV/NUCLEON DEUTERONS
TARGET = [illegible]

	PLAB/Z	PROTONS	DEUTERONS	H-3	HE-3	HE-4
CROSS SECTION	3.531	0.	7.962E+02	0.	0.	0.
CROSS SECTION ERROR		0.	2.537E+01	0.	0.	0.

Table 35 (continued).

2.1 GEV/NUCLEON DEUTERONS
TARGET = BE

	PLAB/Z	PROTONS	DEUTERONS	H-3	HE-3	HE-4
CROSS SECTION	.500	6.260E+01	7.899E-01	0.	2.645E-02	0.
CROSS SECTION ERROR		1.184E+00	7.920E-02	0.	1.080E-02	0.
CROSS SECTION	.750	1.484E+02	6.351E+00	1.176E-01	2.939E-01	0.
CROSS SECTION ERROR		1.669E+00	2.020E-01	2.631E-02	2.953E-02	0.
CROSS SECTION	1.000	1.919E+02	8.204E+00	5.025E-01	2.388E-01	0.
CROSS SECTION ERROR		2.125E+00	2.866E-01	4.733E-02	2.383E-02	0.
CROSS SECTION	1.250	2.733E+02	1.832E+01	3.527E-01	2.863E-01	0.
CROSS SECTION ERROR		2.902E+00	2.165E-01	3.544E-02	1.918E-02	0.
CROSS SECTION	1.500	3.834E+02	1.134E+01	3.262E-01	1.102E-01	0.
CROSS SECTION ERROR		3.977E+00	2.144E-01	3.113E-02	1.277E-02	0.
CROSS SECTION	1.750	4.925E+02	1.382E+01	3.134E-01	9.039E-02	0.
CROSS SECTION ERROR		7.807E+00	3.585E-01	4.373E-02	1.656E-02	0.
CROSS SECTION	2.000	6.372E+02	1.600E+01	3.166E-01	9.452E-02	0.
CROSS SECTION ERROR		9.489E+00	3.606E-01	3.896E-02	1.501E-02	0.
CROSS SECTION	2.250	1.141E+03	1.679E+01	2.841E-01	5.388E-02	0.
CROSS SECTION ERROR		1.150E+01	2.468E-01	2.376E-02	7.285E-03	0.
CROSS SECTION	2.500	2.370E+03	1.564E+01	0.	0.	0.
CROSS SECTION ERROR		2.379E+01	2.278E-01	0.	0.	0.
CROSS SECTION	2.750	6.226E+03	1.414E+01	0.	0.	0.
CROSS SECTION ERROR		1.971E+02	6.528E-01	0.	0.	0.
CROSS SECTION	2.875	8.804E+03	1.399E+01	0.	0.	0.
CROSS SECTION ERROR		2.786E+02	6.396E-01	0.	0.	0.

Table 36.

2.1 GEV/NUCLEON DEUTERONS
TARGET = BE

	PLAB/Z	PROTONS	DEUTERONS	H-3	HE-3	HE-4
CROSS SECTION	3.000	6.368E+03	1.452E+01	0.	0.	0.
CROSS SECTION ERROR		2.014E+02	6.583E-01	0.	0.	0.
CROSS SECTION	3.250	1.180E+03	1.090E+01	0.	0.	0.
CROSS SECTION ERROR		3.751E+01	5.121E-01	0.	0.	0.
CROSS SECTION	3.500	2.553E+02	9.115E+00	8.816E-02	0.	0.
CROSS SECTION ERROR		2.615E+00	1.404E-01	1.057E-02	0.	0.
CROSS SECTION	3.500	2.564E+02	9.453E+00	0.	0.	0.
CROSS SECTION ERROR		2.626E+00	1.441E-01	0.	0.	0.
CROSS SECTION	3.750	6.386E+01	1.110E+01	0.	0.	0.
CROSS SECTION ERROR		8.868E-01	1.591E-01	0.	0.	0.
CROSS SECTION	4.000	3.845E+01	1.479E+01	0.	0.	0.
CROSS SECTION ERROR		4.355E-01	1.951E-01	0.	0.	0.
CROSS SECTION	4.000	3.929E+01	1.390E+01	1.256E-01	0.	0.
CROSS SECTION ERROR		4.443E-01	1.858E-01	1.183E-02	0.	0.
CROSS SECTION	4.500	7.512E+00	4.334E+01	0.	0.	0.
CROSS SECTION ERROR		1.136E-01	4.796E-01	0.	0.	0.
CROSS SECTION	5.000	0.	1.096E+02	0.	0.	0.
CROSS SECTION ERROR		0.	1.139E+00	0.	0.	0.

Table 36 (continued).

2.1 GEV/NUCLEON DEUTERONS
TARGET = C

	PLAB/Z	PROTONS	DEUTERONS	H-3	HE-3	HE-4
CROSS SECTION	.500	1.137E+02	1.120E+00	0.	7.130E-02	0.
CROSS SECTION ERROR		1.657E+00	1.206E-01	0.	2.151E-02	0.
CROSS SECTION	.750	1.818E+02	1.899E+01	1.383E-01	5.790E-01	0.
CROSS SECTION ERROR		2.203E+00	3.262E-01	3.468E-02	5.035E-02	0.
CROSS SECTION	1.000	2.277E+02	1.320E+01	9.593E-01	3.954E-01	0.
CROSS SECTION ERROR		2.577E+00	3.208E-01	7.943E-02	3.601E-02	0.
CROSS SECTION	1.250	3.837E+02	1.422E+01	7.882E-01	3.407E-01	0.
CROSS SECTION ERROR		3.282E+00	3.038E-01	6.441E-02	2.809E-02	0.
CROSS SECTION	1.500	3.976E+02	1.449E+01	5.531E-01	1.491E-01	0.
CROSS SECTION ERROR		4.183E+00	2.885E-01	4.928E-02	1.801E-02	0.
CROSS SECTION	1.750	5.163E+02	1.619E+01	5.889E-01	9.630E-02	0.
CROSS SECTION ERROR		5.362E+00	2.929E-01	4.787E-02	1.339E-02	0.
CROSS SECTION	2.000	6.419E+02	1.701E+01	4.343E-01	1.280E-01	0.
CROSS SECTION ERROR		6.576E+00	2.892E-01	3.777E-02	1.446E-02	0.
CROSS SECTION	2.500	2.246E+03	1.641E+01	0.	0.	0.
CROSS SECTION ERROR		2.259E+01	2.630E-01	0.	0.	0.
CROSS SECTION	2.750	6.613E+03	1.408E+01	0.	0.	0.
CROSS SECTION ERROR		2.895E+02	7.237E-01	0.	0.	0.
CROSS SECTION	2.875	9.308E+03	0.	0.	0.	0.
CROSS SECTION ERROR		2.944E+02	0.	0.	0.	0.
CROSS SECTION	3.000	6.913E+03	1.356E+01	0.	0.	0.
CROSS SECTION ERROR		2.189E+02	6.892E-01	0.	0.	0.

Table 37.

2.1 GEV/NUCLEON DEUTERONS
TARGET = C

	PLAB/Z	PROTONS	DEUTERONS	H-3	HE-3	HE-4
CROSS SECTION	3.250	1.198E+03	1.149E+01	0.	0.	0.
CROSS SECTION ERROR		3.818E+01	5.996E-01	0.	0.	0.
CROSS SECTION	3.500	2.717E+02	9.932E+00	0.	0.	0.
CROSS SECTION ERROR		2.606E+00	1.677E-01	0.	0.	0.
CROSS SECTION	3.750	8.542E+01	1.100E+01	0.	0.	0.
CROSS SECTION ERROR		9.354E-01	1.760E-01	0.	0.	0.
CROSS SECTION	4.000	4.196E+01	1.281E+01	0.	0.	0.
CROSS SECTION ERROR		4.929E-01	1.924E-01	0.	0.	0.
CROSS SECTION	4.000	4.855E+01	1.441E+01	1.701E-01	0.	0.
CROSS SECTION ERROR		4.787E-01	2.037E-01	1.669E-02	0.	0.
CROSS SECTION	4.500	7.510E+00	4.134E+01	0.	0.	0.
CROSS SECTION ERROR		1.277E-01	4.737E-01	0.	0.	0.
CROSS SECTION	5.000	0.	1.898E+02	0.	0.	0.
CROSS SECTION ERROR		0.	1.161E+00	0.	0.	0.

Table 37 (continued).

2.1 GEV/NUCLEON DEUTERONS
TARGET = PB

	PLAB/Z	PROTONS	DEUTERONS	H-3	HE-3	HE-4
CROSS SECTION	.500	1.282E+03	3.068E+01	0.	1.088E+00	0.
CROSS SECTION ERROR		1.776E+01	1.941E+00	0.	3.397E-01	0.
CROSS SECTION	.750	1.224E+03	2.557E+02	1.568E+01	7.067E+00	0.
CROSS SECTION ERROR		1.568E+01	5.196E+00	1.136E+00	5.404E-01	0.
CROSS SECTION	1.000	1.208E+03	2.091E+02	4.484E+01	2.863E+00	0.
CROSS SECTION ERROR		1.465E+01	4.114E+00	1.696E+00	2.967E-01	0.
CROSS SECTION	1.250	1.193E+03	1.483E+02	2.378E+01	1.097E+00	0.
CROSS SECTION ERROR		1.409E+01	2.958E+00	1.103E+00	1.638E-01	0.
CROSS SECTION	1.500	1.378E+03	9.525E+01	1.251E+01	5.877E-01	0.
CROSS SECTION ERROR		1.562E+01	2.186E+00	7.236E-01	1.017E-01	0.
CROSS SECTION	1.750	1.561E+03	7.256E+01	6.719E+00	3.629E-01	0.
CROSS SECTION ERROR		1.721E+01	1.736E+00	4.383E-01	8.173E-02	0.
CROSS SECTION	2.000	1.903E+03	6.881E+01	3.777E+00	3.503E-01	0.
CROSS SECTION ERROR		2.045E+01	1.470E+00	3.413E-01	7.312E-02	0.
CROSS SECTION	2.250	3.490E+03	5.766E+01	2.228E+00	1.218E-01	0.
CROSS SECTION ERROR		3.619E+01	1.368E+00	2.462E-01	4.663E-02	0.
CROSS SECTION	2.500	7.495E+03	4.616E+01	0.	0.	0.
CROSS SECTION ERROR		7.612E+01	1.149E+00	0.	0.	0.
CROSS SECTION	2.500	7.290E+03	4.258E+01	1.511E+00	0.	0.
CROSS SECTION ERROR		7.407E+01	1.097E+00	1.925E-01	0.	0.
CROSS SECTION	2.750	3.600E+04	3.912E+01	0.	0.	0.
CROSS SECTION ERROR		3.610E+02	1.033E+00	0.	0.	0.

Table 38.

2.1 GEV/NUCLEON DEUTERONS
TARGET = PB

	PLAB/Z	PROTONS	DEUTERONS	H-3	HE-3	HE-4
CROSS SECTION	2.875	5.206E+04	3.444E+01	0.	0.	0.
CROSS SECTION ERROR		1.649E+03	2.894E+00	0.	0.	0.
CROSS SECTION	3.000	3.339E+04	3.748E+01	0.	0.	0.
CROSS SECTION ERROR		1.059E+03	2.988E+00	0.	0.	0.
CROSS SECTION	3.250	4.025E+03	2.733E+01	0.	0.	0.
CROSS SECTION ERROR		1.301E+02	2.487E+00	0.	0.	0.
CROSS SECTION	3.250	3.920E+03	3.183E+01	0.622E-01	0.	0.
CROSS SECTION ERROR		5.671E+01	1.174E+00	1.802E-01	0.	0.
CROSS SECTION	3.500	7.879E+02	2.572E+01	0.	0.	0.
CROSS SECTION ERROR		8.680E+00	7.121E-01	0.	0.	0.
CROSS SECTION	3.500	7.727E+02	2.532E+01	2.611E-01	0.	0.
CROSS SECTION ERROR		8.527E+00	7.153E-01	6.746E-02	0.	0.
CROSS SECTION	4.000	9.994E+01	5.108E+01	0.	0.	0.
CROSS SECTION ERROR		1.572E+00	1.813E+00	0.	0.	0.
CROSS SECTION	4.000	9.928E+01	3.615E+01	3.503E-01	0.	0.
CROSS SECTION ERROR		1.565E+00	8.204E-01	7.312E-02	0.	0.

Table 38 (continued).

2.1 GEV/NUCLEON DEUTERONS
TARGET = CH2

	PLAB/Z	PROTONS	DEUTERONS	H-3	HE-3	HE-4
CROSS SECTION	.500	1.396E+02	1.100E+00	0.	6.734E-02	0.
CROSS SECTION ERROR		2.801E+00	1.203E-01	0.	2.246E-02	0.
CROSS SECTION	.750	1.912E+02	1.864E+01	2.394E-01	5.437E-01	0.
CROSS SECTION ERROR		2.353E+00	3.417E-01	4.894E-02	5.236E-02	0.
CROSS SECTION	1.000	2.830E+02	1.251E+01	5.537E-01	3.629E-01	0.
CROSS SECTION ERROR		3.177E+00	3.295E-01	6.461E-02	3.783E-02	0.
CROSS SECTION	1.250	3.651E+02	1.514E+01	6.784E-01	3.173E-01	0.
CROSS SECTION ERROR		4.135E+00	3.368E-01	6.371E-02	3.098E-02	0.
CROSS SECTION	1.500	5.656E+02	1.667E+01	7.383E-01	1.173E-01	0.
CROSS SECTION ERROR		5.896E+00	3.322E-01	6.113E-02	1.714E-02	0.
CROSS SECTION	1.750	6.728E+02	1.839E+01	5.388E-01	1.304E-01	0.
CROSS SECTION ERROR		6.935E+00	3.345E-01	4.838E-02	1.675E-02	0.
CROSS SECTION	2.000	9.482E+02	2.163E+01	3.405E-01	1.141E-01	0.
CROSS SECTION ERROR		9.584E+00	3.566E-01	3.585E-02	1.465E-02	0.
CROSS SECTION	2.500	3.359E+03	2.142E+01	0.	0.	0.
CROSS SECTION ERROR		3.374E+01	3.310E-01	0.	0.	0.
CROSS SECTION	2.750	8.465E+03	1.711E+01	0.	0.	0.
CROSS SECTION ERROR		2.681E+02	8.689E-01	0.	0.	0.
CROSS SECTION	2.875	1.209E+04	1.631E+01	0.	0.	0.
CROSS SECTION ERROR		3.828E+02	8.293E-01	0.	0.	0.
CROSS SECTION	3.000	8.619E+03	1.828E+01	0.	0.	0.
CROSS SECTION ERROR		2.729E+02	8.872E-01	0.	0.	0.

Table 39.

2.1 GEV/NUCLEON DEUTERONS
TARGET = CH2

	PLAB/Z	PROTONS	DEUTERONS	H-3	HE-3	HE-4
CROSS SECTION	3.250	1.519E+03	1.194E+01	0.	0.	0.
CROSS SECTION ERROR		4.838E+01	6.446E-01	0.	0.	0.
CROSS SECTION	3.250	1.599E+03	1.511E+01	4.374E-01	0.	0.
CROSS SECTION ERROR		2.277E+01	3.387E-01	4.531E-02	0.	0.
CROSS SECTION	3.500	3.696E+02	1.330E+01	0.	0.	0.
CROSS SECTION ERROR		3.998E+00	2.152E-01	0.	0.	0.
CROSS SECTION	3.750	1.263E+02	1.510E+01	0.	0.	0.
CROSS SECTION ERROR		1.358E+00	2.296E-01	0.	0.	0.
CROSS SECTION	4.000	6.464E+01	2.137E+01	0.	0.	0.
CROSS SECTION ERROR		7.327E-01	2.921E-01	0.	0.	0.
CROSS SECTION	4.000	6.591E+01	2.146E+01	1.627E-01	0.	0.
CROSS SECTION ERROR		7.455E-01	2.931E-01	1.752E-02	0.	0.
CROSS SECTION	4.500	1.212E+01	6.490E+01	0.	0.	0.
CROSS SECTION ERROR		1.858E-01	7.270E-01	0.	0.	0.
CROSS SECTION	5.000	0.	1.739E+02	0.	0.	0.
CROSS SECTION ERROR		0.	1.812E+00	0.	0.	0.

Table 39 (continued).

1.05 GEV/NUCLEON ALPHAS
TARGET = BE

	PLAB/Z	PROTONS	DEUTERONS	H-3	HE-3	HE-4
CROSS SECTION	.500	1.246E+02	7.785E-01	0.	0.	0.
CROSS SECTION ERROR		5.808E+00	2.449E-01	0.	0.	0.
CROSS SECTION	1.000	4.984E+02	2.454E+01	8.623E-01	1.657E+00	7.137E-01
CROSS SECTION ERROR		8.050E+00	6.221E-01	9.241E-02	9.334E-02	5.988E-02
CROSS SECTION	1.250	9.297E+02	3.823E+01	1.132E+00	1.698E+00	4.284E-01
CROSS SECTION ERROR		1.494E+01	8.125E-01	9.535E-02	8.522E-02	4.140E-02
CROSS SECTION	1.500	3.724E+03	4.832E+01	1.634E+00	2.157E+00	5.777E-01
CROSS SECTION ERROR		5.908E+01	9.455E-01	1.059E-01	9.617E-02	4.425E-02
CROSS SECTION	1.750	1.831E+04	6.109E+01	1.819E+00	3.903E+00	7.678E-01
CROSS SECTION ERROR		2.307E+02	1.593E+00	1.086E-01	1.710E-01	6.757E-02
CROSS SECTION	2.000	2.646E+03	6.483E+01	1.647E+00	1.569E+01	8.568E-01
CROSS SECTION ERROR		5.938E+01	1.651E+00	1.316E-01	4.508E-01	6.736E-02
CROSS SECTION	2.250	2.776E+02	8.202E+01	1.860E+00	2.678E+02	1.817E+00
CROSS SECTION ERROR		9.845E+00	2.852E+00	1.864E-01	8.684E+00	1.380E-01
CROSS SECTION	2.375	1.969E+02	1.377E+02	2.048E+00	8.437E+02	0.
CROSS SECTION ERROR		6.476E+00	3.653E+00	1.935E-01	2.681E+01	0.
CROSS SECTION	2.500	0.	1.156E+02	0.	2.148E+03	1.137E+00
CROSS SECTION ERROR		0.	3.691E+00	0.	6.788E+01	1.837E-01
CROSS SECTION	2.625	0.	2.436E+02	0.	2.565E+03	0.
CROSS SECTION ERROR		0.	7.933E+00	0.	8.123E+01	0.
CROSS SECTION	2.750	0.	4.281E+02	0.	3.668E+02	0.
CROSS SECTION ERROR		0.	1.376E+01	0.	1.171E+01	0.

Table 40.

1.05 GEV/NUCLEON ALPHAS
TARGET = BE

	PLAB/Z	PROTONS	DEUTERONS	H-3	HE-3	HE-4
CROSS SECTION	3.000	0.	1.896E+03	3.049E+00	1.044E+01	3.023E+01
CROSS SECTION ERROR		0.	3.486E+01	2.286E-01	4.282E-01	1.054E+00
CROSS SECTION	3.125	0.	2.145E+03	0.	3.786E+01	1.285E+02
CROSS SECTION ERROR		0.	2.109E+02	0.	4.085E+00	1.290E+01
CROSS SECTION	3.125	0.	2.978E+03	0.	0.	0.
CROSS SECTION ERROR		0.	6.567E+01	0.	0.	0.
CROSS SECTION	3.250	0.	3.668E+03	4.819E+00	0.	3.175E+02
CROSS SECTION ERROR		0.	1.159E+02	2.531E-01	0.	1.013E+01
CROSS SECTION	3.333	0.	0.	0.	0.	0.
CROSS SECTION ERROR		0.	0.	0.	0.	0.
CROSS SECTION	3.375	0.	5.613E+03	0.	0.	1.275E+03
CROSS SECTION ERROR		0.	5.618E+02	0.	0.	1.278E+02
CROSS SECTION	3.438	0.	5.898E+03	0.	0.	3.500E+03
CROSS SECTION ERROR		0.	1.867E+02	0.	0.	1.138E+02
CROSS SECTION	3.470	0.	7.296E+03	0.	0.	1.047E+04
CROSS SECTION ERROR		0.	2.280E+02	0.	0.	3.310E+02
CROSS SECTION	3.625	0.	4.124E+03	3.410E+00	0.	0.
CROSS SECTION ERROR		0.	1.306E+02	2.193E-01	0.	0.
CROSS SECTION	4.000	0.	1.792E+02	2.575E+01	0.	0.
CROSS SECTION ERROR		0.	5.816E+00	9.553E-01	0.	0.
CROSS SECTION	4.500	0.	1.372E+01	3.341E+02	0.	0.
CROSS SECTION ERROR		0.	5.528E-01	1.078E+01	0.	0.

Table 40 (continued).

1.05 GEV/NUCLEON ALPHAS
TARGET = BE

	PLAB/Z	PROTONS	DEUTERONS	H-3	HE-3	HE-4
CROSS SECTION	4.750	0.	0.	1.256E+03	0.	0.
CROSS SECTION ERROR		0.	0.	3.988E+01	0.	0.
CROSS SECTION	4.875	0.	0.	1.068E+03	0.	0.
CROSS SECTION ERROR		0.	0.	5.928E+01	0.	0.
CROSS SECTION	5.000	0.	0.	3.217E+03	0.	0.
CROSS SECTION ERROR		0.	0.	1.018E+02	0.	0.
CROSS SECTION	3.563					0.0
CROSS SECTION ERROR						1.878E+00

Table 40(continued).

1.05 GEV/NUCLEON ALPHAS
TARGET = C

	PLAB/Z	PROTONS	DEUTERONS	H-3	HE-3	HE-4
CROSS SECTION	.500	1.666E+02	2.847E+00	0.	0.	0.
CROSS SECTION ERROR		7.056E+00	5.159E-01	0.	0.	0.
CROSS SECTION	.750	3.844E+02	1.634E+01	3.436E-01	7.381E-01	1.643E+00
CROSS SECTION ERROR		1.343E+01	1.379E+00	1.721E-01	1.706E-01	2.715E-01
CROSS SECTION	1.000	5.661E+02	3.536E+01	1.766E+00	1.986E+00	7.701E-01
CROSS SECTION ERROR		9.787E+00	9.375E-01	1.720E-01	1.276E-01	7.995E-02
CROSS SECTION	1.250	1.075E+03	5.104E+01	2.074E+00	2.274E+00	5.837E-01
CROSS SECTION ERROR		1.739E+01	1.142E+00	1.667E-01	1.263E-01	6.221E-02
CROSS SECTION	1.500	4.232E+03	6.139E+01	2.276E+00	2.786E+00	7.945E-01
CROSS SECTION ERROR		6.725E+01	1.247E+00	1.684E-01	1.308E-01	6.672E-02
CROSS SECTION	1.750	1.142E+04	7.812E+01	3.092E+00	4.620E+00	1.001E+00
CROSS SECTION ERROR		3.616E+02	2.735E+00	3.513E-01	3.261E-01	1.390E-01
CROSS SECTION	2.000	2.077E+03	7.431E+01	1.836E+00	1.681E+01	1.151E+00
CROSS SECTION ERROR		9.149E+01	2.811E+00	2.500E-01	7.439E-01	1.414E-01
CROSS SECTION	2.250	3.108E+02	8.912E+01	2.205E+00	2.755E+02	1.802E+00
CROSS SECTION ERROR		1.826E+01	3.237E+00	2.607E-01	8.934E+00	1.709E-01
CROSS SECTION	2.375	2.817E+02	1.224E+02	2.848E+00	9.448E+02	0.
CROSS SECTION ERROR		6.766E+00	4.277E+00	2.922E-01	3.809E+01	0.
CROSS SECTION	2.500	0.	1.643E+02	0.	2.255E+03	0.
CROSS SECTION ERROR		0.	5.586E+00	0.	7.158E+01	0.
CROSS SECTION	2.625	6.905E+01	2.510E+02	0.	3.817E+03	0.
CROSS SECTION ERROR		2.537E+00	8.315E+00	0.	9.561E+01	0.

Table 41.

1.85 GEV/NUCLEON ALPHAS
TARGET = C

	PLAB/Z	PROTONS	DEUTERONS	H-3	HE-3	HE-4
CROSS SECTION	2.750	0.	3.888E+02	0.	4.544E+02	3.809E+00
CROSS SECTION ERROR		0.	1.263E+01	0.	1.455E+01	2.438E-01
CROSS SECTION	3.000	0.	1.158E+03	2.813E+00	1.178E+01	2.976E+01
CROSS SECTION ERROR		0.	3.694E+01	2.614E-01	5.[illegible]9E-01	1.099E+00
CROSS SECTION	3.125	0.	2.167E+03	0.	0.	1.726E+02
CROSS SECTION ERROR		0.	6.883E+01	0.	0.	5.619E+00
CROSS SECTION	3.250	0.	3.448E+03	3.645E+00	0.	2.923E+02
CROSS SECTION ERROR		0.	1.094E+02	3.817E-01	0.	9.431E+00
CROSS SECTION	3.333	0.	0.	0.	0.	0.
CROSS SECTION ERROR		0.	0.	0.	0.	0.
CROSS SECTION	3.375	0.	5.289E+03	0.	0.	1.228E+03
CROSS SECTION ERROR		0.	1.674E+02	0.	0.	3.899E+01
CROSS SECTION	3.438	0.	6.226E+03	0.	0.	3.149E+03
CROSS SECTION ERROR		0.	1.972E+02	0.	0.	9.973E+01
CROSS SECTION	3.470	0.	6.681E+03	0.	0.	9.614E+03
CROSS SECTION ERROR		0.	2.090E+02	0.	0.	3.042E+02
CROSS SECTION	3.625	0.	4.335E+03	4.727E+00	0.	0.
CROSS SECTION ERROR		0.	1.374E+02	3.261E-01	0.	0.
CROSS SECTION	4.000	0.	1.663E+02	2.031E+01	0.	0.
CROSS SECTION ERROR		0.	5.587E+00	1.121E+00	0.	0.
CROSS SECTION	4.500	0.	1.321E+01	3.135E+02	0.	0.
CROSS SECTION ERROR		0.	6.819E-01	1.014E+01	0.	0.

Table 41 (continued).

1.85 GEV/NUCLEON ALPHAS
TARGET = C

	PLAB/Z	PROTONS	DEUTERONS	H-3	HE-3	HE-4
CROSS SECTION	4.750	0.	0.	1.244E+03	0.	0.
CROSS SECTION ERROR		0.	0.	3.954E+01	0.	0.
CROSS SECTION	4.875	0.	0.	1.929E+03	0.	0.
CROSS SECTION ERROR		0.	0.	6.122E+01	0.	0.
CROSS SECTION	5.000	0.	0.	3.092E+03	0.	0.
CROSS SECTION ERROR		0.	0.	9.798E+01	0.	0.
CROSS SECTION	3.563					0.0
CROSS SECTION ERROR						1.413E+00

Table 41(continued).

1.05 GEV/NUCLEON ALPHAS
TARGET = PB

	PLAB/Z	PROTONS	DEUTERONS	H-3	HE-3	HE-4
CROSS SECTION	.750	1.926E+03	3.835E+02	7.281E+01	2.944E+01	2.465E+01
CROSS SECTION ERROR		2.230E+01	5.427E+00	2.336E+00	1.040E+00	9.516E-01
CROSS SECTION	1.000	2.231E+03	3.369E+02	5.958E+01	7.633E+00	6.551E+00
CROSS SECTION ERROR		1.559E+01	3.358E+00	1.163E+00	2.825E-01	2.628E-01
CROSS SECTION	1.250	3.209E+03	2.887E+02	4.253E+01	5.329E+00	2.468E+00
CROSS SECTION ERROR		5.375E+01	6.910E+00	2.184E+00	5.269E-01	3.584E-01
CROSS SECTION	1.500	1.104E+04	2.268E+02	2.411E+01	5.879E+00	2.657E+00
CROSS SECTION ERROR		1.772E+02	5.635E+00	1.478E+00	5.072E-01	3.400E-01
CROSS SECTION	1.750	3.210E+04	2.197E+02	1.552E+01	1.030E+01	3.335E+00
CROSS SECTION ERROR		7.210E+02	7.450E+00	1.540E+00	8.941E-01	4.983E-01
CROSS SECTION	2.000	7.648E+03	2.097E+02	1.472E+01	3.692E+01	3.471E+00
CROSS SECTION ERROR		2.457E+02	9.818E+00	1.988E+00	2.459E+00	6.769E-01
CROSS SECTION	2.250	7.943E+02	2.551E+02	7.218E+00	7.597E+02	3.999E+00
CROSS SECTION ERROR		2.836E+01	1.103E+01	1.296E+00	2.575E+01	6.877E-01
CROSS SECTION	2.375	5.490E+02	2.901E+02	7.266E+00	2.622E+03	0.
CROSS SECTION ERROR		2.837E+01	1.205E+01	1.267E+00	8.458E+01	0.
CROSS SECTION	2.500	3.362E+02	4.399E+02	0.	8.636E+03	0.
CROSS SECTION ERROR		1.338E+01	1.678E+01	0.	2.747E+02	0.
CROSS SECTION	2.625	2.424E+02	7.294E+02	0.	8.345E+03	0.
CROSS SECTION ERROR		1.028E+01	2.598E+01	0.	2.654E+02	0.
CROSS SECTION	2.750	0.	1.858E+03	0.	1.032E+03	1.449E+01
CROSS SECTION ERROR		0.	3.596E+01	0.	3.406E+01	1.251E+00

Table 42.

1.05 GEV/NUCLEON ALPHAS
TARGET = PB

	PLAB/Z	PROTONS	DEUTERONS	H-3	HE-3	HE-4
CROSS SECTION	3.000	0.	2.671E+03	8.459E+00	2.605E+01	7.337E+01
CROSS SECTION ERROR		0.	8.705E+01	1.226E+00	1.698E+00	3.433E+00
CROSS SECTION	3.125	0.	5.858E+03	0.	0.	4.862E+02
CROSS SECTION ERROR		0.	1.875E+02	0.	0.	1.663E+01
CROSS SECTION	3.250	0.	1.048E+04	7.183E+00	0.	8.995E+02
CROSS SECTION ERROR		0.	3.338E+02	1.083E+00	0.	2.967E+01
CROSS SECTION	3.333	0.	0.	0.	0.	0.
CROSS SECTION ERROR		0.	0.	0.	0.	0.
CROSS SECTION	3.375	0.	1.496E+04	0.	0.	4.328E+03
CROSS SECTION ERROR		0.	4.753E+02	0.	0.	1.381E+02
CROSS SECTION	3.438	0.	1.715E+04	0.	0.	1.237E+04
CROSS SECTION ERROR		0.	5.445E+02	0.	0.	3.924E+02
CROSS SECTION	3.470	0.	3.386E+04	0.	0.	4.522E+04
CROSS SECTION ERROR		0.	1.073E+03	0.	0.	1.431E+03
CROSS SECTION	3.625	0.	1.075E+04	1.232E+01	0.	0.
CROSS SECTION ERROR		0.	3.420E+02	1.378E+00	0.	0.
CROSS SECTION	4.000	0.	4.896E+02	6.369E+01	0.	0.
CROSS SECTION ERROR		0.	1.480E+01	3.484E+00	0.	0.
CROSS SECTION	4.500	0.	3.277E+01	8.330E+02	0.	0.
CROSS SECTION ERROR		0.	2.171E+00	2.807E+01	0.	0.
CROSS SECTION	4.750	0.	0.	3.216E+03	0.	0.
CROSS SECTION ERROR		0.	0.	1.034E+02	0.	0.

Table 42 (continued).

1.05 GEV/NUCLEON ALPHAS
TARGET = PB

	PLAB/Z	PROTONS	DEUTERONS	H-3	HE-3	HE-4
CROSS SECTION	4.675	0.	0.	5.872E+03	0.	0.
CROSS SECTION ERROR		0.	0.	1.873E+02	0.	0.
CROSS SECTION	5.000	0.	0.	9.438E+03	0.	0.
CROSS SECTION ERROR		0.	0.	2.998E+02	0.	0.
CROSS SECTION	3.563					0.0
CROSS SECTION ERROR						1.231E+01

Table 42(continued).

1.05 GEV/NUCLEON ALPHAS
TARGET = CH2

	PLAB/Z	PROTONS	DEUTERONS	H-3	HE-3	HE-4
CROSS SECTION	.750	4.339E+02	1.668E+01	0.	0.	7.497E-01
CROSS SECTION ERROR		1.502E+01	1.324E+00	0.	0.	1.034E-01
CROSS SECTION	1.000	7.354E+02	3.638E+01	1.528E+00	1.807E+00	7.773E-01
CROSS SECTION ERROR		1.213E+01	9.615E-01	1.682E-01	1.251E-01	8.110E-02
CROSS SECTION	1.250	1.375E+03	5.446E+01	1.997E+00	2.352E+00	7.012E-01
CROSS SECTION ERROR		2.214E+01	1.205E+00	1.651E-01	1.298E-01	6.900E-02
CROSS SECTION	1.500	4.832E+03	6.709E+01	2.073E+00	3.019E+00	7.160E-01
CROSS SECTION ERROR		8.852E+01	1.429E+00	1.618E-01	1.439E-01	6.697E-02
CROSS SECTION	1.750	1.437E+04	8.871E+01	2.046E+00	5.801E+00	1.399E+00
CROSS SECTION ERROR		3.218E+02	2.364E+00	2.013E-01	2.670E-01	1.131E-01
CROSS SECTION	2.000	3.358E+03	6.297E+01	1.938E+00	2.285E+01	1.025E+00
CROSS SECTION ERROR		1.067E+02	3.897E+00	2.597E-01	9.473E-01	1.342E-01
CROSS SECTION	2.250	4.328E+02	1.138E+02	2.365E+00	3.998E+02	2.455E+00
CROSS SECTION ERROR		1.413E+01	4.832E+00	2.733E-01	1.287E+01	2.052E-01
CROSS SECTION	2.375	3.599E+02	1.414E+02	3.154E+00	1.332E+03	0.
CROSS SECTION ERROR		1.180E+01	4.867E+00	3.118E-01	4.233E+01	0.
CROSS SECTION	2.500	8.727E+01	2.016E+02	0.	3.180E+03	0.
CROSS SECTION ERROR		3.142E+00	6.777E+00	0.	1.008E+02	0.
CROSS SECTION	2.625	1.021E+02	2.969E+02	0.	4.131E+03	2.936E+00
CROSS SECTION ERROR		3.596E+00	9.775E+00	0.	1.308E+02	2.136E-01
CROSS SECTION	2.750	0.	5.508E+02	0.	5.002E+02	9.814E+00
CROSS SECTION ERROR		0.	1.779E+01	0.	1.601E+01	4.630E-01

Table 43.

1.05 GEV/NUCLEON ALPHAS
TARGET = CH2

	PLAB/Z	PROTONS	DEUTERONS	H-3	HE-3	HE-4
CROSS SECTION	3.000	0.	1.543E+03	4.038E+00	2.175E+01	4.520E+01
CROSS SECTION ERROR		0.	4.915E+01	3.233E-01	8.433E-01	1.594E+00
CROSS SECTION	3.125	0.	3.033E+03	0.	0.	2.535E+02
CROSS SECTION ERROR		0.	9.625E+01	0.	0.	8.182E+00
CROSS SECTION	3.250	0.	4.845E+03	5.014E+00	0.	3.852E+02
CROSS SECTION ERROR		0.	1.535E+02	3.557E-01	0.	1.234E+01
CROSS SECTION	3.333	0.	0.	0.	0.	0.
CROSS SECTION ERROR		0.	0.	0.	0.	0.
CROSS SECTION	3.375	0.	7.435E+03	0.	0.	1.535E+03
CROSS SECTION ERROR		0.	2.354E+02	0.	0.	4.869E+01
CROSS SECTION	3.438	0.	8.812E+03	0.	0.	4.557E+03
CROSS SECTION ERROR		0.	2.798E+02	0.	0.	1.443E+02
CROSS SECTION	3.478	0.	2.270E+04	0.	0.	1.445E+04
CROSS SECTION ERROR		0.	7.181E+02	0.	0.	4.571E+02
CROSS SECTION	3.625	0.	5.239E+03	6.416E+00	0.	0.
CROSS SECTION ERROR		0.	1.659E+02	3.960E-01	0.	0.
CROSS SECTION	4.000	0.	2.578E+02	3.017E+01	0.	0.
CROSS SECTION ERROR		0.	8.405E+00	1.186E+00	0.	0.
CROSS SECTION	4.500	0.	1.781E+01	4.468E+02	0.	0.
CROSS SECTION ERROR		0.	7.585E-01	1.436E+01	0.	0.
CROSS SECTION	4.750	0.	0.	2.715E+03	0.	0.
CROSS SECTION ERROR		0.	0.	5.446E+01	0.	0.

Table 43 (continued).

1.05 GEV/NUCLEON ALPHAS
TARGET = CH2

	PLAB/Z	PROTONS	DEUTERONS	H-3	HE-3	HE-4
CROSS SECTION	4.675	0.	0.	3.127E+03	0.	0.
CROSS SECTION ERROR		0.	0.	9.909E+01	0.	0.
CROSS SECTION	5.000	0.	0.	3.916E+03	0.	0.
CROSS SECTION ERROR		0.	0.	1.240E+02	0.	0.

Table 43 (continued).

2.1 GEV/NUCLEON ALPHAS
TARGET = BE

	PLAB/Z	PROTONS	DEUTERONS	H-3	HE-3	HE-4
CROSS SECTION	.500	1.061E+02	4.698E-01	0.	0.	0.
CROSS SECTION ERROR		3.566E+00	1.779E-01	0.	0.	0.
CROSS SECTION	.750	2.033E+02	7.122E+00	0.	3.248E-01	0.
CROSS SECTION ERROR		3.446E+00	3.710E-01	0.	5.420E-02	0.
CROSS SECTION	1.000	3.093E+02	1.212E+01	4.185E-01	3.983E-01	0.
CROSS SECTION ERROR		4.823E+00	4.392E-01	7.548E-02	5.216E-02	0.
CROSS SECTION	1.250	4.322E+02	1.421E+01	5.400E-01	4.158E-01	0.
CROSS SECTION ERROR		4.582E+00	3.106E-01	5.427E-02	3.377E-02	0.
CROSS SECTION	1.500	6.177E+02	1.747E+01	6.030E-01	4.635E-01	0.
CROSS SECTION ERROR		6.395E+00	3.296E-01	5.244E-02	3.263E-02	0.
CROSS SECTION	1.750	8.270E+02	2.117E+01	5.400E-01	5.400E-01	0.
CROSS SECTION ERROR		1.196E+01	5.020E-01	6.500E-02	4.628E-02	0.
CROSS SECTION	2.000	1.147E+03	2.599E+01	4.894E-01	6.750E-01	0.
CROSS SECTION ERROR		2.601E+01	8.771E-01	9.154E-02	7.697E-02	0.
CROSS SECTION	2.250	2.039E+03	3.126E+01	6.380E-01	1.020E+00	0.
CROSS SECTION ERROR		6.495E+01	1.382E+00	1.389E-01	1.278E-01	0.
CROSS SECTION	2.500	3.750E+03	3.355E+01	0.	0.	0.
CROSS SECTION ERROR		1.190E+02	1.424E+00	0.	0.	0.
CROSS SECTION	2.750	7.697E+03	4.361E+01	0.	0.	0.
CROSS SECTION ERROR		2.438E+02	1.722E+00	0.	0.	0.
CROSS SECTION	2.813	7.702E+03	0.	0.	0.	0.
CROSS SECTION ERROR		2.439E+02	0.	0.	0.	0.

Table 44.

2.1 GEV/NUCLEON ALPHAS
TARGET = BE

	PLAB/Z	PROTONS	DEUTERONS	H-3	HE-3	HE-4
CROSS SECTION	2.875	7.845E+03	0.	0.	0.	0.
CROSS SECTION ERROR		2.484E+02	0.	0.	0.	0.
CROSS SECTION	3.000	7.043E+03	3.617E+01	0.	0.	0.
CROSS SECTION ERROR		2.231E+02	1.455E+00	0.	0.	0.
CROSS SECTION	3.250	2.636E+03	3.610E+01	0.	0.	0.
CROSS SECTION ERROR		1.513E+02	2.588E+00	0.	0.	0.
CROSS SECTION	3.500	9.694E+02	4.891E+01	0.	0.	0.
CROSS SECTION ERROR		5.507E+01	3.246E+00	0.	0.	0.
CROSS SECTION	3.750	0.	5.825E+01	8.641E-01	9.467E+01	0.
CROSS SECTION ERROR		0.	2.106E+00	1.277E-01	3.133E+00	0.
CROSS SECTION	4.000	2.502E+02	5.485E+01	0.	3.667E+02	0.
CROSS SECTION ERROR		1.273E+01	3.888E+00	0.	1.828E+01	0.
CROSS SECTION	4.250	0.	0.	0.	6.543E+02	0.
CROSS SECTION ERROR		0.	0.	0.	2.081E+01	0.
CROSS SECTION	4.500	0.	0.	0.	1.277E+02	0.
CROSS SECTION ERROR		0.	0.	0.	4.154E+00	0.
CROSS SECTION	4.750	0.	0.	0.	2.076E+01	0.
CROSS SECTION ERROR		0.	0.	0.	7.605E-01	0.
CROSS SECTION	5.000	0.	7.188E+02	0.	0.	0.
CROSS SECTION ERROR		0.	2.294E+01	0.	0.	0.

Table 44 (continued).

2.1 GEV/NUCLEON ALPHAS
TARGET = C

	PLAB/Z	PROTONS	DEUTERONS	H-3	HE-3	HE-4
CROSS SECTION	.500	1.498E+02	1.450E+00	0.	0.	0.
CROSS SECTION ERROR		3.289E+00	2.495E-01	0.	0.	0.
CROSS SECTION	.750	2.627E+02	1.358E+01	0.	8.380E-01	0.
CROSS SECTION ERROR		4.605E+00	7.818E-01	0.	1.096E-01	0.
CROSS SECTION	1.000	3.823E+02	1.930E+01	1.224E+00	8.694E-01	0.
CROSS SECTION ERROR		6.109E+00	6.978E-01	1.630E-01	9.738E-02	0.
CROSS SECTION	1.250	5.412E+02	2.270E+01	1.082E+00	8.286E-01	0.
CROSS SECTION ERROR		5.819E+00	4.931E-01	9.699E-02	6.022E-02	0.
CROSS SECTION	1.500	7.431E+02	2.581E+01	1.138E+00	8.121E-01	0.
CROSS SECTION ERROR		7.775E+00	5.000E-01	9.094E-02	5.451E-02	0.
CROSS SECTION	1.750	9.705E+02	2.935E+01	1.349E+00	7.053E-01	0.
CROSS SECTION ERROR		1.415E+01	7.279E-01	1.301E-01	6.652E-02	0.
CROSS SECTION	2.000	1.567E+03	4.120E+01	1.154E+00	1.140E+00	0.
CROSS SECTION ERROR		3.563E+01	1.395E+00	1.778E-01	1.263E-01	0.
CROSS SECTION	2.250	2.198E+03	3.672E+01	1.049E+00	7.633E-01	0.
CROSS SECTION ERROR		7.024E+01	1.757E+00	2.262E-01	1.371E-01	0.
CROSS SECTION	2.500	4.254E+03	4.166E+01	7.728E-01	0.	0.
CROSS SECTION ERROR		1.352E+02	1.674E+00	1.838E-01	0.	0.
CROSS SECTION	2.750	7.115E+03	4.836E+01	0.	0.	0.
CROSS SECTION ERROR		2.256E+02	2.852E+00	0.	0.	0.
CROSS SECTION	2.813	9.299E+03	0.	0.	0.	0.
CROSS SECTION ERROR		2.946E+02	0.	0.	0.	0.

Table 45.

2.1 GEV/NUCLEON ALPHAS
TARGET = C

	PLAB/Z	PROTONS	DEUTERONS	H-3	HE-3	HE-4
CROSS SECTION	2.875	8.599E+03	0.	0.	0.	0.
CROSS SECTION ERROR		2.725E+02	0.	0.	0.	0.
CROSS SECTION	3.000	1.149E+04	5.841E+01	0.	0.	0.
CROSS SECTION ERROR		6.170E+02	3.971E+00	0.	0.	0.
CROSS SECTION	3.250	4.615E+03	5.799E+01	0.	0.	0.
CROSS SECTION ERROR		2.648E+02	4.148E+00	0.	0.	0.
CROSS SECTION	3.500	1.148E+03	5.199E+01	0.	0.	0.
CROSS SECTION ERROR		3.676E+01	2.067E+00	0.	0.	0.
CROSS SECTION	3.750	0.	6.685E+01	0.	1.171E+02	0.
CROSS SECTION ERROR		0.	2.588E+00	0.	3.924E+00	0.
CROSS SECTION	4.000	2.844E+02	5.527E+01	0.	3.967E+02	0.
CROSS SECTION ERROR		1.429E+01	3.234E+00	0.	1.939E+01	0.
CROSS SECTION	4.250	0.	0.	0.	6.518E+02	0.
CROSS SECTION ERROR		0.	0.	0.	3.417E+01	0.
CROSS SECTION	4.500	0.	0.	0.	1.120E+02	0.
CROSS SECTION ERROR		0.	0.	0.	3.727E+00	0.
CROSS SECTION	4.750	0.	0.	0.	2.191E+01	0.
CROSS SECTION ERROR		0.	0.	0.	8.529E-01	0.
CROSS SECTION	5.000	0.	0.	0.	0.	0.
CROSS SECTION ERROR		0.	0.	0.	0.	0.

Table 45 (continued).

2.1 GEV/NUCLEON ALPHAS
TARGET = PB

	PLAB/Z	PROTONS	DEUTERONS	H-3	HE-3	HE-4
CROSS SECTION	.500	1.985E+03	3.555E+01	0.	3.292E+00	0.
CROSS SECTION ERROR		2.936E+01	2.944E+00	0.	6.345E-01	0.
CROSS SECTION	.750	2.465E+03	4.377E+02	0.	2.260E+01	0.
CROSS SECTION ERROR		3.155E+01	9.448E+00	0.	1.374E+00	0.
CROSS SECTION	1.000	2.328E+03	4.189E+02	8.670E+01	1.055E+01	0.
CROSS SECTION ERROR		2.858E+01	8.237E+00	3.365E+00	8.089E-01	0.
CROSS SECTION	1.250	2.446E+03	3.444E+02	7.278E+01	6.195E+00	0.
CROSS SECTION ERROR		2.888E+01	6.789E+00	2.762E+00	5.532E-01	0.
CROSS SECTION	1.500	2.736E+03	2.508E+02	4.935E+01	4.065E+00	0.
CROSS SECTION ERROR		3.184E+01	5.135E+00	2.063E+00	4.085E-01	0.
CROSS SECTION	1.750	3.086E+03	2.063E+02	3.212E+01	3.031E+00	0.
CROSS SECTION ERROR		3.486E+01	4.292E+00	1.538E+00	3.264E-01	0.
CROSS SECTION	2.000	4.147E+03	1.880E+02	2.012E+01	1.982E+00	0.
CROSS SECTION ERROR		9.911E+01	6.589E+00	2.517E+00	5.514E-01	0.
CROSS SECTION	2.250	6.166E+03	1.607E+02	9.755E+00	4.065E+00	0.
CROSS SECTION ERROR		2.031E+02	1.056E+01	2.328E+00	1.057E+00	0.
CROSS SECTION	2.500	1.292E+04	1.302E+02	0.	0.	0.
CROSS SECTION ERROR		4.168E+02	8.917E+00	0.	0.	0.
CROSS SECTION	2.750	2.916E+04	1.594E+02	0.	0.	0.
CROSS SECTION ERROR		9.288E+02	9.749E+00	0.	0.	0.
CROSS SECTION	2.813	3.192E+04	0.	0.	0.	0.
CROSS SECTION ERROR		1.816E+03	0.	0.	0.	0.

Table 46.

2.1 GEV/NUCLEON ALPHAS
TARGET = PB

	PLAB/Z	PROTONS	DEUTERONS	H-3	HE-3	HE-4
CROSS SECTION	2.875	2.846E+04	0.	0.	0.	0.
CROSS SECTION ERROR		9.064E+02	0.	0.	0.	0.
CROSS SECTION	3.000	2.678E+04	1.317E+02	0.	0.	0.
CROSS SECTION ERROR		9.162E+02	6.372E+00	0.	0.	0.
CROSS SECTION	3.250	1.196E+04	1.778E+02	0.	0.	0.
CROSS SECTION ERROR		3.848E+02	9.864E+00	0.	0.	0.
CROSS SECTION	3.500	3.323E+03	1.452E+02	0.	0.	0.
CROSS SECTION ERROR		1.103E+02	8.420E+00	0.	0.	0.
CROSS SECTION	3.750	0.	1.730E+02	2.927E+00	3.863E+02	0.
CROSS SECTION ERROR		0.	6.531E+00	6.929E-01	8.475E+00	0.
CROSS SECTION	4.000	7.130E+02	1.516E+02	0.	1.418E+03	0.
CROSS SECTION ERROR		2.601E+01	8.278E+00	0.	4.719E+01	0.
CROSS SECTION	4.250	0.	0.	0.	2.716E+03	0.
CROSS SECTION ERROR		0.	0.	0.	8.813E+01	0.
CROSS SECTION	4.500	0.	0.	0.	3.862E+02	0.
CROSS SECTION ERROR		0.	0.	0.	1.004E+01	0.
CROSS SECTION	4.750	0.	0.	0.	6.238E+01	0.
CROSS SECTION ERROR		0.	0.	0.	2.439E+00	0.
CROSS SECTION	5.000	0.	2.521E+03	0.	0.	0.
CROSS SECTION ERROR		0.	8.345E+01	0.	0.	0.

Table 46 (continued).

2.1 GEV/NUCLEON ALPHAS
TARGET = CH2

	PLAB/Z	PROTONS	DEUTERONS	H-3	HE-3	HE-4
CROSS SECTION	.500	1.545E+02	6.052E-01	0.	0.	0.
CROSS SECTION ERROR		3.309E+00	1.569E-01	0.	0.	0.
CROSS SECTION	.750	2.798E+02	1.124E+01	0.	6.771E-01	0.
CROSS SECTION ERROR		4.889E+00	5.725E-01	0.	9.623E-02	0.
CROSS SECTION	1.000	3.591E+02	1.872E+01	1.341E+00	7.313E-01	0.
CROSS SECTION ERROR		4.061E+00	4.732E-01	1.175E-01	6.130E-02	0.
CROSS SECTION	1.250	4.369E+02	2.225E+01	1.406E+00	6.906E-01	0.
CROSS SECTION ERROR		5.353E+00	4.786E-01	1.078E-01	5.342E-02	0.
CROSS SECTION	1.500	8.338E+02	2.375E+01	9.953E-01	6.399E-01	0.
CROSS SECTION ERROR		8.657E+00	4.649E-01	8.269E-02	4.698E-02	0.
CROSS SECTION	1.750	1.134E+03	2.824E+01	1.010E+00	7.835E-01	0.
CROSS SECTION ERROR		1.643E+01	5.965E-01	1.092E-01	6.834E-02	0.
CROSS SECTION	2.000	1.578E+03	3.667E+01	7.189E-01	9.776E-01	0.
CROSS SECTION ERROR		3.584E+01	1.264E+00	1.353E-01	1.135E-01	0.
CROSS SECTION	2.250	2.667E+03	4.152E+01	5.868E-01	1.151E+00	0.
CROSS SECTION ERROR		8.534E+01	1.853E+00	1.638E-01	1.652E-01	0.
CROSS SECTION	2.500	4.913E+03	3.631E+01	0.	0.	0.
CROSS SECTION ERROR		1.560E+02	1.669E+00	0.	0.	0.
CROSS SECTION	2.750	1.836E+04	5.752E+01	0.	0.	0.
CROSS SECTION ERROR		3.281E+02	2.328E+00	0.	0.	0.
CROSS SECTION	2.813	1.852E+04	0.	0.	0.	0.
CROSS SECTION ERROR		3.333E+02	0.	0.	0.	0.

Table 47.

2.1 GEV/NUCLEON ALPHAS
TARGET = CH2

	PLAB/Z	PROTONS	DEUTERONS	H-3	HE-3	HE-4
CROSS SECTION	2.875	1.003E+04	0.	0.	0.	0.
CROSS SECTION ERROR		3.176E+02	0.	0.	0.	0.
CROSS SECTION	3.000	6.410E+03	2.560E+01	0.	0.	0.
CROSS SECTION ERROR		3.679E+02	2.226E+00	0.	0.	0.
CROSS SECTION	3.250	2.666E+03	3.745E+01	0.	0.	0.
CROSS SECTION ERROR		1.536E+02	2.980E+00	0.	0.	0.
CROSS SECTION	3.500	1.353E+03	5.833E+01	0.	0.	0.
CROSS SECTION ERROR		4.324E+01	2.255E+00	0.	0.	0.
CROSS SECTION	3.750	0.	7.132E+01	0.	1.306E+02	0.
CROSS SECTION ERROR		0.	2.637E+00	0.	4.339E+00	0.
CROSS SECTION	4.000	3.171E+02	7.861E+01	0.	4.882E+02	0.
CROSS SECTION ERROR		1.842E+01	2.601E+00	0.	1.564E+01	0.
CROSS SECTION	4.250	0.	0.	0.	8.209E+02	0.
CROSS SECTION ERROR		0.	0.	0.	2.615E+01	0.
CROSS SECTION	4.500	0.	0.	0.	1.278E+02	0.
CROSS SECTION ERROR		0.	0.	0.	4.217E+03	0.
CROSS SECTION	4.750	0.	0.	0.	2.358E+01	0.
CROSS SECTION ERROR		0.	0.	0.	8.991E-01	0.
CROSS SECTION	5.000	0.	1.858E+03	0.	0.	0.
CROSS SECTION ERROR		0.	3.353E+01	0.	0.	0.

Table 47 (continued).

Cu or Pb Target 1/4" Thick					
Fragment / Observed Momentum (MeV/c)	p	d	^{3}H	^{3}He	^{4}He
1250	1250	1266±13	1285±28	1269±16	1281±25
1000	1000	1025±20	1053±35	1028±22	1050±41
900	909±7	931±24	970±57	933±27	954±44
750	762±10	793±33	857±87	796±37	832±65
500	521±17	594±77	--	597±80	666±54

Be or C Target 1/4" Thick					
Fragment / Observed Momentum (MeV/c)	p	d	^{3}H	^{3}He	^{4}He
1250	1250	1250	1250	1250	1250
1000	1000	1000	1013±11	1000	1000
900	900	900	917±14	907±6	914±11
750	750	760±8	776±21	760±9	770±16
500	505±4	526±21	--	526±21	536±29

Table 48. Momentum of Observed Particle Corrected for Energy Loss in Target (MeV/c)

Reaction	$\frac{E}{k^2}\frac{d^2\sigma}{d\Omega dk}$ (1.05 GeV/nucleon) / $\frac{E}{k^2}\frac{d^2\sigma}{d\Omega dk}$ (2.1 GeV/nucleon)
d + Be → p + X	2.29
d + C → p + X	3.04
d + Pb → p + X	3.60
d + CH_2 → p + X	3.16
Average	3.02 ± .47
α + Be → p + X	2.33
α + C → p + X	2.35
α + Pb → p + X	2.00
α + CH_2 → p + X	2.54
Average	2.31 ± .10

Overall average 2.67 ± 0.48

Table 49. Ratio of invariant cross sections at two energies at the proton peak

1.03 GEV/NUCLEON CARBON BEAM
TARGET = C

	PLAB/Z	PROTONS	DEUTERONS	H-3	HE-3	HE-4
CROSS SECTION	1.000	2.035E+03	9.543E+01	0.	1.091E+01	0.
CROSS SECTION ERROR		8.728E+01	1.723E+01	0.	4.691E+00	0.
CROSS SECTION	1.250	4.470E+03	2.203E+02	0.	1.839E+01	0.
CROSS SECTION ERROR		2.297E+02	4.983E+01	0.	8.246E+00	0.
CROSS SECTION	1.500	1.767E+04	2.875E+02	0.	3.054E+01	0.
CROSS SECTION ERROR		6.480E+02	3.618E+01	0.	9.705E+00	0.
CROSS SECTION	1.625	3.888E+04	2.250E+02	0.	3.939E+01	0.
CROSS SECTION ERROR		1.315E+03	3.628E+01	0.	1.060E+01	0.
CROSS SECTION	1.750	5.096E+04	2.818E+02	0.	4.176E+01	0.
CROSS SECTION ERROR		1.692E+03	3.937E+01	0.	1.052E+01	0.
CROSS SECTION	1.875	3.525E+04	3.165E+02	1.948E+01	9.496E+01	0.
CROSS SECTION ERROR		1.189E+03	4.051E+01	9.759E+00	1.550E+01	0.
CROSS SECTION	2.000	1.478E+04	2.921E+02	0.	1.620E+02	0.
CROSS SECTION ERROR		5.346E+02	3.766E+01	0.	1.990E+01	0.
CROSS SECTION	2.250	2.199E+03	5.233E+02	1.217E+01	1.673E+03	0.
CROSS SECTION ERROR		1.173E+02	4.895E+01	7.037E+00	7.870E+01	0.
CROSS SECTION	2.500	6.169E+02	9.765E+02	2.198E+01	6.973E+03	0.
CROSS SECTION ERROR		3.628E+01	4.753E+01	6.342E+00	1.751E+02	0.
CROSS SECTION	2.625	3.755E+02	1.533E+03	6.953E+00	7.889E+03	0.
CROSS SECTION ERROR		3.803E+01	8.764E+01	4.922E+00	2.756E+02	0.
CROSS SECTION	2.750	0.	2.486E+03	4.148E+00	4.211E+03	0.
CROSS SECTION ERROR		0.	5.868E+01	1.456E+00	7.861E+01	0.

Table 50.

1.05 GEV/NUCLEON CARBON BEAM
TARGET = C

	PLAB/Z	PROTONS	DEUTERONS	H-3	HE-3	HE-4
CROSS SECTION	2.800	0.	2.830E+03	0.	2.738E+03	0.
CROSS SECTION ERROR		0.	6.564E+01	0.	5.468E+01	0.
CROSS SECTION	2.900	0.	4.056E+03	0.	1.465E+03	0.
CROSS SECTION ERROR		0.	1.709E+02	0.	6.672E+01	0.
CROSS SECTION	3.063	0.	4.419E+03	3.278E+01	6.437E+02	3.828E+03
CROSS SECTION ERROR		0.	1.279E+02	7.027E+00	2.628E+01	1.089E+02
CROSS SECTION	3.125	0.	8.964E+03	3.504E+01	4.213E+02	3.796E+03
CROSS SECTION ERROR		0.	2.338E+02	7.196E+00	1.991E+01	9.966E+01
CROSS SECTION	3.250	0.	1.327E+04	4.212E+01	0.	5.755E+03
CROSS SECTION ERROR		0.	3.266E+02	7.748E+00	0.	2.333E+02
CROSS SECTION	3.375	0.	1.818E+04	0.	0.	1.846E+04
CROSS SECTION ERROR		0.	6.151E+02	0.	0.	6.046E+02
CROSS SECTION	3.500	0.	1.723E+04	0.	0.	1.699E+04
CROSS SECTION ERROR		0.	5.846E+02	0.	0.	5.574E+02
CROSS SECTION	3.625	0.	1.366E+04	8.560E+01	0.	7.911E+03
CROSS SECTION ERROR		0.	3.324E+02	1.056E+01	0.	1.934E+02
CROSS SECTION	3.750	0.	4.114E+03	1.071E+02	0.	1.743E+03
CROSS SECTION ERROR		0.	1.151E+02	1.166E+01	0.	5.079E+01
CROSS SECTION	3.850	0.	1.903E+03	1.517E+02	0.	2.133E+02
CROSS SECTION ERROR		0.	9.019E+01	1.956E+01	0.	1.727E+01

Table 50 (continued).

1.05 GEV/NUCLEON CARBON BEAM
TARGET = CU

	PLAB/Z	PROTONS	DEUTERONS	H-3	HE-3	HE-4
CROSS SECTION	1.000	4.319E+03	4.266E+02	0.	4.800E+01	0.
CROSS SECTION ERROR		2.525E+02	7.581E+01	0.	1.635E+01	0.
CROSS SECTION	1.250	7.805E+03	9.598E+02	0.	3.199E+01	0.
CROSS SECTION ERROR		5.573E+02	1.778E+02	0.	2.265E+01	0.
CROSS SECTION	1.500	3.220E+04	7.997E+02	0.	6.665E+01	0.
CROSS SECTION ERROR		1.377E+03	1.482E+02	0.	2.988E+01	0.
CROSS SECTION	1.625	6.213E+04	7.874E+02	4.922E+01	9.843E+01	0.
CROSS SECTION ERROR		2.321E+03	1.414E+02	3.484E+01	3.494E+01	0.
CROSS SECTION	1.750	8.343E+04	8.454E+02	6.855E+01	7.997E+01	0.
CROSS SECTION ERROR		2.978E+03	1.415E+02	3.963E+01	3.033E+01	0.
CROSS SECTION	1.875	5.834E+04	8.316E+02	6.397E+01	1.279E+02	0.
CROSS SECTION ERROR		2.156E+03	1.357E+02	3.699E+01	3.716E+01	0.
CROSS SECTION	2.000	2.415E+04	7.796E+02	9.996E+01	1.999E+02	0.
CROSS SECTION ERROR		1.032E+03	1.273E+02	4.481E+01	4.515E+01	0.
CROSS SECTION	2.250	4.122E+03	8.884E+02	7.108E+01	3.812E+03	0.
CROSS SECTION ERROR		3.004E+02	1.287E+02	3.561E+01	1.893E+02	0.
CROSS SECTION	2.500	1.007E+03	1.591E+03	1.599E+01	1.891E+04	0.
CROSS SECTION ERROR		9.253E+01	1.153E+02	1.131E+01	3.212E+02	0.
CROSS SECTION	2.625	6.701E+02	2.684E+03	4.569E+01	1.109E+04	0.
CROSS SECTION ERROR		1.032E+02	2.155E+02	2.642E+01	4.554E+02	0.
CROSS SECTION	2.750	0.	3.823E+03	0.	5.732E+03	0.
CROSS SECTION ERROR		0.	1.325E+02	0.	1.365E+02	0.

Table 51.

1.05 GEV/NUCLEON CARBON BEAM
TARGET = CU

	PLAB/Z	PROTONS	DEUTERONS	H-3	HE-3	HE-4
CROSS SECTION	2.800	0.	4.508E+03	0.	4.816E+03	0.
CROSS SECTION ERROR		0.	9.202E+01	0.	6.693E+01	0.
CROSS SECTION	2.900	0.	6.493E+03	8.271E+01	1.047E+03	0.
CROSS SECTION ERROR		0.	3.629E+02	7.387E+01	1.271E+02	0.
CROSS SECTION	3.063	0.	1.216E+04	6.005E+01	1.063E+03	4.263E+03
CROSS SECTION ERROR		0.	2.476E+02	1.255E+01	4.016E+01	9.592E+01
CROSS SECTION	3.125	0.	1.419E+04	8.699E+01	7.010E+02	6.057E+03
CROSS SECTION ERROR		0.	2.768E+02	1.497E+01	3.155E+01	1.228E+02
CROSS SECTION	3.250	0.	1.995E+04	9.021E+01	0.	1.527E+04
CROSS SECTION ERROR		0.	4.631E+02	1.930E+01	0.	3.303E+02
CROSS SECTION	3.375	0.	2.541E+04	0.	0.	2.627E+04
CROSS SECTION ERROR		0.	4.352E+02	0.	0.	4.113E+02
CROSS SECTION	3.500	0.	2.627E+04	0.	0.	2.452E+04
CROSS SECTION ERROR		0.	3.147E+02	0.	0.	2.722E+02
CROSS SECTION	3.625	0.	1.914E+04	1.059E+02	0.	9.935E+03
CROSS SECTION ERROR		0.	3.398E+02	1.535E+01	0.	1.752E+02
CROSS SECTION	3.750	0.	1.044E+04	1.599E+02	0.	2.013E+03
CROSS SECTION ERROR		0.	2.788E+02	2.402E+01	0.	7.012E+01
CROSS SECTION	3.850	0.	1.504E+04	3.530E+02	0.	2.845E+03
CROSS SECTION ERROR		0.	6.182E+02	6.157E+01	0.	1.512E+02

Table 51 (continued).

1.05 GEV PER NUCLEON CARBON - HEAVY FRAGMENTS
TARGET = CU

	PLAB/Z	LI	BE	B	C
CROSS SECTION	2.750	0.	7.730E+01	1.804E+01	0.
CROSS SECTION ERROR		0.	5.540E+00	2.439E+00	0.
CROSS SECTION	2.000	0.	1.505E+02	2.099E+01	0.
CROSS SECTION ERROR		0.	7.729E+00	3.004E+00	0.
CROSS SECTION	2.900	0.	4.000E+02	2.471E+01	0.
CROSS SECTION ERROR		0.	1.416E+01	2.724E+00	0.
CROSS SECTION	3.063	0.	4.295E+02	5.216E+01	0.
CROSS SECTION ERROR		0.	1.290E+01	3.070E+00	0.
CROSS SECTION	3.125	1.796E+02	2.241E+02	1.094E+02	0.
CROSS SECTION ERROR		9.170E+00	9.040E+00	5.606E+00	0.
CROSS SECTION	3.250	5.106E+02	0.	0.	0.
CROSS SECTION ERROR		1.573E+01	0.	0.	0.
CROSS SECTION	3.375	1.191E+03	0.	1.057E+02	6.257E+01
CROSS SECTION ERROR		2.520E+01	0.	7.140E+00	3.727E+00
CROSS SECTION	3.500	0.741E+02	0.	0.043E+01	4.590E+01
CROSS SECTION ERROR		2.070E+01	0.	4.527E+00	3.127E+00
CROSS SECTION	3.625	2.062E+02	0.	0.	0.
CROSS SECTION ERROR		1.546E+01	0.	0.	0.
CROSS SECTION	3.750	1.575E+02	4.249E+01	5.711E+01	0.
CROSS SECTION ERROR		7.055E+00	3.507E+00	3.671E+00	0.
CROSS SECTION	3.050	2.765E+02	7.499E+01	6.056E+01	0.
CROSS SECTION ERROR		2.333E+01	1.034E+01	0.351E+00	0.

Table 52.

1.05 GEV PER NUCLEON CARBON - HEAVY FRAGMENTS
TARGET = C

	PLAB/Z	LI	BE	B	C
CROSS SECTION	2.750	0.	4.886E+01	5.077E+00	0.
CROSS SECTION ERROR		0.	3.058E+00	9.461E-01	0.
CROSS SECTION	2.800	0.	8.710E+01	1.289E+01	0.
CROSS SECTION ERROR		0.	4.527E+00	1.503E+00	0.
CROSS SECTION	2.900	0.	2.473E+02	1.262E+01	0.
CROSS SECTION ERROR		0.	1.151E+01	2.066E+00	0.
CROSS SECTION	3.063	0.	2.714E+02	2.812E+01	0.
CROSS SECTION ERROR		0.	7.557E+00	1.616E+00	0.
CROSS SECTION	3.125	9.719E+01	1.333E+02	3.466E+01	0.
CROSS SECTION ERROR		5.192E+00	5.472E+00	2.375E+00	0.
CROSS SECTION	3.250	2.769E+02	0.	0.	0.
CROSS SECTION ERROR		1.316E+01	0.	0.	0.
CROSS SECTION	3.375	6.693E+02	0.	0.	0.
CROSS SECTION ERROR		3.279E+01	0.	0.	0.
CROSS SECTION	3.500	5.695E+02	0.	0.	3.283E+01
CROSS SECTION ERROR		2.897E+01	0.	0.	4.032E+00
CROSS SECTION	3.625	2.090E+02	0.	0.	0.
CROSS SECTION ERROR		1.063E+01	0.	0.	0.
CROSS SECTION	3.750	9.466E+01	1.696E+01	2.854E+01	0.
CROSS SECTION ERROR		4.218E+00	1.498E+00	1.461E+00	0.
CROSS SECTION	3.850	1.484E+02	2.940E+01	2.434E+01	0.
CROSS SECTION ERROR		6.046E+00	2.529E+00	2.063E+00	0.

Table 53.

Figure Captions

Fig. 1. Expected general shape of single particle inclusive cross sections showing three kinematic regions.

Fig. 2. Regge exchange diagrams applicable to (a) beam fragmentation region, (b) target fragmentation region, (c) central region.

Fig. 3. Illustration of the model used to calculate pion production by heavy ions.

Fig. 4. Set-up of spectrometer and detection system.

Fig. 5. Effect of (a) intermediate focus collimator and (b) upstream collimator on the flux of particles at the spectrometer's final focus.

Fig. 6. Logic system for measuring negative particle production.

Fig. 7. Gas Cerenkov counter pressure curve showing separation of pions and leptons.

Fig. 8. Logic system for identification of positive fragments by time-of-flight and dE/dx.

Fig. 9. Logic system for measuring dE/dx spectra.

Fig. 10. Typical time-of-flight spectrum showing ^{3}H near channel 113, deuterons and alphas near channel 149, ^{3}He near channel 166, protons near channel 179, and pions near 191. Vertical scales are logarithmic.

Fig. 11. Electron fraction of negative produced particles from 3.5 GeV protons on various targets.

Fig. 12. Range of parameters involved in the experiment.

Fig. 13. Negative pion production by proton beams with a carbon target.

Fig. 14. Positive pion production by proton beams with a carbon target.

Fig. 15. Negative pion production by 1.05 GeV/nucleon deuterons, alphas, and protons on carbon.

Fig. 16. Negative pion production by 2.1 GeV/nucleon deuterons, alphas, and protons on carbon.

Fig. 17. Negative pion production by protons on carbon as a function of the scaling variable x'.

Fig. 18. Negative pion production by deuterons on carbon as a function of the scaling variable x'.

Fig. 19. Negative pion production by alphas on carbon as a function of the scaling variable x'.

Fig. 20. Comparison of the data for π^- production by 1.05 and 2.1 GeV/nucleon deuterons with the predictions of the model described in the text (solid line).

Fig. 21. Comparison of the data for π^- production by 1.05 and 2.1 GeV/nucleon alphas with the predictions of the model described in the text (solid line).

Fig. 22. Negative pion production by 2.1 GeV/nucleon alphas as a function of the atomic mass of the target.

Fig. 24. Fragmentation cross sections of 1.05 GeV/nucleon alphas into protons, deuterons, ^{3}H, ^{3}He, and ^{4}He.

Fig. 25. Fragmentation cross sections of 1.05 GeV/nucleon alphas as a function of fragment rapidity y.

Fig. 26. Fragmentation cross sections for 1.05 GeV/nucleon deuterons on carbon.

Fig. 27. Comparison of data on fragmentation of deuterons into protons with the predictions of the model described in the text (solid lines).

Fig. 28. Comparison of data on fragmentation of alphas into protons with the predictions of the model described in the text (solid line).

Fig. 29. Fragmentation of alphas into ^{3}He at two energies.

Fig. 30. Plot of the exponent N obtained from fitting the target dependence of various cross sections with an A^{N} type function.

Fig. 31. Fragmentation of a 1.05 GeV/nucleon carbon beam on a carbon target.

Fig. 32. Fragmentation of a 1.05 GeV/nucleon carbon beam into heavy fragments (A > 4).

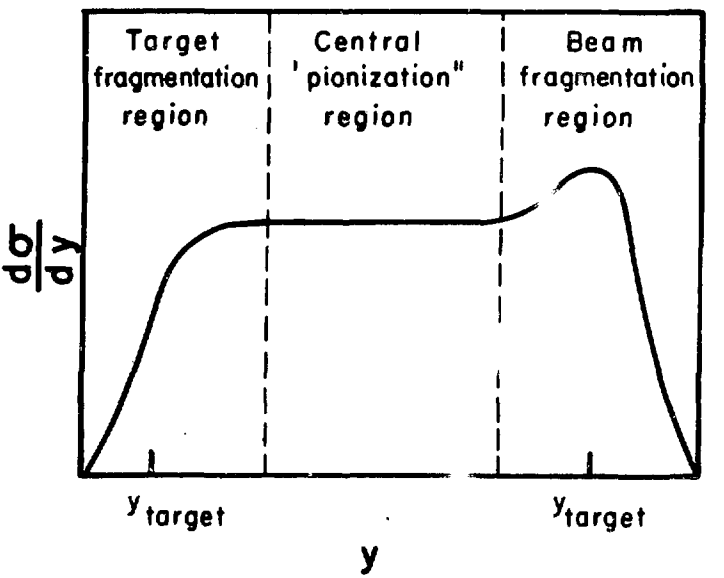
Target fragmentation region
Central "pionization" region
Beam fragmentation region
dσ/dy
y target
y target
y
XBL748-3811

Fig. 1

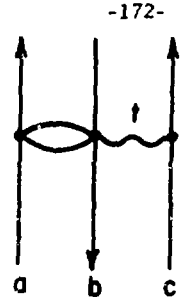

XBL748-3805

Fig. 2

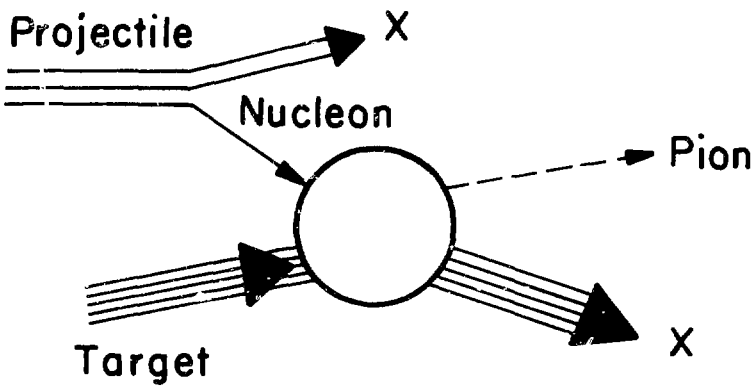

XBL7411-8316

Fig. 3

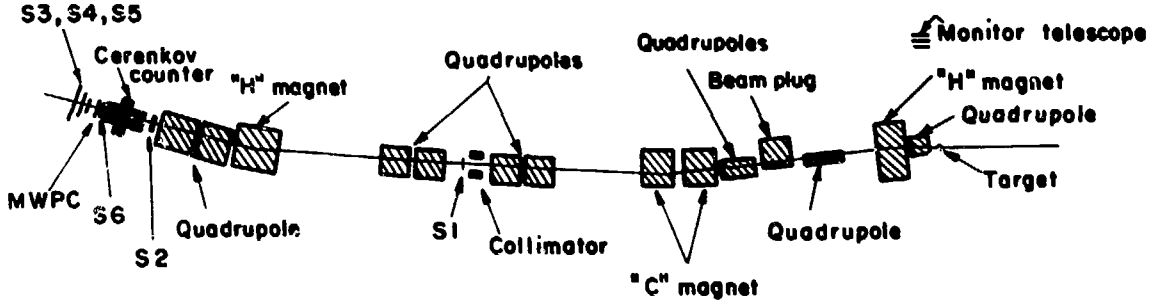

XBL7411-8317

Fig. 4

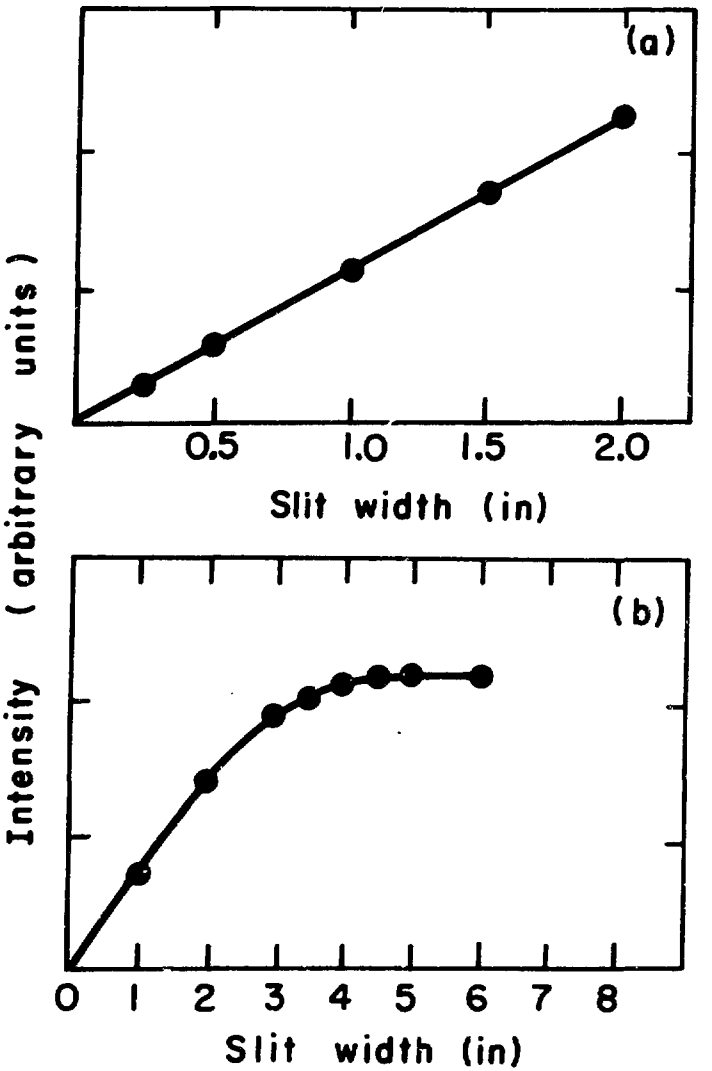
(a)
0.5
1.0
1.5
2.0
Slit width (in)
Intensity (arbitrary units)
(b)
0 1 2 3 4 5 6 7 8
Slit width (in)
XBL748-3813

Fig. 5

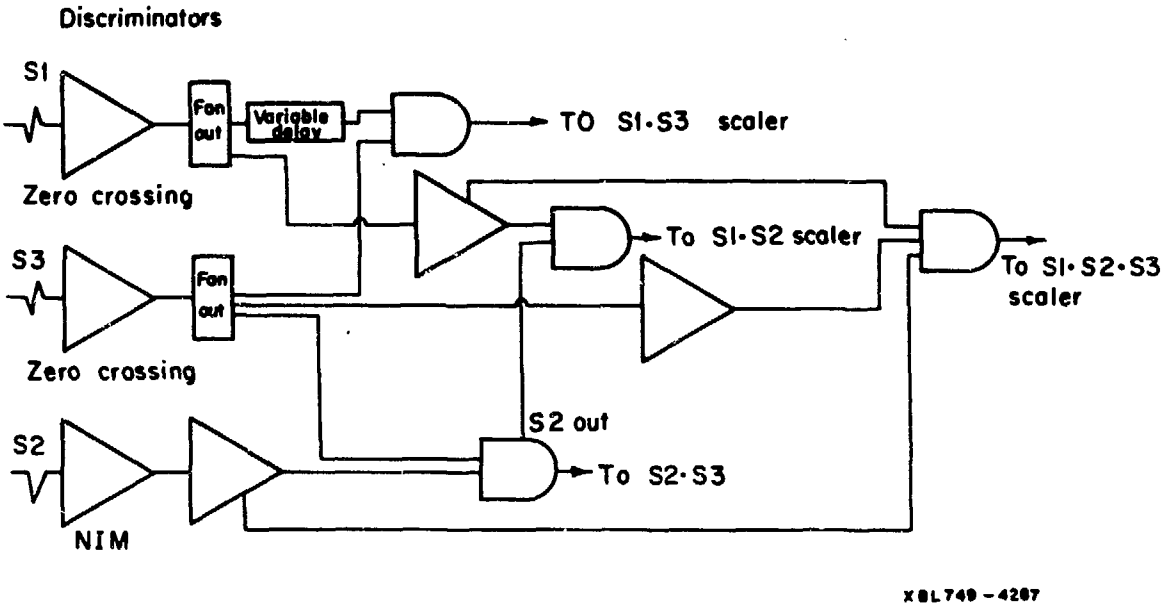
Discriminators
S1
Fan out
Variable delay
TO S1·S3 scaler
Zero crossing
To S1·S2 scaler
To S1·S2·S3 scaler
S3
Fan out
Zero crossing
S2 out
S2
To S2·S3
NIM
XBL749-4287

Fig. 6

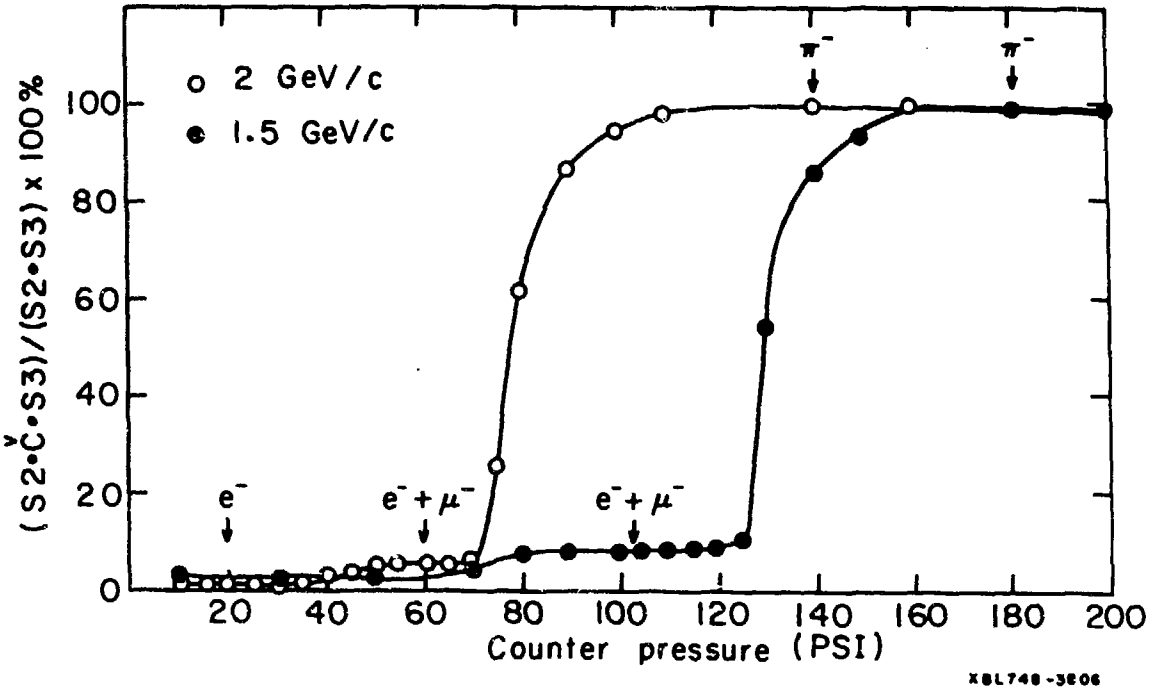
o 2 GeV/c
● 1.5 GeV/c
π⁻
π⁻
e⁻
e⁻ + μ⁻
e⁻ + μ⁻
(S2•C̄•S3)/(S2•S3) x 100%
0
20
40
60
80
100
20
40
60
80
100
120
140
160
180
200
Counter pressure (PSI)
XBL748-3806

Fig. 7

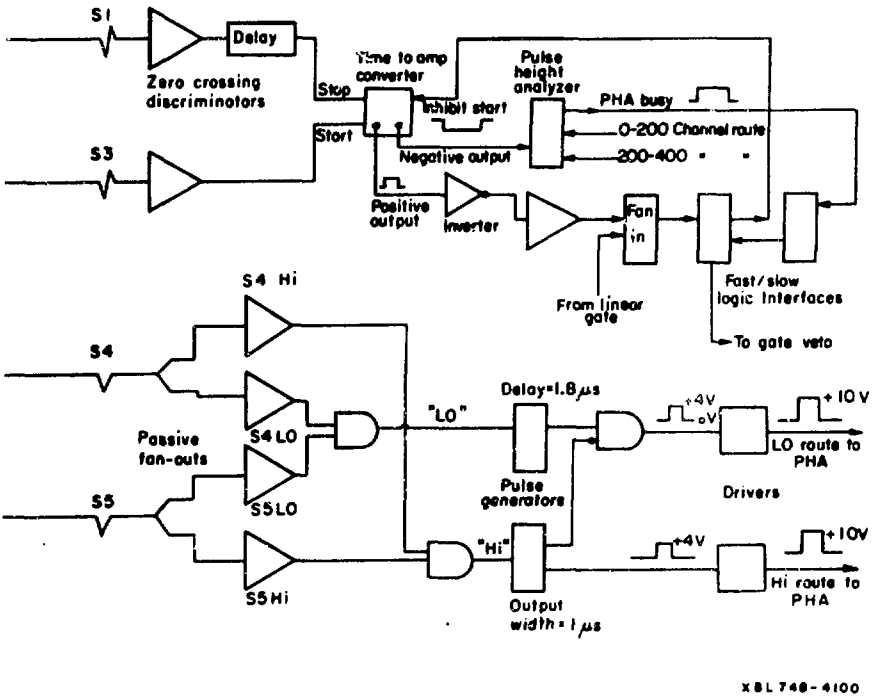
S1
Delay
Zero crossing discriminators
Stop
Time to amp converter
Pulse height analyzer
PHA busy
Inhibit start
Start
0-200 Channel route
S3
Negative output
200-400
Positive output
Inverter
Fan in
From linear gate
Fast/slow logic Interfaces
To gate veto
S4 Hi
S4
Delay=1.8μs
"LO"
+4V
0V
+10V
Passive fan-outs
S4 LO
LO route to PHA
S5
S5 LO
Pulse generators
Drivers
"Hi"
+4V
+10V
S5 Hi
Hi route to PHA
Output width = 1μs
XBL 748-4100

Fig. 8

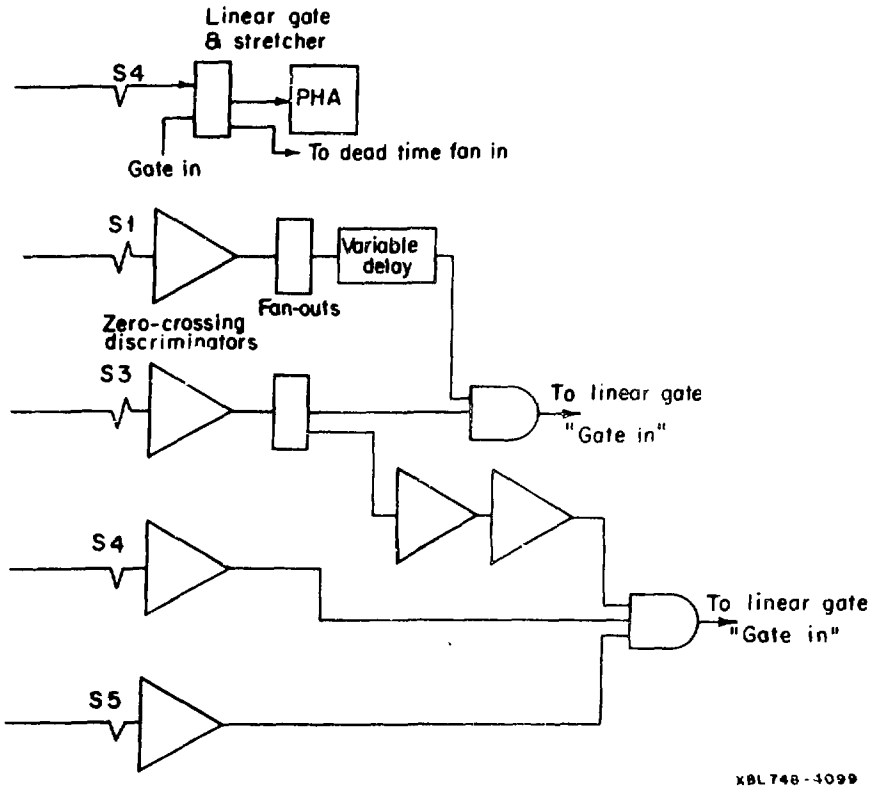
Linear gate
& stretcher
S4
PHA
To dead time fan in
Gate in
S1
Variable
delay
Fan-outs
Zero-crossing
discriminators
S3
To linear gate
"Gate in"
S4
To linear gate
"Gate in"
S5
XBL 748-4099

Fig. 9

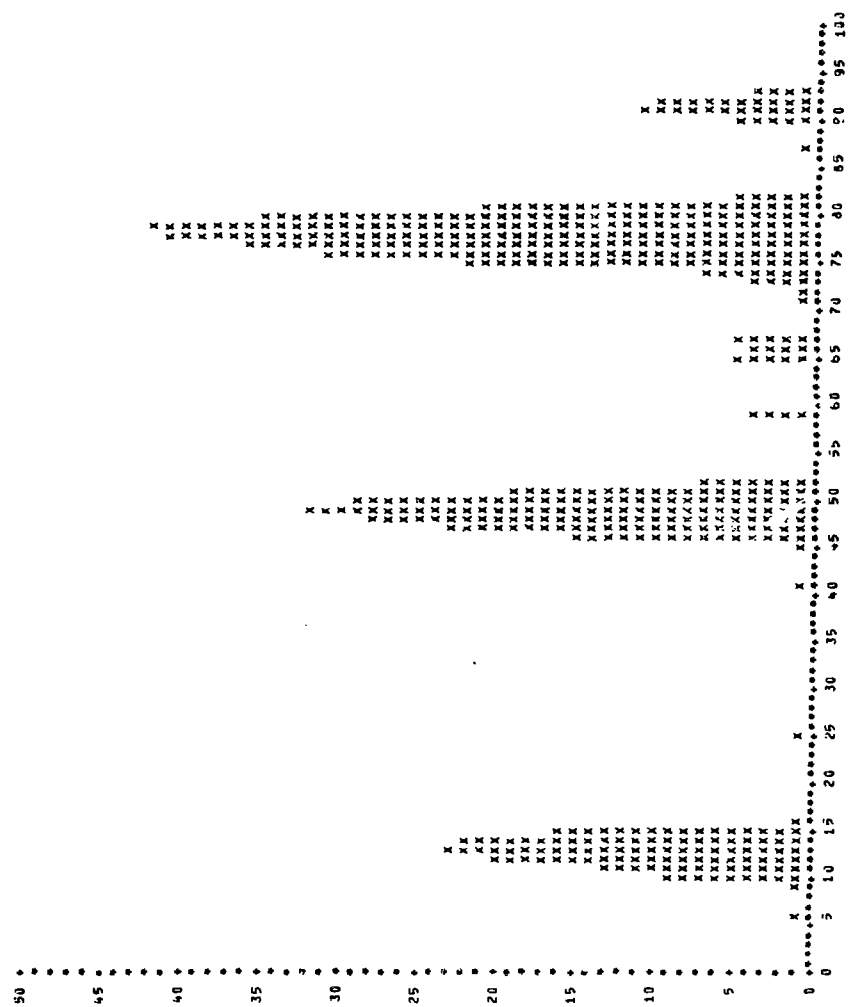

Fig. 10

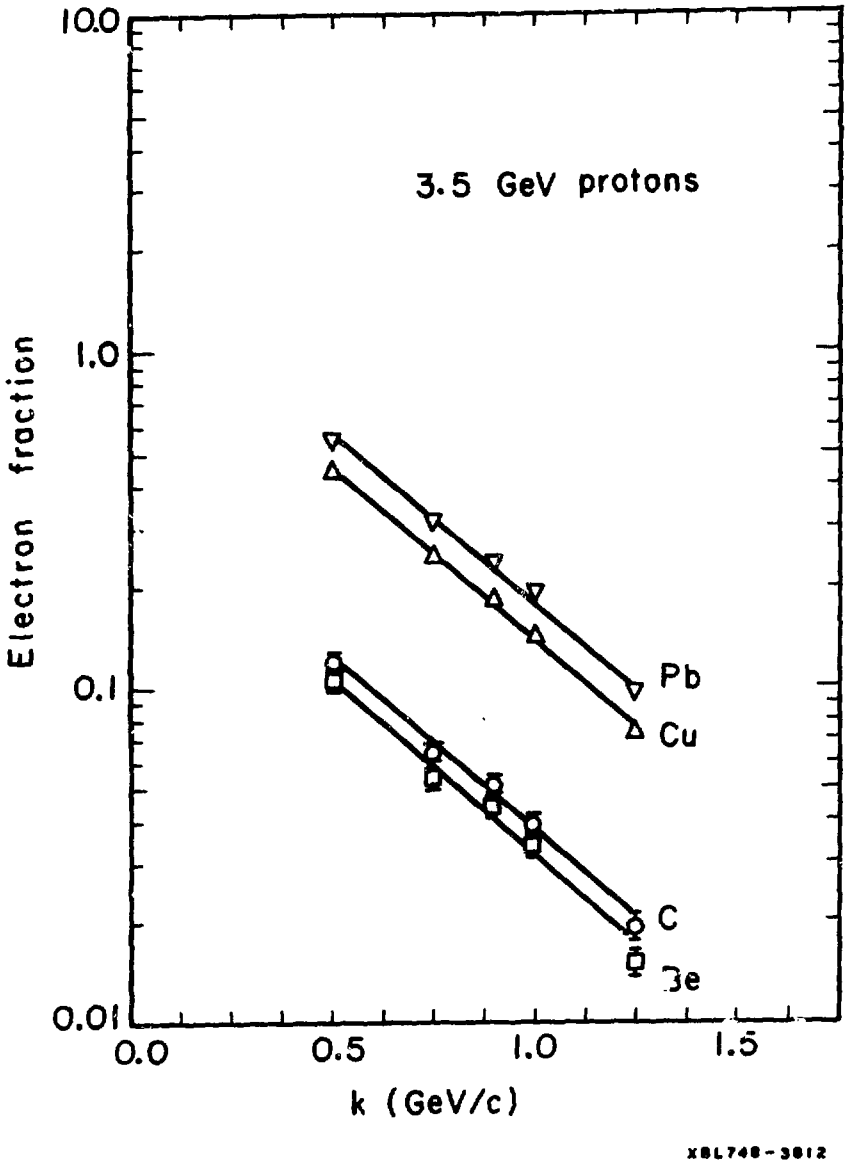
10.0
1.0
0.1
0.01
Electron fraction
3.5 GeV protons
Pb
Cu
C
Be
0.0
0.5
1.0
1.5
k (GeV/c)
XBL748-3812

Fig. 11

Beams

Protons: 1.05, 1.73, 2.1, 2.66, 3.5, 4.2 GeV

Deuterons: 1.05, 2.1 GeV/nucleon

Alphas: 1.05, 2.1 GeV/nucleon

^{12}C: 1.05 GeV/nucleon

Targets

Be, C, Cu, Pb, CH_2

Fragments

$e^{\pm}$, $\mu^{\pm}$, $\pi^{\pm}$, p, d, ^{3}H, ^{3}He, ^{4}He

Li, Be, B, C

Fragment momentum/charge

0.56 GeV/c $\leq$ k $\leq$ 5 GeV/c

Production angle

θ = 2.5° (lab) = 43.6 milliradians

Fig. 12. Range of Parameters

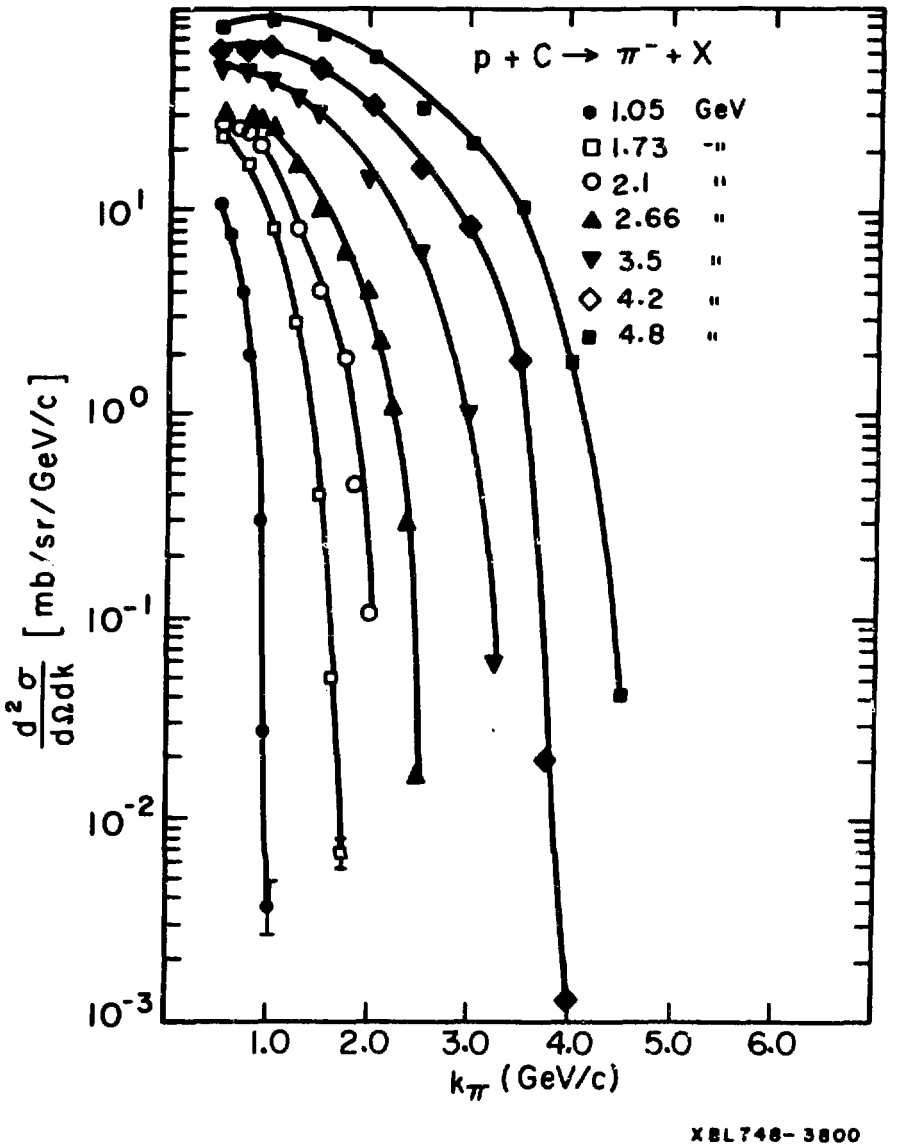
p + C → π⁻ + X
● 1.05 GeV
□ 1.73 "
○ 2.1 "
▲ 2.66 "
▼ 3.5 "
◇ 4.2 "
■ 4.8 "
$\frac{d^2\sigma}{d\Omega dk}$ [mb/sr/GeV/c]
10^1
10^0
10^{-1}
10^{-2}
10^{-3}
1.0
2.0
3.0
4.0
5.0
6.0
k_π (GeV/c)
XBL748-3800

Fig. 13

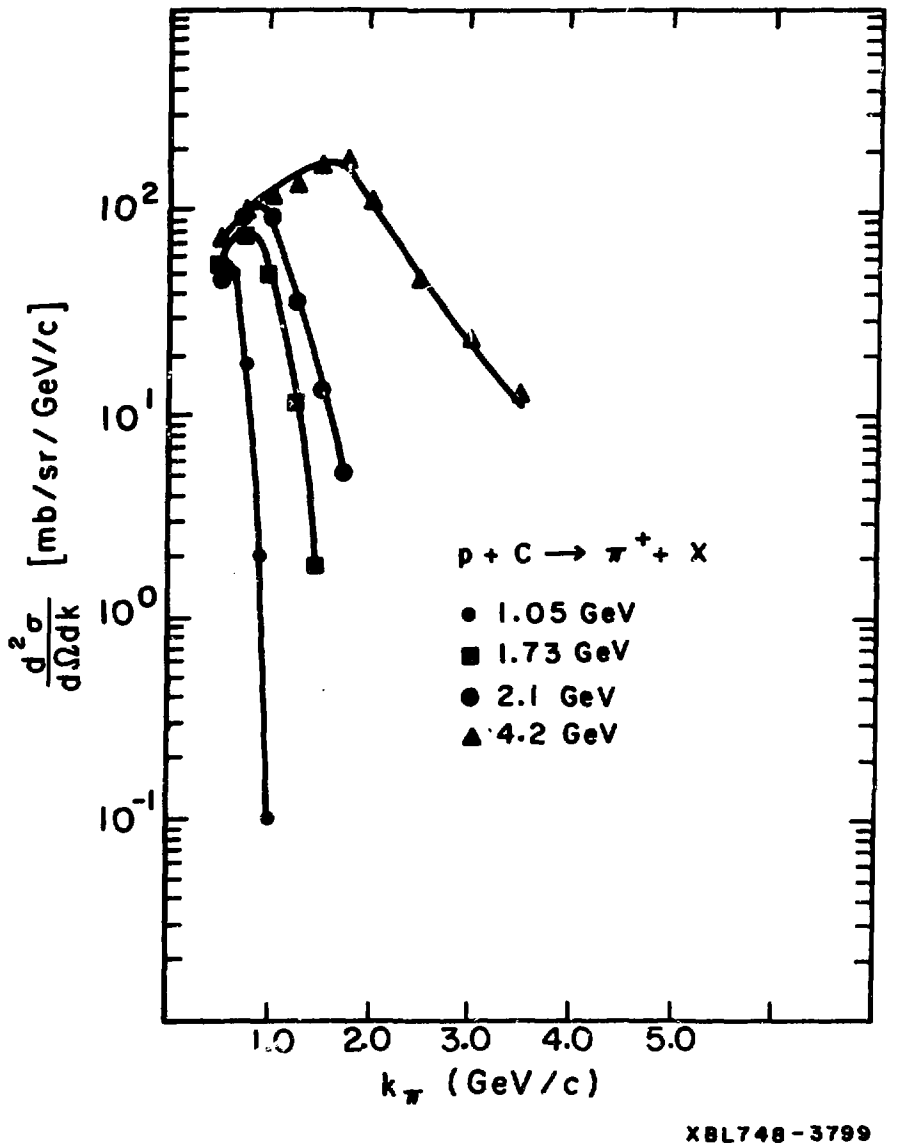
$\frac{d^2\sigma}{d\Omega dk}$ [mb/sr/GeV/c]
10^2
10^1
10^0
10^{-1}
p + C → π⁺ + X
1.05 GeV
1.73 GeV
2.1 GeV
4.2 GeV
1.0
2.0
3.0
4.0
5.0
k_π (GeV/c)
XBL748-3799

Fig. 14

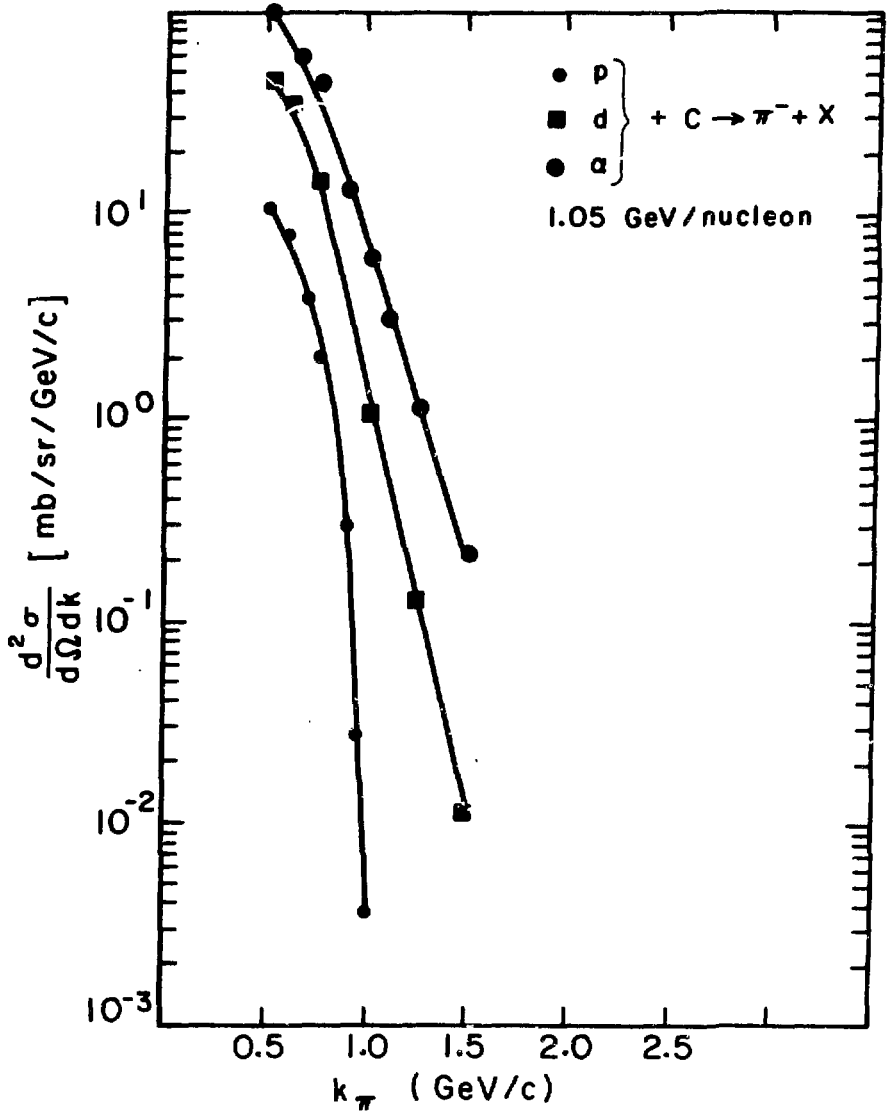

XBL 7411-8590

Fig. 15

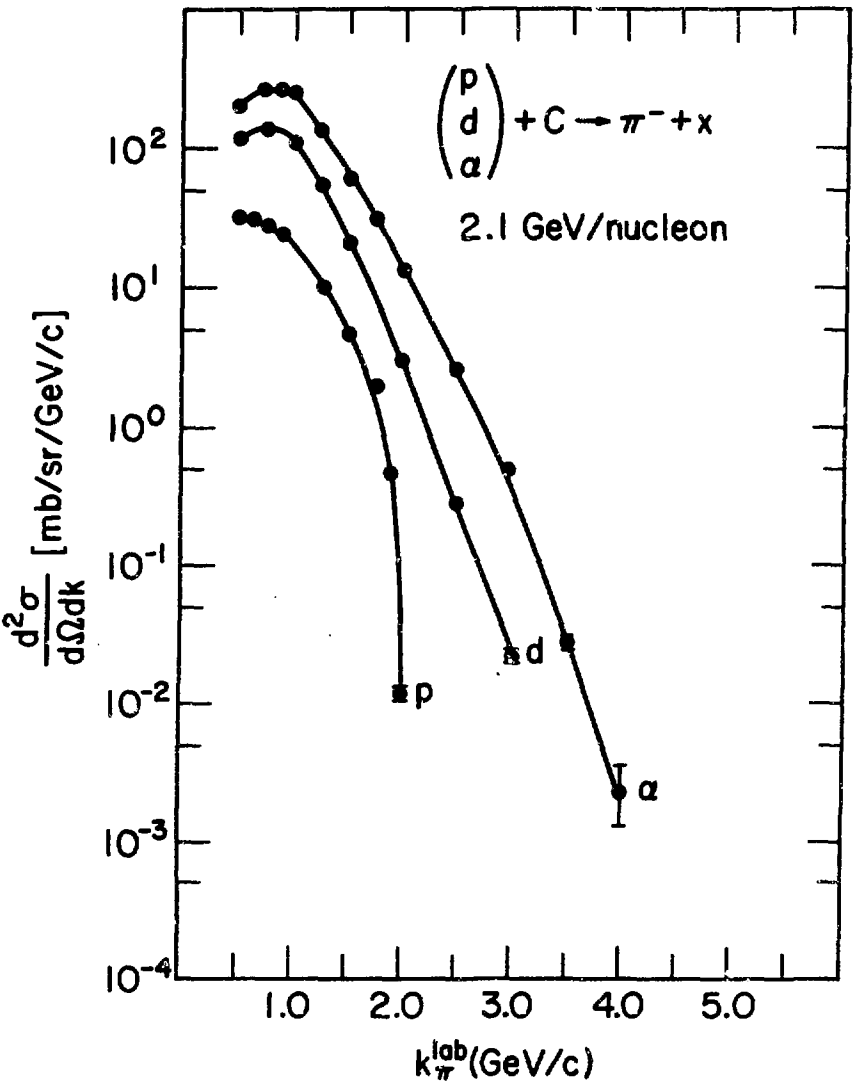

XBL 708-3897

Fig. 16

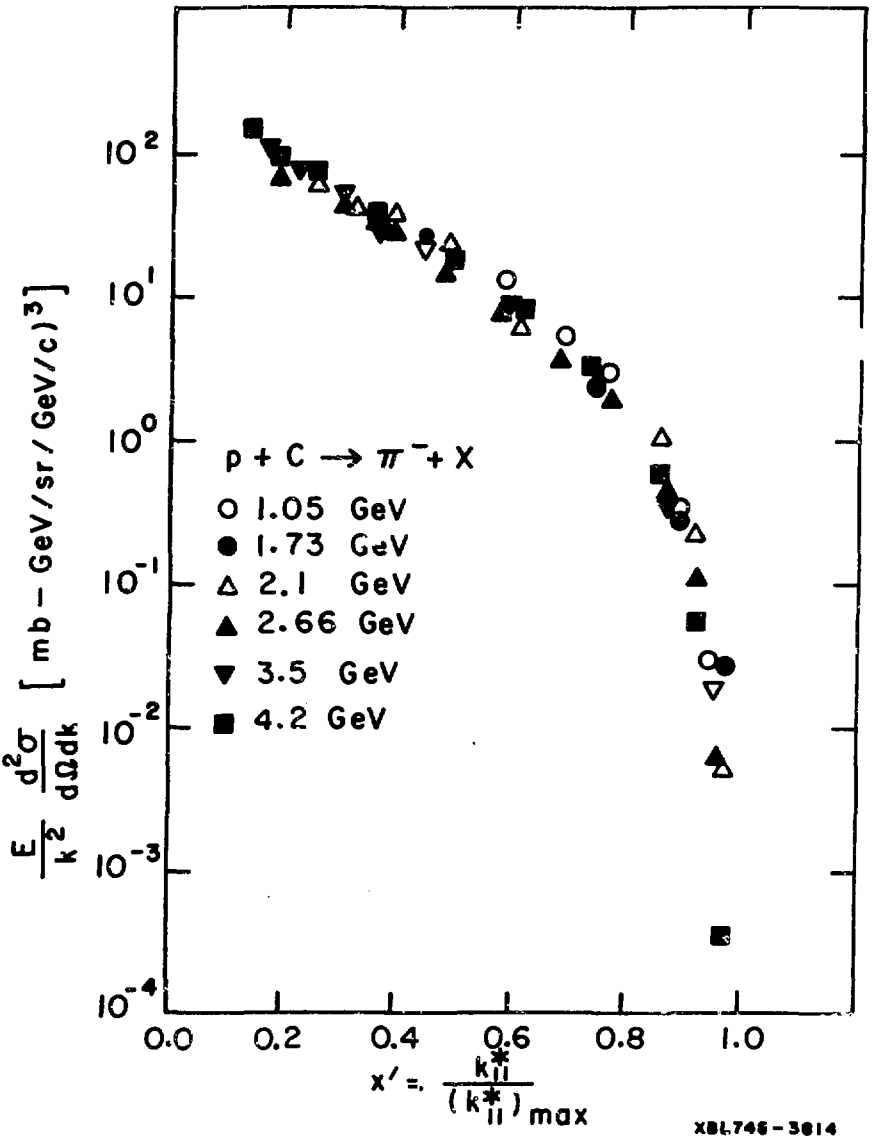
$\frac{E}{k^2}\frac{d^2\sigma}{d\Omega dk}$ [mb − GeV/sr/GeV/c)^3]
10^2
10^1
10^0
10^{-1}
10^{-2}
10^{-3}
10^{-4}
p + C → π⁻ + X
○ 1.05 GeV
● 1.73 GeV
△ 2.1 GeV
▲ 2.66 GeV
▼ 3.5 GeV
■ 4.2 GeV
0.0
0.2
0.4
0.6
0.8
1.0
$x' = \frac{k^*_{\parallel}}{(k^*_{\parallel})_{max}}$
XBL746-3814

Fig. 17

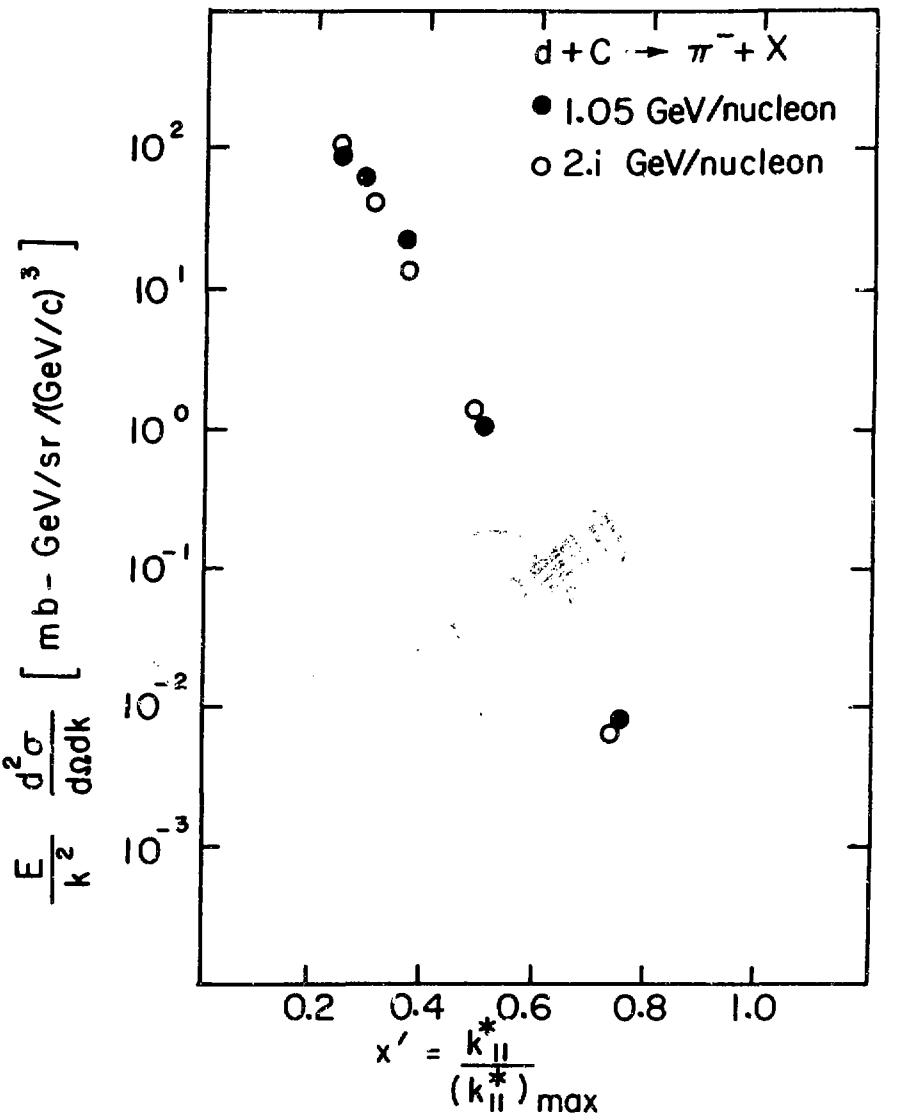
d + C → π⁻ + X
● 1.05 GeV/nucleon
o 2.1 GeV/nucleon
$\frac{E}{k^2}\frac{d^2\sigma}{d\Omega dk}$ [mb - GeV/sr /(GeV/c)^3]
10^2
10^1
10^0
10^{-1}
10^{-2}
10^{-3}
0.2
0.4
0.6
0.8
1.0
$x' = \frac{k^*_{\parallel}}{(k^*_{\parallel})_{max}}$
XBL748-3809

Fig. 18

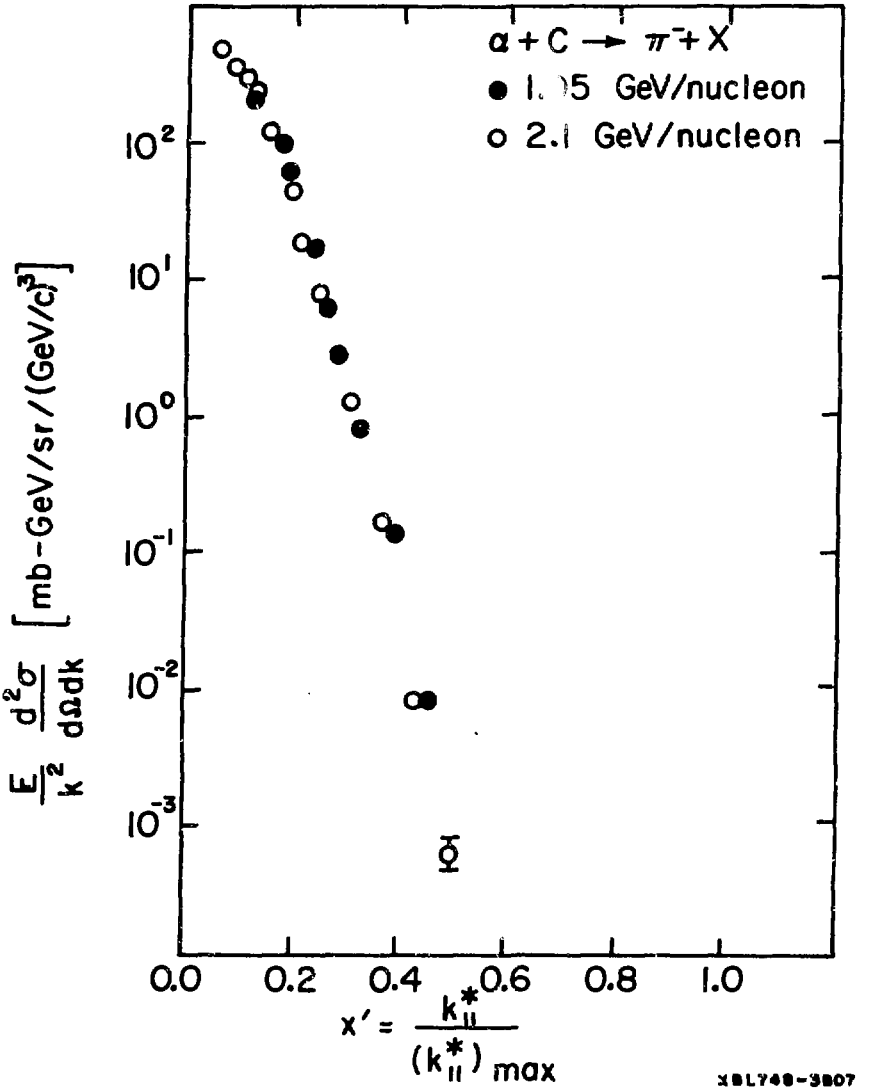
α + C → π⁻ + X
● 1.05 GeV/nucleon
○ 2.1 GeV/nucleon
$\frac{E}{k^2}\frac{d^2\sigma}{d\Omega dk}$ [mb-GeV/sr/(GeV/c)³]
10²
10¹
10⁰
10⁻¹
10⁻²
10⁻³
0.0
0.2
0.4
0.6
0.8
1.0
$x' = \frac{k_{\parallel}^*}{(k_{\parallel}^*)_{max}}$
XBL748-3807

Fig. 19

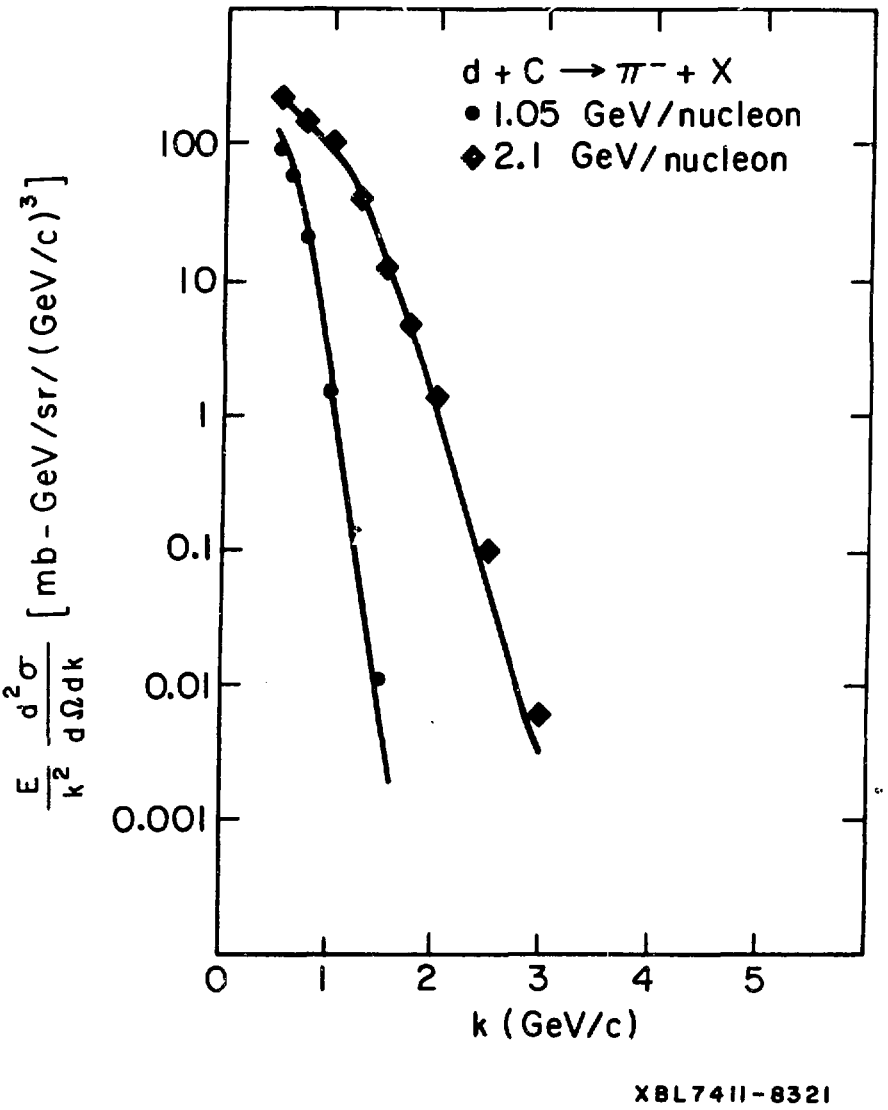
d + C → π⁻ + X
• 1.05 GeV/nucleon
◆ 2.1 GeV/nucleon
100
10
1
0.1
0.01
0.001
0
1
2
3
4
5
k (GeV/c)
E/k² d²σ/dΩdk [mb-GeV/sr/(GeV/c)³]
XBL7411-8321

Fig. 20

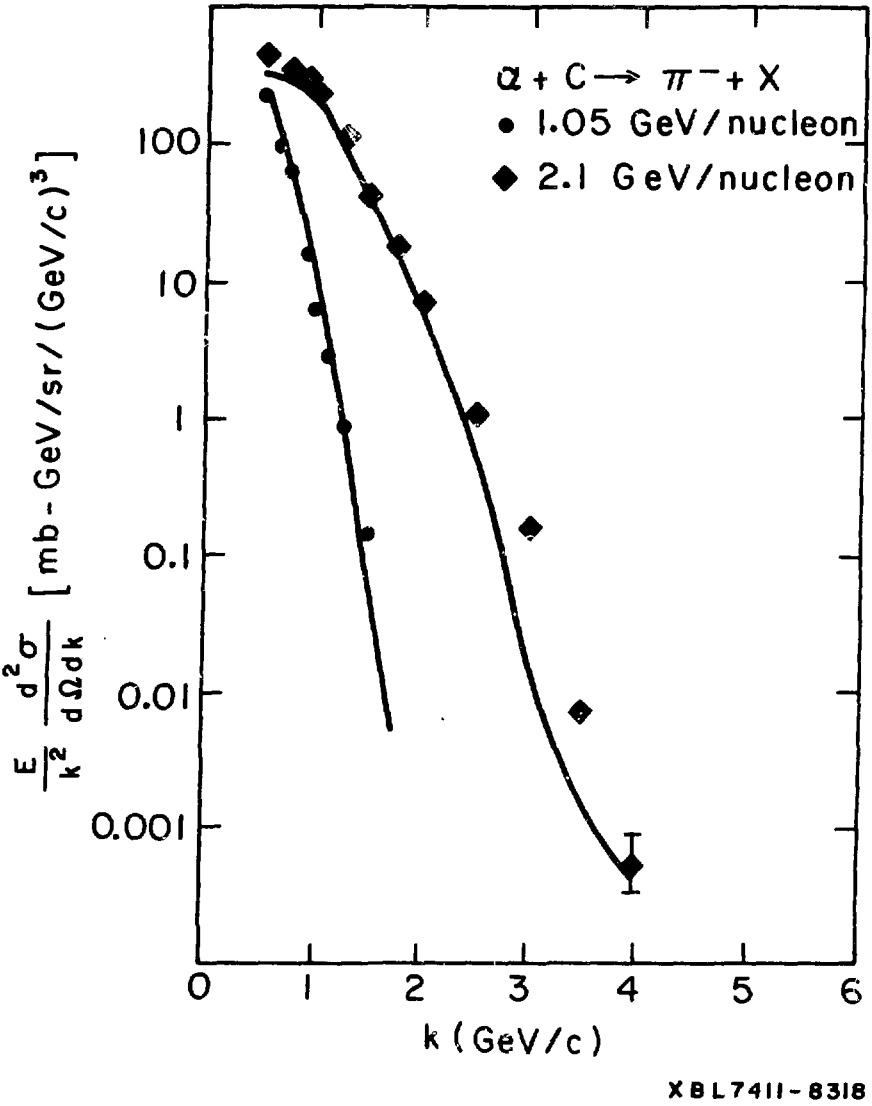
α + C → π⁻ + X
• 1.05 GeV/nucleon
◆ 2.1 GeV/nucleon
100
10
1
0.1
0.01
0.001
$\frac{E}{k^2}\frac{d^2\sigma}{d\Omega dk}$ [mb-GeV/sr/(GeV/c)³]
0
1
2
3
4
5
6
k (GeV/c)
XBL7411-8318

Fig. 21

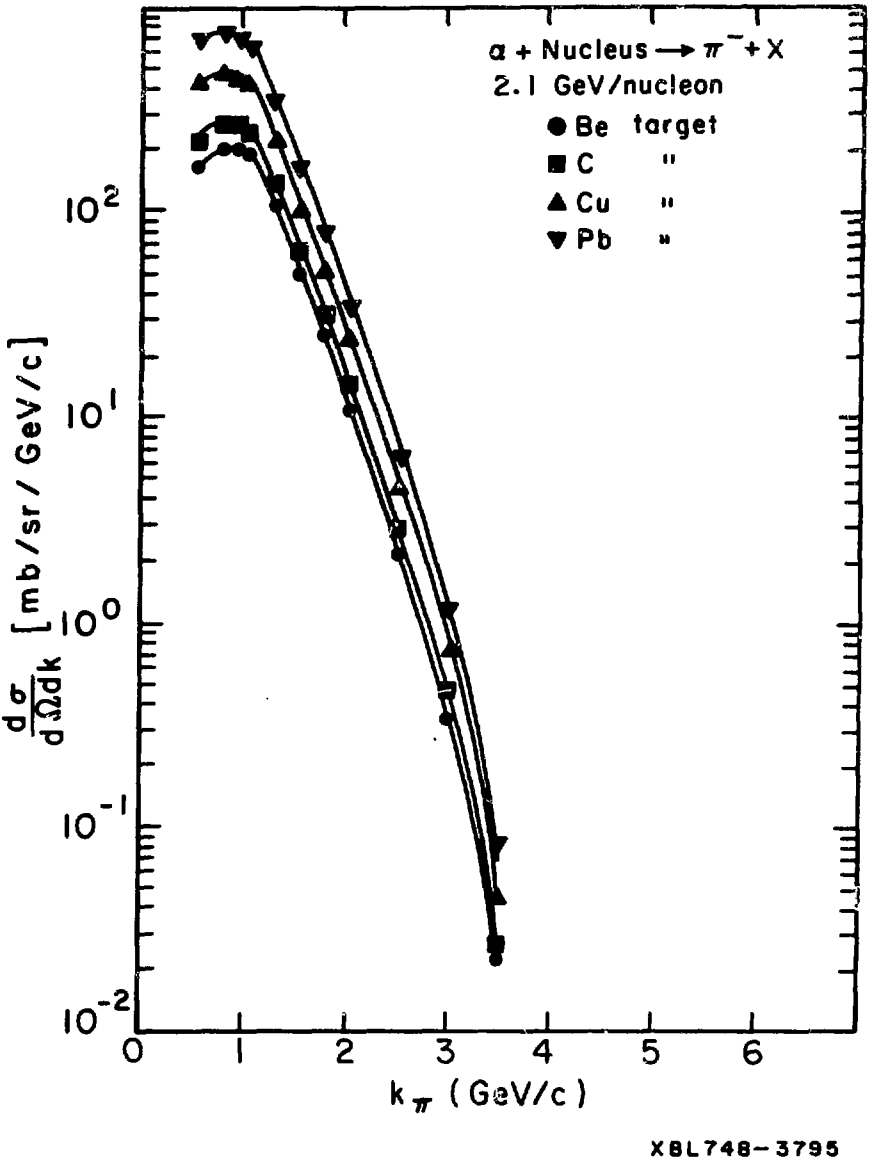
α + Nucleus → π⁻ + X
2.1 GeV/nucleon
● Be target
■ C "
▲ Cu "
▼ Pb "
$\frac{d\sigma}{d\Omega dk}$ [mb/sr/GeV/c]
10^2
10^1
10^0
10^{-1}
10^{-2}
0
1
2
3
4
5
6
k_π (GeV/c)
XBL748-3795

Fig. 22

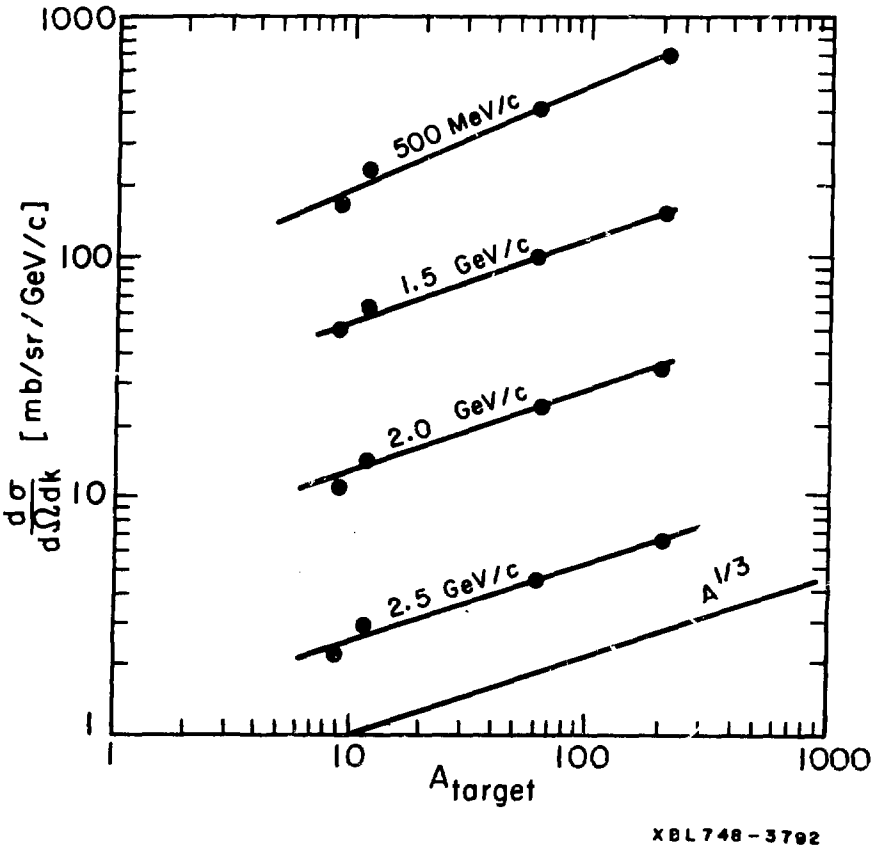
1000
100
10
1
$\frac{d\sigma}{d\Omega dk}$ [mb/sr/GeV/c]
500 MeV/c
1.5 GeV/c
2.0 GeV/c
2.5 GeV/c
$A^{1/3}$
1
10
100
1000
A_{target}
XBL748-3792

Fig. 23

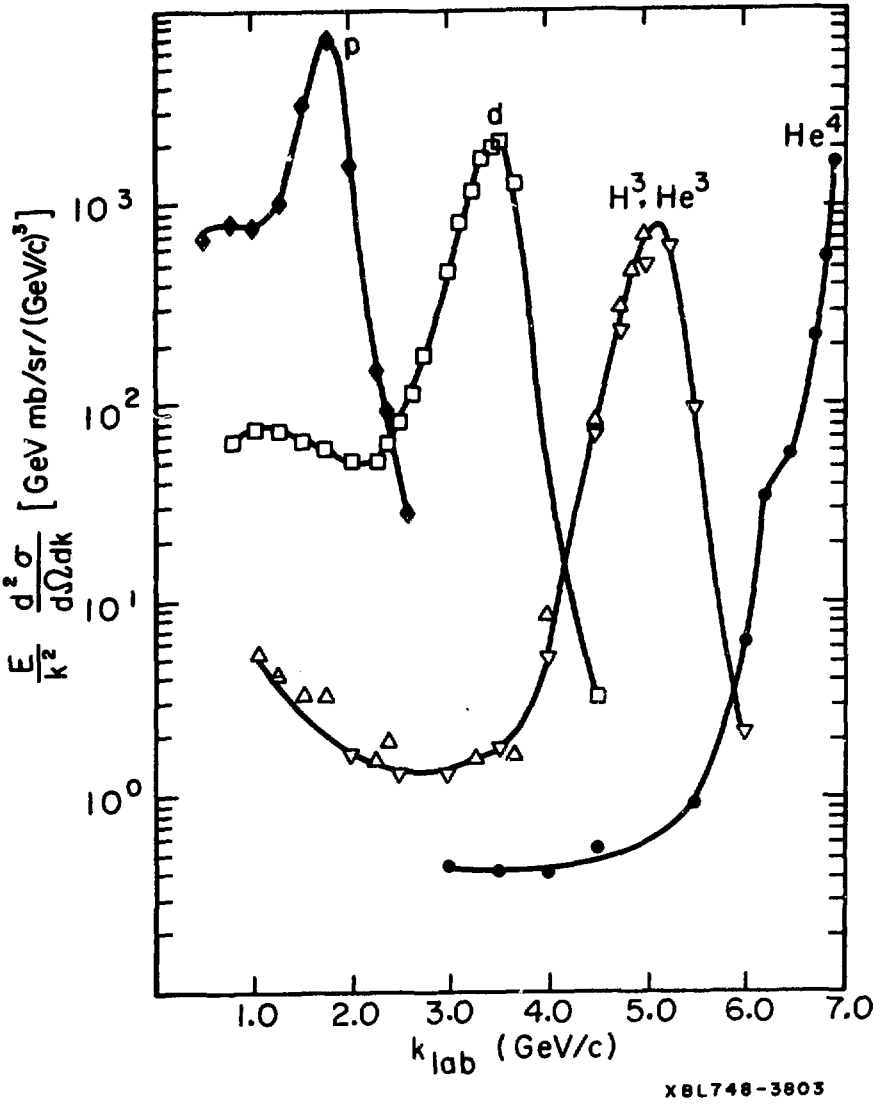
p
d
H³, He³
He⁴
10³
10²
10¹
10⁰
E/k² d²σ/dΩdk [GeV mb/sr/(GeV/c)³]
1.0
2.0
3.0
4.0
5.0
6.0
7.0
k lab (GeV/c)
XBL748-3803

Fig. 24

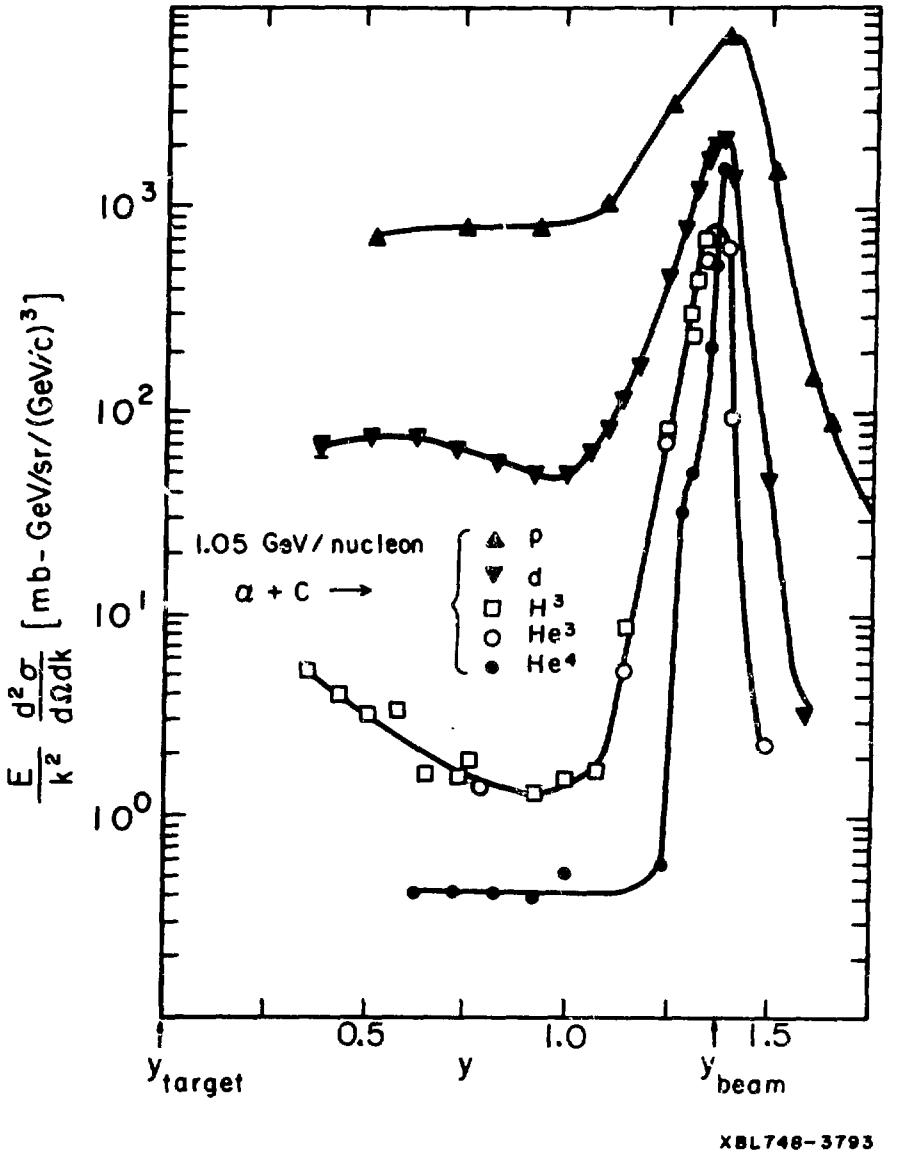
$\frac{E}{k^2}\frac{d^2\sigma}{d\Omega dk}$ [mb-GeV/sr/(GeV/c)^3]
10^3
10^2
10^1
10^0
1.05 GeV/nucleon
α + C
p
d
H^3
He^3
He^4
0.5
1.0
1.5
y_{target}
y
y_{beam}
XBL748-3793

Fig. 25

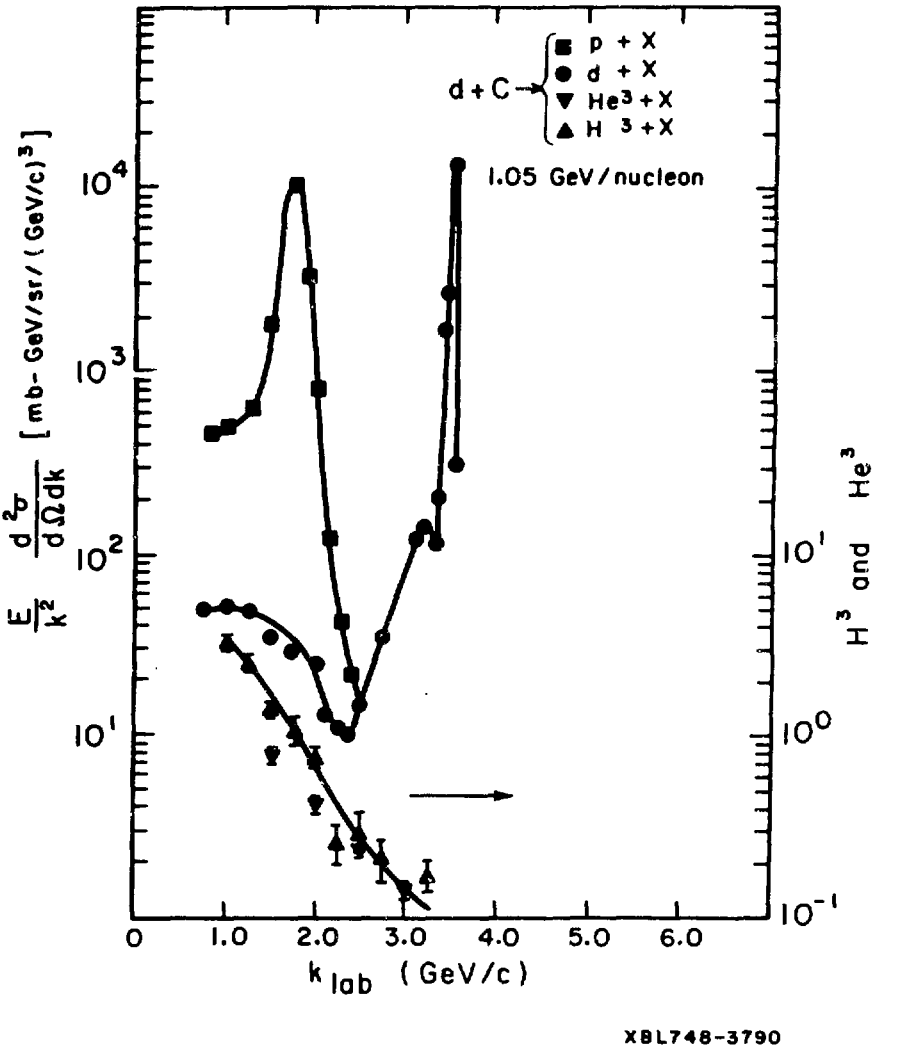
d + C
p + X
d + X
He3 + X
H 3 + X
1.05 GeV/nucleon
E/k² d²σ/dΩdk [mb-GeV/sr/(GeV/c)³]
H³ and He³
k lab (GeV/c)
XBL748-3790

Fig. 26

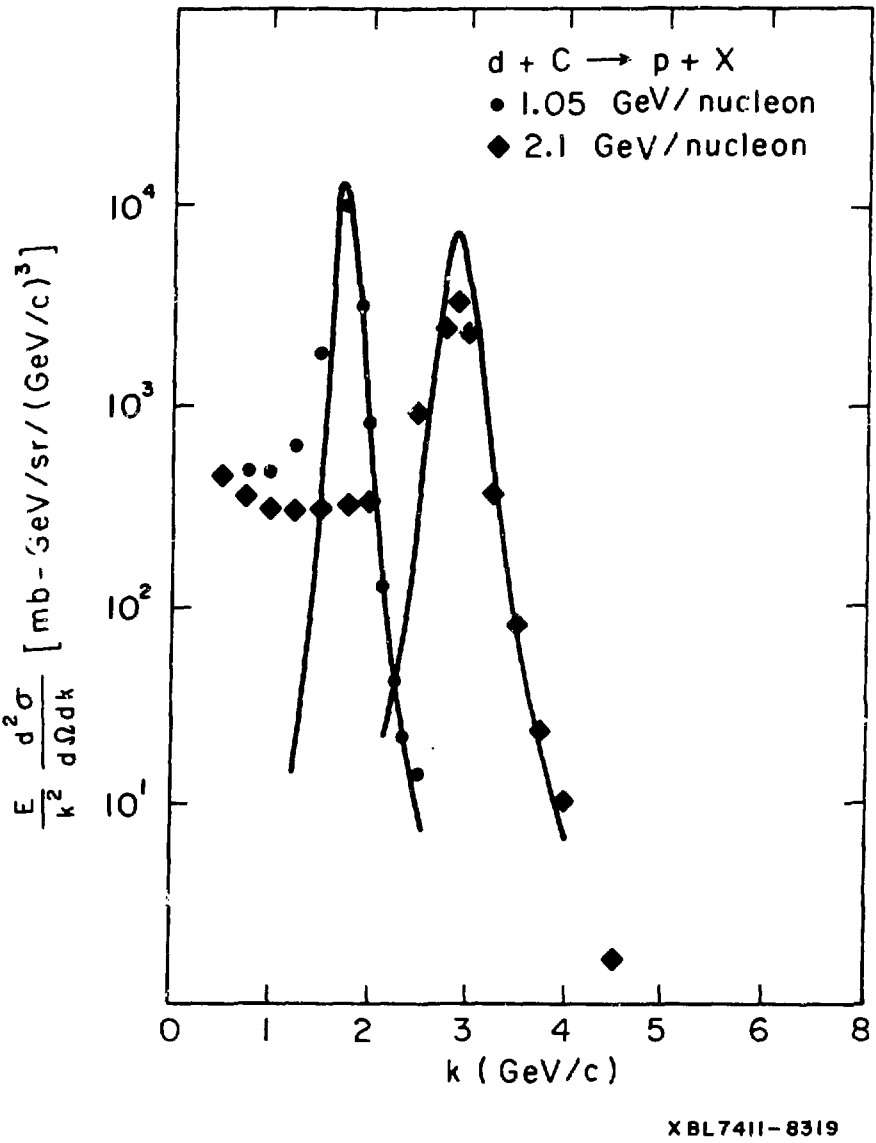
d + C → p + X
• 1.05 GeV/nucleon
◆ 2.1 GeV/nucleon
$\frac{E}{k^2}\frac{d^2\sigma}{d\Omega dk}$ [mb-GeV/sr/(GeV/c)^3]
10^4
10^3
10^2
10^1
0
1
2
3
4
5
6
8
k (GeV/c)
XBL7411-8319

Fig. 27

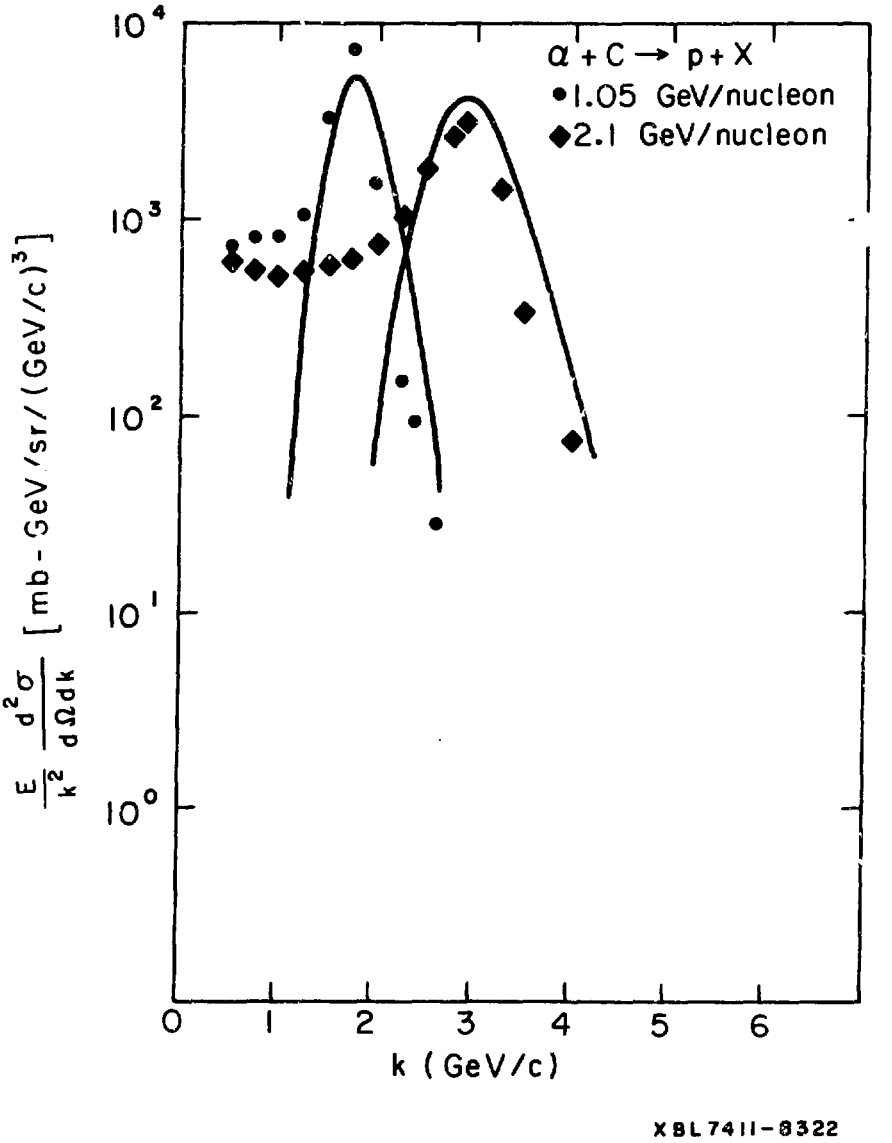
α + C → p + X
●1.05 GeV/nucleon
◆2.1 GeV/nucleon
$\frac{E}{k^2}\frac{d^2\sigma}{d\Omega dk}$ [mb-GeV/sr/(GeV/c)^3]
10^4
10^3
10^2
10^1
10^0
0
1
2
3
4
5
6
k (GeV/c)
XBL7411-8322

Fig. 28

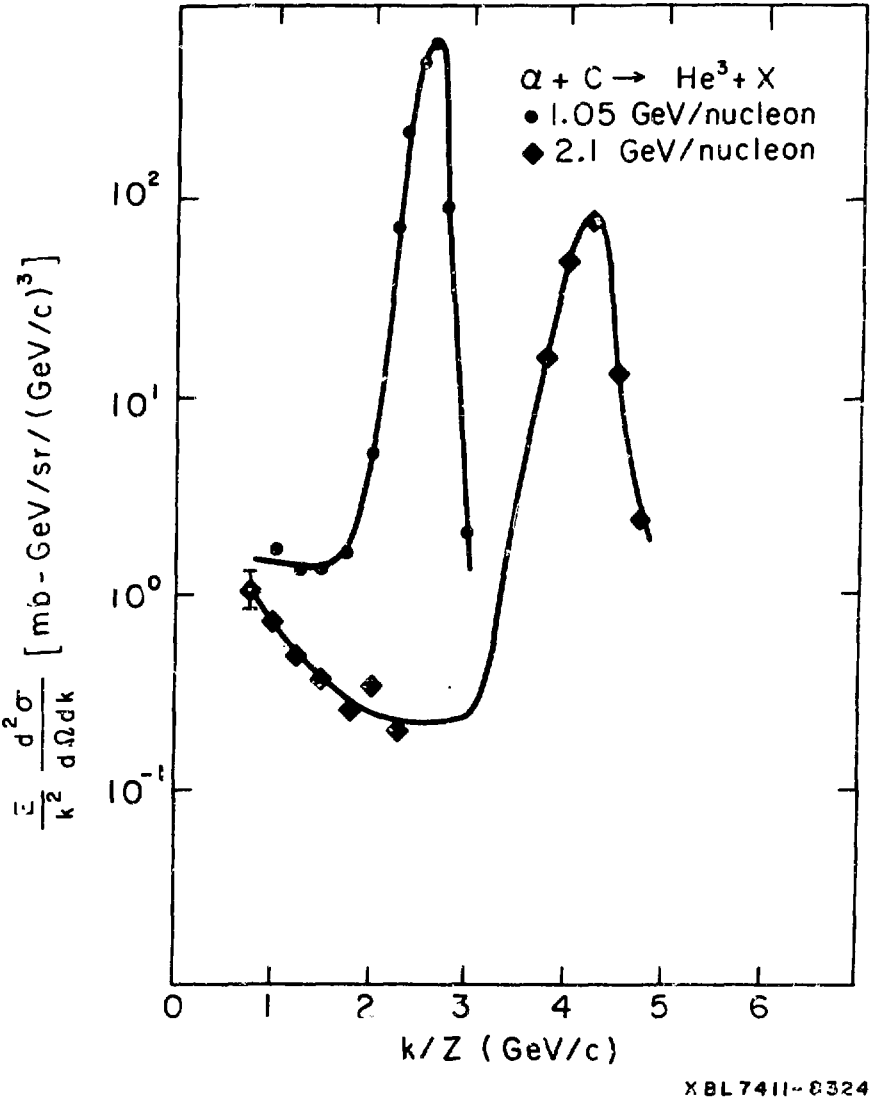
α + C → He³ + X
• 1.05 GeV/nucleon
◆ 2.1 GeV/nucleon
10²
10¹
10⁰
10⁻¹
0
1
2
3
4
5
6
k/Z (GeV/c)
XBL7411-6324

Fig. 29

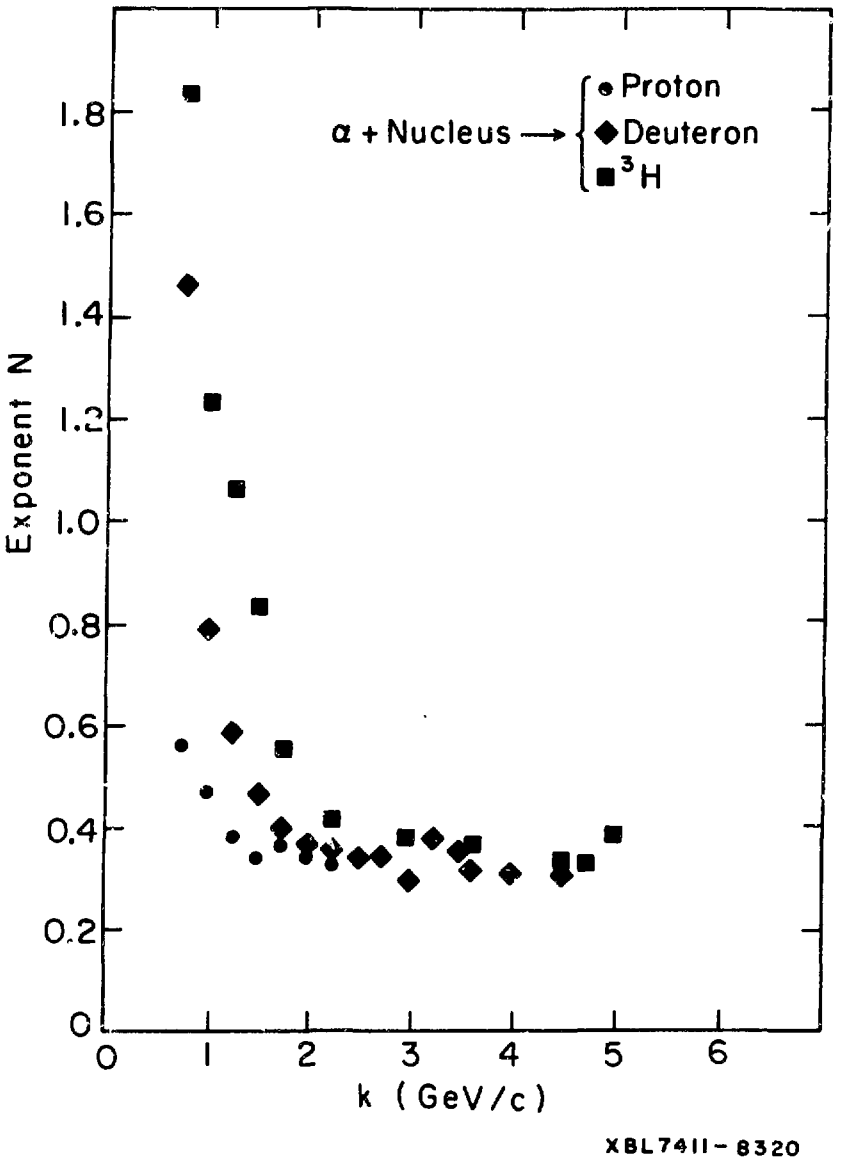
α + Nucleus →
Proton
Deuteron
^{3}H
Exponent N
1.8
1.6
1.4
1.2
1.0
0.8
0.6
0.4
0.2
0
0
1
2
3
4
5
6
k (GeV/c)
XBL7411-8320

Fig. 30

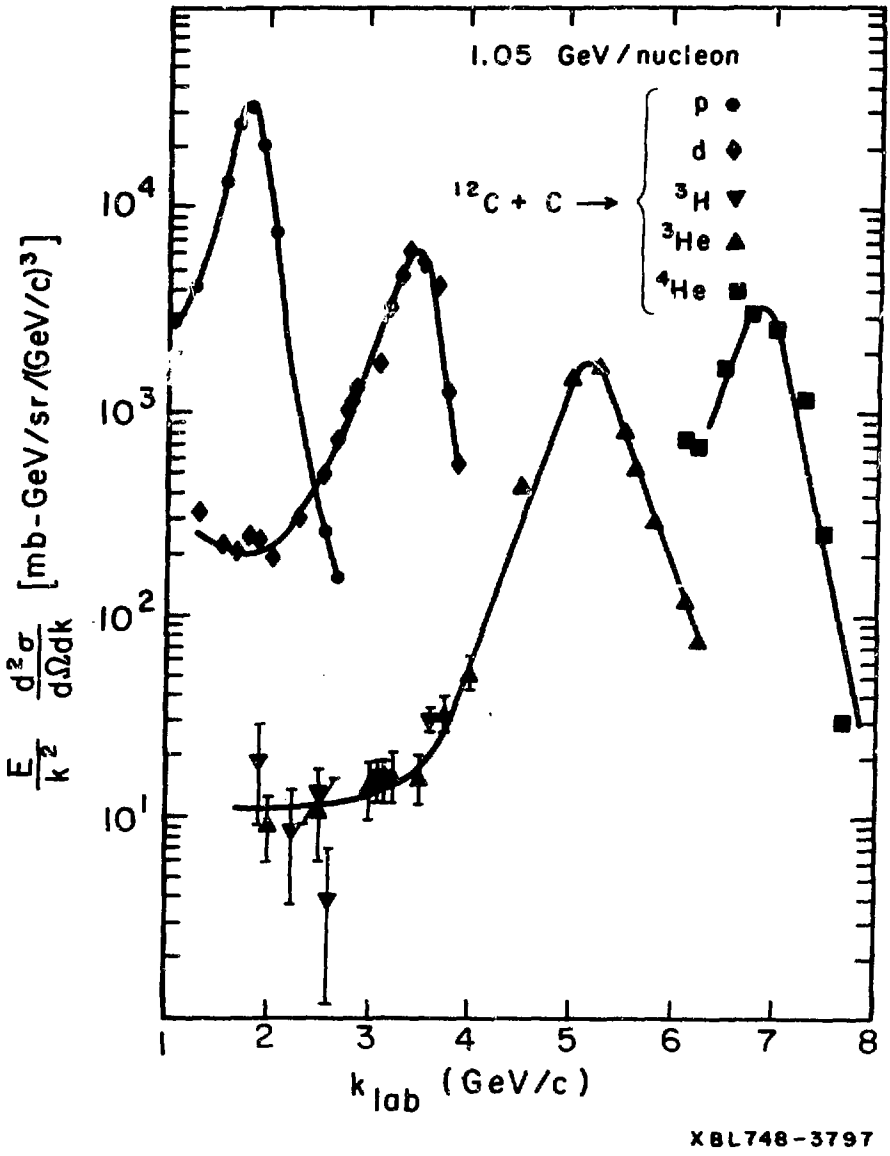
1.05 GeV/nucleon
$^{12}C + C \rightarrow$
p
d
^3H
^3He
^4He
$\frac{E}{k^2}\frac{d^2\sigma}{d\Omega dk}$ [mb-GeV/sr/(GeV/c)^3]
10^4
10^3
10^2
10^1
1
2
3
4
5
6
7
8
k_{lab} (GeV/c)
XBL748-3797

Fig. 31

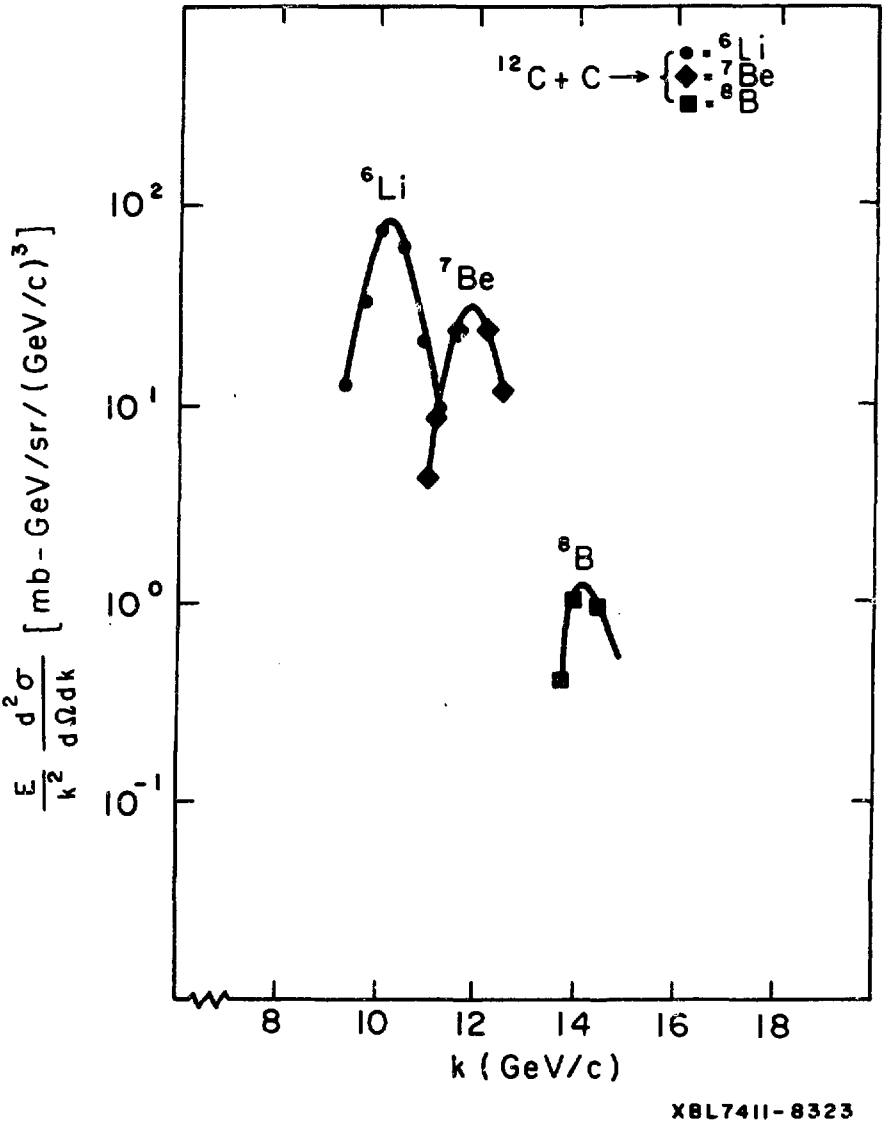
$^{12}C + C \rightarrow$ {● = ^{6}Li, ◆ = ^{7}Be, ■ = ^{8}B}
^{6}Li
^{7}Be
^{8}B
10^{2}
10^{1}
10^{0}
10^{-1}
$\frac{E}{k^2}\frac{d^2\sigma}{d\Omega dk}$ [mb - GeV/sr/(GeV/c)^3]
8
10
12
14
16
18
k (GeV/c)
XBL7411-8323

Fig. 32